ROBERT GORDON UNIVERSITY ABERDEEN

OpenAIR@RGU

The Open Access Institutional Repository at Robert Gordon University

http://openair.rgu.ac.uk

Citation Details

Citation for the version of the work held in 'OpenAIR@RGU':

CHEN, C. C., 2010. Development and testing of thin composite palladium membrane for membrane fuel cell processors. Available from *OpenAIR@RGU*. [online]. Available from: http://openair.rgu.ac.uk

Copyright

Items in 'OpenAIR@RGU', Robert Gordon University Open Access Institutional Repository, are protected by copyright and intellectual property law. If you believe that any material held in 'OpenAIR@RGU' infringes copyright, please contact openair-help@rgu.ac.uk with details. The item will be removed from the repository while the claim is investigated.

Development and Testing of Thin Composite Palladium Membrane for Membrane Fuel Cell Processors

By

Chee Chong, Chen

A thesis submitted in partial fulfilment of the requirements for the degree of Doctor of Philosophy

THE
ROBERT GORDON
UNIVERSITY
ABERDEEN

The Robert Gordon University, Sept 2010

Abstract

The Palladium (Pd) based membranes have long been the focus of studies for the separation of hydrogen due to its high permeability and selectivity toward hydrogen. However, palladium is a precious metal and extremely expensive and its wider applications will depend largely on its ability to become economically feasible to compete with other separation technologies. Hence, the main focus of this study is to produce a supported, thin and defect free palladium composite membrane in a cost effective manner. This thesis also highlights some of current advances in palladium research, especially the membrane preparation methods.

In this study, the Pd composite membranes were fabricated by depositing Pd metal as a thin layer by using advanced electroless plating coupled with partial suction method onto a 30nm γ-Al_2O_3 support. The suction pressure creates a pressure difference between the bore and tube side of the support and this will eventually encourage the transfer of more Pd metal onto the ceramic support, at the same time densifying the deposited layer and simultaneously prevent mass transfer from the film back into the solution, which is the major problem with conventional electroless plating techniques.

The final membrane produced has a thickness of about 6 microns with flux in the order of ~0.1 mol/m^2s and H_2/N_2 selectivity of 140 at 673K. The membrane also show its capability in purifying H_2 gas using a reformate gas mixtures containing 67% H_2, up to the value of 97.3% pure H_2 in a single stage pass at 673K at low pressure differentials of 0.8 barg.

Studies conducted also investigate the effects of electroless plating condition and parameters in their resulting relationship with the pore sizes of the ceramic support have on the palladium layer deposited.

Dedication

I would like to dedicate this work to those who supported and believed in me the most:

My parents, Mr. Chen Fun Keong and Madam Lau Siew Wan,

My sister, Miss Chen Fei Shun,

My grandparents (gone but not forgotten), Mr. Chen Kin Sui and Madam Dai Thye

My best friends, Mr. Robert Scott McIntyre and Mr. Winkin Leung

Acknowledgement

I would like to express my sincere gratitude to the following people and organisations that have made this work possible:

Firstly, I would like express my appreciation and thanks to Prof. Edward Gobina who was my academic supervisor for all his encouragement, support and guidance throughout the duration of this PhD.

Vivien MacKinlay from Univation Ltd, The Robert Gordon University for funding my PhD study and the financial support provided during times of difficulty.

I would also like to thank all the technical staff from the School of Engineering and the School of Life Sciences for their help, guidance, and also the used of their analytical equipment. Special thanks to Ian Tough, Bill Walker, Milton Montgomery, Steve Pirie and Stan Buchan.

Gas2 Ltd for their support, especially Willie Reid.

My friends and colleagues over the years, Ramagopal Uppalari, Susanne Olsen, Luciana, Aurik Andreu, Maurizio Falco, Barry McKenzie, Ruben Umoh, and Ali for their support and friendship.

Contents

List of Figures

List of Tables

Nomenclature

A	Membrane Area	m^2
C	Gas Concentration	mol/m^3
C_p	Concentration of Permeate	mol/m^3
C_r	Concentration of Retentate	mol/m^3
D	Diffusion Coefficient	m^2/s
D_A	Diffusivity of Species A	m^2/s
D_B	Diffusivity of Species B	m^2/s
d_c/d_x	Concentration Gradient	-
E_A	Activation Energy	KJ/mol
J, G	Gas Flux	$mol/m^2.s$
K_o	Knudsen Coefficient	$mol.m/m^2.s.Pa$
L	Length	m
l	Membrane Thickness	µm
M	Molecular Mass	kg/Kmol
n	Constant Power of Pressure	-
P	Permeability Coefficient	$mol.m/m^2.s.Pa^n$
P_A	Permeability of Species A	$mol.m/m^2.s.Pa^n$
P_B	Permeability of Species B	$mol.m/m^2.s.Pa^n$
p	Partial Pressure	Bar, Pa
p_r	Partial Pressure of Retentate	Bar, Pa
p_p	Partial Pressure of Permeate	Bar, Pa
P_1, P_r, P_{high}	Retentate Pressure	Bar, Pa
P_2, P_p, P_{low}	Permeate Pressure	Bar, Pa
Q_H	Temperature Dependant Constant	$mol.m/m^2.s.Pa^n$
Q_O	Pre-Exponential Factor	$mol.m/m^2.s.Pa^n$
R	Gas Constant	J/K.mol
r	Average Pore Radius	nm
S	Solubility Coefficient	$mol/m^3.Pa^n$
S_A	Solubility of Species A	$mol/m^3.Pa^n$

S_B	Solubility of Species B	$mol/m^3.Pa^n$
T	Temperature	^OC, K
V_O	Viscous Flow Co-efficient	kg/m.s
Greek Letters		
$\alpha_{A/B}$	Selectivity of Species A over B	-
λ	Mean Free Path	Å, nm
μ	Viscosity	kg/m.s
π	Pi	-
σ	Collision Diameter of Gas molecules	nm

Abbreviations

AFC	Alkaline Fuel Cell
Ag	Silver
Ar	Argon
Au	Gold
CAS	Chemical Abstracts Service number
CH_4	Methane
CH_3OH	Methanol
CO	Carbon Monoxide
CO_2	Carbon Dioxide
CPIMT	Centre for Process Integration and Membrane Technology
Cu	Copper
$CuSO_4$	Copper (II) Sulfate
CVD	Chemical Vapour Deposition
DME	Dimethyl Ether
DOE	US Department of Energy
EDTA	Ethylene Diamine Tetra Acetic
EDXA	Energy Dispersive X-ray Analysis
EERE	Office of Energy Efficiency and Renewable Energy
ELP	Electroless Plating
Fe	Iron
GC	Gas Chromatography
H_2	Hydrogen
H_2O	Water
HCl	Hydrochloric Acid
H_4N_4	Hydrazine
HI	Hydroiodic Acid
IC	Internal Combustion
MCFC	Molten Carbonate Fuel Cells
N_2	Nitrogen
NaCl	Sodium Chloride

NH_3	Ammonia
NH_4	Ammonium
Ni	Nickel
NOx	Nitrogen Oxide
OPEC	Organization of the Petroleum Exporting Countries
PAFC	Phosphoric acid Fuel Cells
PCBs	Polychlorinated Biphenyls
Pd	Palladium
$PdCl_2$	Palladium(II) Chloride
PEMFC	Proton Exchange Membrane Fuel Cell
Pt	Platinum
SEM	Scanning Electron Microscope
SG	Specific Gravity
SI	Sulphur Iodine
$SnCl_2$	Tin (II) Chloride
SOFC	Solid Oxide Fuel Cells
SS	Stainless Steel
TCD	Thermal Conductivity Detector
VOC	Volatile Organic Compounds
Wt%	Weight Percentage
Y	Yttrium
YSZ	Yttria-stabilized Zirconia

CHAPTER 1

1.0 Introduction

Due to its high energy density and relative abundance, fossil fuels have become the world's most important source of energy over the last few decades. For that reason, the consumption level has increased every year and it is becoming scarcer [1]. As the supply becomes more limited and oil prices escalate, society has begun to look toward other alternative sources.

It is known that scientists today is exploring possible future energy sources and technologies that will produce lower toxic and greenhouse gas emissions, greater efficiency in energy use, and most importantly affordability. For many, the future invokes the idea of renewable energies such as hydrogen power (if hydrogen is produced from electrolysis of water with electricity generated from renewable sources like the sun and wind), solar power, wind power, tidal power, and biomass. Although, existing technologies for new energy sources are promising, there are still commercial and environmental uncertainties associated with renewable energy. Therefore, these technologies still require substantial research and sustained development before they could become economically viable.

1.1 Hydrogen Energy

In recent years, as one of the alternative energy sources, hydrogen power has started to gain international recognition as a key component to a clean and sustainable energy system. However, the transition to hydrogen will take some time to realize a hydrogen based economy. The technology is still associated with uncertainties such as the development of efficient fuel cell technologies, problems in hydrogen production, purification, distribution infrastructure, and the response of petroleum markets [2]. Therefore, it has encouraged more research and development in finding the solutions to these uncertainties and to ensure a smooth future implementation.

President Bush, during his State of the Union Address in 2003 announced a $1.2 billion to stimulate the hydrogen economy [3] and in 2006 said that US is addicted to oil and the best way to go forward is through renewable energies [4]. Therefore, the US government will invest more in zero emission coal-fired plant, revolutionary solar and wind technologies, clean and safe nuclear energy and hydrogen energy [4]. In fact, currently healthy competition has emerged between nations as diverse as Iceland, China, Germany, Japan, US and many more in the race to commercialise a hydrogen powered vehicle in the 21st century [5].

Presently, hydrogen production is still a growing industry. Globally, about 50 million metric tonnes of hydrogen were produced in 2004 compared to 41 million metric tonnes in 2003 [6]. The overall US hydrogen market is estimated at $798 million in 2005 and is expected to rise to $1,605 million in 2010. Meanwhile, the overall European market is estimated to be about $368 million in 2005 and is expected to grow at an average annual growth rate of 15% to $740 million in 2010 [7]. This unprecedented growth has motivated more research into new methods and technologies for hydrogen production, separation, purification, transportation, distribution, storage and application.

1.2 Background of This Work

Although hydrogen is widely used in space craft launches, petroleum refining and methanol production, the technology is not yet advanced enough to be commercially viable, particularly in the sector of production and storage [8]. Hence, the main focus of this research is to address one of the sectors, which is purification of hydrogen gas. Presently, there are a variety of different technologies that can be targeted for the purification of hydrogen. The main ones include pressure swing adsorption, cryogenic processing, membrane separation, and metal hydrides. Amongst them, membrane separation technology is considered most suitable for small and medium scale applications but also have the potential for large scale applications [9] (see chapter 2.2.2).

In this work, the membrane technology being applied refers to metallic or multi-metallic membrane, mainly using Palladium based metal or alloying Palladium with other metals. Although the ability of metals, particularly Palladium to selectively permeate hydrogen has been known for a century [8], the commercial utilisation of this property for the production and purification of hydrogen is relatively recent [8].

The development of Palladium-Silver alloys as diffusion membrane material in the late 1950s, overcame the principal technical difficulties associated with the technique. Thus it has enabled the successful development of commercial equipment [8].

However, a general issue in these membrane technologies is the attainment of high selectivity and high permeability. Both of these properties contribute significantly in the reduction of component size and cost [10]. Furthermore, complete hydrogen selectivity with high permeability is required for applications with ultra-pure hydrogen such as fuel cells. Hence, the study conducted in this work using gas mixture is of vital importance.

Currently, most commercial Palladium and Palladium alloy membranes are made of free-standing foils and tubes (monolithic system). In the initial phase of applications, Palladium and its alloy foil of high thickness (50-200µm) are suggested [11]. The higher thickness is usually required to achieve mechanical strength to withstand pressure differentials (about 15 bars) during operation. However, by doing so the membrane is then prone to other limitations including low flux and the high cost of palladium. The membrane will be expensive and will have lower hydrogen production per unit area due to the high thickness. In addition, the higher the thickness of Palladium membrane, the lower the flux, as the later is inversely proportional to the membrane thickness [11]. Nevertheless, these limitations have provided incentives for the preparation of thinner membranes in order to lower cost and to achieve higher hydrogen permeation rate.

1.3 Target of This Work

As a significant amount of time in this research involves experimental work, the method or technique being applied to produce the membrane is crucial. Currently, there are various techniques of membrane preparation (fabrication) available such as electroless plating, magnetron sputtering, chemical vapour deposition etc [12]. Extensive review of literature and other related texts have revealed that the electroless plating method is one of the most suitable in terms of commercial suitability. The method and the reasons for using this technique will be discussed more in detail in chapter 3, 4 and 5.

In the first phase of research developments and subsequent applications, preparation and utilisation of composite membranes has received considerable attention due to the fact that deposition of a thin palladium layer on the surface of a highly porous support has the potential to overcome the limitation of using higher thickness (which at present have about 20 – 40μm palladium metal layer on porous alumina or stainless steel supports). For these composite membranes, certain limitations do exist. The hydrogen flux is a function of the thickness of the palladium/palladium alloy film. The lower the thickness of the film the lower the cost and the higher the hydrogen produced per unit membrane area. Because of this problem, achievement of lower thickness (1 – 5 μm) for successful industrial applications is not practical [13 - 18] as it will not be able to withstand the operational pressure..

The optimal thickness of palladium film in a composite membrane depends upon a number of factors such as method of preparation, mechanical stability, dense film formation, surface defects of the support and type and quality of the support [19]. The effect of these factors is discussed in chapter 4 and 5. In this research the optimal thickness of Pd film produced would be in the range of approximately 6 – 20μm on porous ceramic supports (alumina) having the pore size range of 30 – 6000nm.

Hence, the aim for the research work is **"Fabrication of metallic composite membrane for the production of hydrogen/high-purity hydrogen".** While the objectives of the research are as follows:

1. To promote the development of H_2 gas separation membranes and their applications in association to the emergence of H_2 economy.
2. To be able to produce high-purity hydrogen or hydrogen gas using membrane separation.
3. To be able to produce a metallic composite membrane for separation and purification purpose.
4. To identify crucial parameters in the preparation methods (membrane manufacturing).
5. To identify suitable preparation method for possible industrial processing (commercialisation)
6. To identify possible ways for simultaneous decrease in membrane cost and increase in separation capability.

Based on the knowledge of available literatures, it is known that the selectivity of the membrane towards hydrogen gas is dependent on the successful formation of a dense layer of Pd or Pd-alloy metal. However, there are still so many other factors that might influence the performance of the membrane in its operating environment. Therefore, there are still further tests that need to be carried out in understanding the effect of temperature (up to 500 ^{0}C), effect of feed gas purity (gas mixtures), and the effect of higher pressure.

1.4 References:

1. Factsheets & FAQ. **Electricity, Nuclear Power and Global Environment**. *International Atomic Energy Agency (IAEA).* Available from: http://www.iaea.org/Publications/Factsheets/English/electric.html [Accessed 03 August 2010].
2. PHILIP TSENG, JOHN LEE and PAUL FRILEY, 2003. **Hydrogen Economy: Opportunities and Challenges**, *The International Journal of Energy, Volume 30, Issue 14, November 2005, International Energy Workshop, pg 2703-2720.*
3. **Hydrogen Fuel: A Clean and Secure Energy Future**, *State of the Union Address 2003*. Available from: http://groups.google.com/group/rechargeit-blog/browse_thread/thread/e333ef540744dc94 [Accessed 03 August 2010].
4. **The Advance Energy Initiative**, *State of the Union Address 2006*. Available from: http://www.aip.org/fyi/2006/017.html [Accessed 03 August 2010].
5. BARRY D. SOLOMOM and ABHIJIT BANARJEE, 2004. **A Global Survey of Hydrogen Energy Research, Development & Policy**, *pg 2-4*.
6. U.S. Department of Energy Laboratory managed by UChicago Argonne, LLC. **Assessing Current, Near-term, and Long-term U.S. Hydrogen Markets**, *for Energy, Environmental, and Economic Systems Analysis.* Available from: http://www.dis.anl.gov/news/HydrogenMarkets.html [Accessed 03 August 2010].
7. MRG Multimedia Research Group, Inc. **Hydrogen Market, Hydrogen R&D and Commercial Implication in the US and EU May 2005**. Available from: http://mrgco.com/TOC_HydrogenMarket_May05.html [Accessed 03 August 2010].
8. GRASHOFF, G.J.; PILKINGTON, C.E.; CORTI, C.W., 1983. **The Purification of Hydrogen – A Review of the Technology Emphasizing the Current Status of Palladium Membrane Diffusion**, *Platinum Metal Reviews*, *27(4), pg 157-169*.
9. MARK C. PORTER, 1990. **Handbook of Industrial Membrane Technology**, *New Jersey, Noyes Publication ISBN 0-8155-1205-8*.
10. S.TOSTI, L. BETTINALI, S. CASTELLI, F. SARTO, S. SCAGLIONE, and V. VIOLANTE, 2002. **Sputtered, Electroless, and Rolled Palladium-Ceramic Membranes**, *Journal of Membrane Science, 196 (2)*, pg. 241-249.

11. ITOH N., 1987. **A Membrane Reactor Using Palladium**, *AIChE Journal*, *33(9), pg 1576-1578.*
12. QUICKER P, HOLLIEN V. and DITTMEYER R, 2000. **Catalytic Dehydrogenation of Hydrocarbons in Palladium Composite Membrane Reactors**, *Catalysis Today, 56 (1-3), pg. 21-34.*
13. LOFFLER D.G., TAYLOR K.G., MASON D, 2003. **A Light Hydrocarbon Fuel Processor Producing High-purity Hydrogen**, *Journal of Power Sources, 117 (1-2), pg. 84-91.*
14. FUNKE H.H., RAVNOR M.W., HOULDING V.H., BOSSAD P., FABIANO P. and STUCKY D., 2003. **Optimization of Palladium Cell for Reliable Purification of Hydrogen in MOCVD**, *Journal of Crystal Growth, 248, pg. 72-76.*
15. HAN J., LEE S., and CHANG H., 2002. **Metal Membrane-type 25-kW Methanol Fuel Processor for Fuel-cell Hybrid Vehicle**, *Journal of Power Sources, 112 (2), pg. 484-490.*
16. LIN Y. and REI M., 2001. **Separation of Hydrogen from the Gas Mixture out of Catalytic Reformer by using Supported Palladium Membrane**, *Separation and Purification Technology, 25 (1-3), pg. 87-95.*
17. NEILSEN A.T., AMANDUSSON H., BJORKLUND R., DANNETUN H., EILERTSSON J., EKEDAHL L, LUNDSTROM I. and SVENSSON B.H., 2001. **Hydrogen Production from Organic Waste**, *International Journal of Hydrogen Energy, 26 (6), pg. 547-550.*
18. LIN Y. and REI M., 2000. **Process Development for Generating High Purity Hydrogen by Using Supported Palladium Membrane Reactor as Steam Reformer**, *International Journal of Hydrogen Energy, 25 (3), pg.211-219.*
19. LI A., LIANG W., and HUGHES R., 2000. **Fabrication of Dense Palladium Composite Membranes for Hydrogen Separation**, *Catalysis Today, 56(1-3), pg 45-51.*

CHAPTER 2

2.0 Review of Literatures, Technologies and Membranes

2.1 Hydrogen Gas Review

The need for hydrogen energy is caused by the concern about the depletion of fossil fuel and most importantly, the reduction and elimination of all harmful and climate affecting emissions. These factors will be the main drivers in propelling the next energy transition.

Fossil fuels are non-renewable resource and although in abundance, they were initially used with little consideration for efficiency/performance. In addition, in recent history fossil fuel has been consumed at an increasing rate and supply is getting limited while demand is still increasing, particularly in China, India and other developing countries. Most non-OPEC (Organisation of Petroleum Exporting Countries) countries are nearing their peak production and most of them cannot produce enough oil to meet their own demand and started importing from oil-rich countries [1].

2.1.1 Hydrogen Economy

The term 'hydrogen economy' refers to all the infrastructures supporting the energy requirement of the society based on the use of hydrogen rather than fossil fuel [1]. It will feature hydrogen as an energy carrier in stationary power, transportation, industrial, residential and commercial sectors [2]. The concept of using hydrogen as an energy system is not new and goes as far back as 1875 when the famous French writer Jules Verne projected in his book 'The Mysterious Island' that water would one day replace coal as fuel by splitting it into hydrogen and oxygen to supply endless electricity and heat [3].

The current economy is primarily fuelled by fossil fuel to provide energy has caused the emission of greenhouse gases and other pollutants. The release of CO_2 into atmosphere may bring about climate change by contributing to global warming. Other air pollutants such as Carbon Monoxide, Nitrogen Oxide, Sulphur Oxide, volatile organic compounds and fine particulates causes acid rain or react with sunlight to create ground level smog [4].

2.1.2 Hydrogen Gas

Hydrogen is the first element on the periodic table of elements and is represented by the symbol H. It is the simplest element with a single electron orbiting around a single proton. It is also the most common and abundant element in the universe accounting for 90% of the universe by weight [6]. However, little exists as free gas since it readily/always combines with other elements.

Under normal conditions, hydrogen is colourless, odourless, tasteless, non-poisonous and highly flammable gas. It burns with a pale-blue, almost invisible flame (difficult to see with the naked eye) and produces no carbon dioxide, particulate or sulphur emissions although it can produce nitrous oxide (NOx) under some conditions [6].

Hydrogen has the highest energy content of any common fuel by weight, about 3 times more than gasoline and 7 times more than coal in equal weight, but it has the lowest energy content by volume [7]. It also has a very low density at standard temperature and pressure, and usually stored under high pressure or extremely low temperature in liquid form.

2.1.3 Hydrogen Gas Safety

Like any fuel, hydrogen is flammable and can be dangerous under certain conditions. It has a flammability range of 4% to 75% in air by volume [8]. However, due to its buoyancy and low density, hydrogen disperses rapidly if leaked to atmosphere. Therefore, it is difficult for it to concentrate in an un-enclosed area to create a combustible situation. Even if hydrogen is ignited, it burns upward and is quickly consumed. By comparison, gasoline vapour and natural gas are heavier than air making it difficult to disperse, making them more dangerous.

Hydrogen gas is also non-toxic and non-poisonous compared to other fuels (petroleum fuels) which are harmful to humans [8]. When it leaks, it will not pollute the atmosphere or cause an environmental concern that is usually associated with fossil fuel.

2.1.4 Hydrogen Gas Production

Although hydrogen can be produced from a wide variety of feedstocks, the great potential for the diversity and renewability of supply is an important reason why it is a promising energy carrier.

Hydrogen can be produced from a variety of feedstocks; from fossil resources (such as natural gas and coal), from renewable sources such as water with input from renewable energy sources (e.g. solar, wind or hydro-power), and from biomass [10]. However, each technology is currently at a different stage of development and complexity, and each has its own opportunities and challenges.

Although the usage of hydrogen produces little or no emission at all, some H_2 production method can release greenhouse gases and other harmful by-products depending on the method and the feedstock. Generally, the production method of hydrogen can easily be categorised by the feedstocks or sources use:

- fossil fuels
- biomass
- water

2.1.4.1 Hydrogen from Fossil Fuel

Hydrogen production from fossil fuel system is the oldest method and also a proven technology. It also tends to have the lowest production cost due to it being a mature technology and, the relative availability and lower costs of resources (especially coal). However, fossil fuels are carbon-based, so they will release carbon monoxide (CO) or carbon dioxide (CO_2) as by-products during the conversion process [11]. Presently, technologies that use fossil fuel as resources in hydrogen production are:

- steam reforming
- partial oxidation
- auto-thermal reforming
- gasification

2.1.4.1.1 Steam Reforming

Steam reforming refers to a reaction process that utilizes hydrocarbon fuel in the presence of water (steam). In this process hydrocarbon gas often methane rich (CH_4) is mixed with steam at high temperatures (750-1000 ^oC) and pressure (3-25 bars) in the presence of catalyst to produce synthesis gas, which consist of H_2 and CO (see Eq1).

$$CH_4 + H_2O \rightarrow CO + 3H_2 \qquad \text{(Eq 1)}$$

$$CO + H_2O \rightarrow CO_2 + H_2 \qquad \text{(Eq 2)} \quad \text{---------- [1]}$$

At the same time, the CO produced from the initial reaction will react further with steam in the presence of the same catalyst to produce H_2 and CO_2 (see Eq 2). This process is also known as the 'water gas shift' reaction. In the final step, a process known as pressure swing adsorption* removes the CO_2 and other impurities, leaving only pure H_2. This whole process makes 4 parts of H_2 from 1 part of methane and 2 parts of water. This process can also be used to produce hydrogen from other fuels such as ethanol, propane, or even gasoline [12].

Steam reforming is a relatively efficient, well proven, widely implemented and the most cost effective way of producing hydrogen on a large scale. However, steam reforming uses natural gas in the process; hence the cost is heavily influence by the fluctuation price of natural gas and it also produces some emissions of CO_2. To avoid emissions of CO_2 into the atmosphere, it can be used by pumping it into the reservoir for enhanced oil recovery or it can be captured and sequestered (carbon sequestration). Nonetheless, steam reforming is poised to be the near term hydrogen production method of choice before other methods become more economically viable [13].

(**Pressure swing adsorption is a separation technology at utilizes high pressure at ambient temperature to separate some gas species from a mixture of gases according to their individual molecular characteristics and affinity to the adsorbent material. The process then swing to low pressure to release the gas species from the adsorbent material hence, the name pressure swing adsorption. The adsorbent material used for the process is dependent on the target gas.)*

2.1.4.1.2 Partial Oxidation and Auto-Thermal Reforming

Partial oxidation process refers to the incomplete oxidation of hydrocarbon with a limited amount of oxygen gas so that it does not completely oxidize the hydrocarbons. The partial oxidation process directly oxidizes methane in a one step reaction, while auto-thermal reforming combines the partial oxidation with reforming process by catalytically reacting methane with a mixture of oxygen and steam [11]. Partial oxidation is therefore different from steam reforming since in the latter process methane reaction with steam only.

With less than the stoichiometric amount of oxygen available for reaction, the partial oxidation process produces syngas (a mixture of CO and H_2), following the reaction:

$$CH_4 + {}^1/_2O_2 \rightarrow CO + 2H_2 \qquad \text{(Eq 3)} \quad \text{---------- [11]}$$

For auto-thermal reforming, the CO produced from initial partial oxidation reaction is further converted to H_2 and CO_2 with water gas shift reaction (Eq 2). However, the product also contains a small amount of CO_2 and other compounds since it is in competition with the total oxidation reaction as shown in equation 4:

$$CH_4 + 2O_2 \rightarrow CO_2 + 2H_2O \qquad \text{(Eq 4)} \quad \text{---------- [11]}$$

Although, both processes do not require the presence of catalyst, the use of a catalyst will definitely increase hydrogen yield and reduce the operating temperature. The partial oxidation is an exothermic process and hence requires careful control and reactor design to facilitate the heat exchange.

2.1.4.1.3 Gasification

Gasification is a process in which coal is converted into a gaseous state. There are 3 steps involved, which are:

1. treatment of coal at high temperature with steam,
2. catalytic shift reaction (water gas shift), and
3. purification of the product (pressure swing adsorption).

In the first step, coal is chemically broken down by high temperature (1330 ^oC) and high pressure steam to produce syngas (Eq 5), as shown below [11]:

$$\text{Coal} + H_2O \rightarrow H_2 + CO \qquad \text{(Eq 5)} \quad \text{---------- [11]}$$

In the second step, the CO produced will then be further reacted with steam in a 'water gas shift reaction' to produce more H_2 (see Eq 2). Subsequently, pressure swing adsorption is then used to remove the impurities from the product stream to produce pure H_2.

Although coal is an attractive energy source due to its abundance and low raw material cost, there are additional technical and economic consideration needed for the handling and, also capture and storage of CO_2 produced [11]. This method of H_2 production can be more environmentally viable if CO_2 produced is sequestered or used to recover methane trapped in un-minable coal beds [14].

2.1.4.2 Hydrogen from Biomass

Similar to coal, biomass can also be gasified to produce hydrogen in a three step gasification process. In this process, biomass such as forestry by-products, straw, municipal solid waste or sewage is heated at high temperature in a reactor to break the bonds in the biomass molecules [9]. This will then produce a raw syngas mixture consisting of CH_4, H_2, CO and CO_2. It is then followed by the catalytic water gas shift reaction and purification process.

Alternatively, biomass can first be reformed to a liquid biofuel state in a process called pyrolysis (thermal decomposition of biomass). The biofuel is then steam reformed using a nickel-based catalyst at 750-850 ^{o}C, followed by the same shift reaction and purification process as in gasification [11]. However, in this process the CO_2 emissions from biomass gasification or pyrolysis do not contribute to a net increase in greenhouse gas emissions because it consumes CO_2 in the atmosphere as part of its natural growth process [15].

2.1.4.3 Hydrogen from Water

Hydrogen can be produced sustainably and cleanly from water splitting processes using energy supplied from renewable sources such as solar, wind, wave, hydropower and nuclear heat. These processes are considered as newer technologies and tend to be more complex and expensive than fossil fuel processes, but it does not produce harmful emissions or consume large quantities of non-renewable feedstocks [11]. Presently, the varieties of technologies available for water splitting processes are:

- Electrolysis of water
- Thermo-chemical water splitting (high-temperature water decomposition)
- Photo-electrochemical water splitting (Photo-electrolysis/catalytic)
- Photo-biological water splitting (Photo-synthetic)

2.1.4.3.1 Electrolysis of Water

Electrolysis is a process of splitting water into molecules of H_2 and O_2 by passing electricity through the water. The whole reaction takes place in a unit known as an electrolyzer and it contains two electrodes within a conducting medium, which is generally an alkaline electrolyte solution (such as an aqueous solution of potassium hydroxide (KOH)) [11]. When an electric potential is applied across the electrodes, H_2 gas will be generated from the negative cathode and O_2 at the positive anode [14]:

Cathode: $2H_2O + 2e^- \rightarrow H_2 + 2OH^-$

Anode: $2OH^- \rightarrow {}^1/_2O_2 + H_2O + 2e^-$

Total: $H_2O \rightarrow H_2 + {}^1/_2O_2$ ---------- [11]

The only product produced are H_2 and O_2, resulting reduced harmful and greenhouse gas emissions. However, this is only true if the electricity used for the splitting process is generated from clean renewable sources (e.g. solar and wind power) and the life cycle assessment. On the other hand, the process has a disadvantage of requiring a large amount of electricity to split the water, thus increasing its hydrogen production cost.

Currently, there are only limited types of industrial electrolyzers available, with the most common one such as alkaline, polymer electrolyte membrane (PEM), and solid oxide (SOE) electrolyzers. Although each of them functions a little differently, their basic operating principle is the same with the only main distinction being the types of electrolyte they use.

2.1.4.3.2 Thermo-chemical Water Splitting (high-temperature water decomposition)

Thermo-chemical water splitting process involves separating water into H_2 and O_2 through chemical reactions in multiple steps at high temperature. High temperature heat ranging from 500-2000 ^oC needed for the process are supplied by the heat from nuclear reactors (up to 1000 ^oC) or from sunlight with solar concentrators (up to 2000 ^oC), while the chemical used are chosen such that it could recycled and reused within each cycle, thus creating a closed loop system that produces only H_2 and O_2 [16].

The main advantage of the process is that it reduces the consumption of electricity by using high temperature heat. An example of the process is the sulphur-iodine (SI) cycle that used water through a series of reactions involving sulphur and iodine at different temperature as described by the reactions below:

$$2H_2O + SO_2 + I_2 \rightarrow H_2SO_4 + 2HI \qquad (<120\ ^oC)$$

$$2HI \rightarrow H_2 + I_2 \qquad (>300\ ^oC)$$

$$H_2SO_4 \rightarrow H_2O + SO_2 + {}^1/_2O_2 \qquad (>800\ ^oC)$$

$$\text{Net:} \quad H_2O \rightarrow H_2 + {}^1/_2O_2 \quad \text{---------- [11]}$$

There are many other thermo-chemical processes that can be utilised, but like SI cycle, still require more research and developments before they could reach industrial scale. However, like most processes, it comes with a drawback. The process is usually associated with the corrosion of the process reactors, system materials, and also the safety issues of chemical handling [16].

2.1.4.3.3 Photo-electrochemical Water Splitting (Photo-electrolysis/catalytic)

In this process, H_2 is produced from water using a special semiconductor also known as photo-catalyst materials with energy input from sunlight irradiation to directly disassociate water into H_2 and O_2. There is a variety of semiconductor materials available and each work at particular wavelength of light and energies [17].

This technology is still in its infancy stage and not yet economically feasible for hydrogen production, however it does have similar advantages to other water splitting processes. The process is clean, producing no harmful emissions and relies on solar energy, thus having the potential to offer long-term sustainable hydrogen production. Currently, more research is being carried out in order to the increase the efficiency of the process to make it more economically viable [11].

2.1.4.3.4 Photo-biological Water Splitting (Photo-synthetic)

This process while similar to photo-electrochemical technique, but differs in that it uses specialized micro-organisms to consume water in the presence of sunlight to produce H_2 as a by-product of their natural metabolic process just like plants producing O_2 during photosynthesis.

Micro-organisms such as green algae and cynobacteria are used because they contain the hydrogenase enzymes that are needed in the process. The current limitation of this process is that the amount of hydrogen produced is limited by the amount of light and is too slow for efficient H_2 production. Nonetheless, like other water splitting processes, with sustained research and development, it does have the potential to offer long-term sustainable H_2 production with no environmental impact.

The process is based on two steps, photosynthesis and hydrogen production catalyzed by hydrogenase enzyme:

Photosynthesis: $2H_2O \rightarrow 4H^+ + 4e^- + O_2$

Hydrogen production: $4H^+ + 4e^- \rightarrow 2H_2$ ---------- [11]

A more detailed explanation of the process can be found in reference 18 and 19.

2.1.5 Hydrogen Storage

Developing a safe and reliable hydrogen storage technology is important to the implementation of hydrogen economy. However, hydrogen storage is proving to be one of the biggest obstacles [20], because hydrogen has the highest energy content per unit weight but it is also the lightest element; therefore it has very low energy content per unit volume. Hence, hydrogen is either stored under high pressure or extremely low temperature in liquid form.

Nevertheless, for hydrogen to be used as fuel, the methods for storing hydrogen will certainly depend on the safety, ease of use, and also other factors such as volume and weight of the storage unit, space restrictions, and the end use purpose. Presently, there are a variety of storage methods available to store hydrogen in different states (solid, liquid and gaseous) and in addition there are some other new methods that are still in research and development stage. The most common hydrogen storage methods are:

- Compressed hydrogen (*gaseous state*)
- Liquid hydrogen (*liquid state*)
- Metal hydride tank (*gaseous/liquid state*)
- Chemically stored hydrogen (*solid state – e.g.: NH_3, HI, CH_3OH*)
- Carbon nanotubes (*solid state*)

The simplest option is to store hydrogen in its gaseous form, but it has to be compressed to a high pressure. This process requires substantial amount of energy to compress the hydrogen and it would also require specialized tanks that can withstand high pressure and to keep it from bursting and leaking in the event of an impact. Despite all these, the weight of hydrogen stored in gaseous form only represents a few percentages (1 - 2%) of the total weight of the tank [3]. For this reason, more research is still needed to find lightweight and inexpensive materials strong enough to withstand the high pressure [23].

Hydrogen can also be stored in its liquid form but has to be at an extremely low temperature (- 253 ^{o}C). Like compression, a considerable amount of energy is required to chill hydrogen to its liquid form [22]. In addition, special equipments are also needed for its storage and tanks have to be properly insulated to maintain the temperature, the two main challenges of liquid hydrogen storage (the efficiency of the liquefaction process and thermal insulation to limit boil off (evaporation) [24]).

More recently, H_2 has been stored in its solid form instead of the more common gaseous or liquid form by using metal hydride system [21]. Metal hydride systems consist of a specific type of metallic alloys that can absorb and store hydrogen. It functions much like a sponge absorbing water. It has a unique ability to absorb, then store hydrogen within its structure and later release it either at room temperature or through heating of the tank [22]. Currently, there is a vast variety metallic alloys being developed to store H_2 which include lithium hydride, sodium borohydride, and the new emerging class of ultraporous nanotech materials [23].

The metal hydride system does offers the potential for volume efficiency, high safety, low pressure containment, and ambient temperature of operation [21]. However, the percentage of gas absorbed to the volume of the metal hydride is still low (1 - 7% of the total weight of the tank), and some hydrides required high temperature to release the hydrogen [22].

Hydrogen can also be stored in solid form by using carbon nanotubes or chemical reactions. Since hydrogen is often found in compound forms in nature, many of these compounds can be utilized as a storage method. A chemical reaction is used to combine hydrogen in a compound form while a second reaction can then release it later for subsequent use.

Carbon nanotubes are microscopic tubes of carbon that can store hydrogen in its microscopic pores within the tube structure [20]. The mechanism of storing and releasing hydrogen is similar to that of metal hydrides but it has the advantage of storing more hydrogen than metal hydride. Carbon nanotubes are capable of storing from 4.2 – 65% of their own weight in hydrogen [22]. However, like other storing methods, further research is still needed in order to understand the material nature and potentials of using carbon nanotubes and chemical hydrides for increasing the storage efficiency [21].

2.1.6 Hydrogen Distribution

One of the key elements in the successful implementation of a future hydrogen economy is the delivery and distribution of produced hydrogen to end use such as hydrogen refuelling station or a fuel cell plant. However, like storage, the transportation of hydrogen poses some unique challenges due to its properties [25]. Presently, hydrogen is usually transported and distributed in its gaseous form through pipelines or in liquid form by special tankers.

Pipelines are considered the cheapest and safest way to deliver hydrogen in large volume, but the current pipeline infrastructure is very small and limited, it exists only for a short distance. It totalled 1500 km in Western Europe [27] and 900 km in America compared to more than 1 million km of natural gas pipelines in America alone [26]. Hydrogen is also transported in its gaseous form but in a much smaller volume for short distances by road using tube trailers [26].

Due to its low energy density by volume, transportation of hydrogen using pipeline is three times more expensive compare to natural gas [3]. Besides that, there is a problem always associated with pipelines where the pipes and fittings can become brittle and cracked as hydrogen diffuses into the metal (hydrogen embrittlement) [28]. Although the problem can be prevented, this would eventually bring up the cost of transportation significantly.

Hydrogen is more commonly transported in its liquid form by two modes of transportation; by road using cryogenic liquid hydrogen tankers or by sea using ocean tankers. Although the liquefaction process cost is high, it is still the preferred method for transportation due to the unavailability of transport pipeline [24]. Besides that, liquefied hydrogen is denser and has higher energy content in a given volume than its gaseous form.

2.1.7 Hydrogen Utilization

The importance of hydrogen has been known since Isaac de Rivaz (Switzerland) developed the first combustion engine fuelled with hydrogen in 1805 [2]. Although the interest and potential is long known, there are still some obstacles that need to be overcome before a hydrogen economy can be realized [5, 8, 29]. Besides that, smooth transition to a hydrogen economy will requires a large amount of investments into further research toward the end use technologies and potential applications.

Hydrogen has the highest energy to weight ratio and a much wider limit of flammability in air compare to fossil fuels. For that reason, it is more efficient, powerful, light weight and more importantly, burns much cleaner. Hence, it is extremely suitable to be used as transportation fuel [29]. Its combustion properties will also enable the development of an engine that would meet all current and future emissions standards and regulations [30].

Thus, a wide range of hydrogen energy related technologies are being developed or modified to run on hydrogen or hydrogen-blended fuels with reduced emission. These includes vehicles powered by internal combustion engines, fuel cell powered vehicles, and hybrid vehicle [29]. Hydrogen can also be used as fuel directly in an internal combustion (IC) engine which requires little or no modification and crucially, the combustion product is clean, consisting of water and little amount of nitrogen oxides [31].

In a longer term, fuel cell vehicles are more attractive compare to IC engine vehicles because they can offer similar performance but with several more advantages, including better environmental performance, quiet operation, rapid acceleration from a standstill, and potentially lower maintenance requirements [32]. However, for the time being, the hybrid powered vehicles have been more successful in penetrating the transport market largely due to the convenience of fossil fuel distribution system (distribution and refuelling station). This is also one of the major drawbacks in utilizing hydrogen within the transportation sector.

Besides transportation, hydrogen can also play a more important role in the industrial and power generation sectors. Currently, industrial boilers and process heaters are fuelled by combustion of fossil fuels (natural gas and coal). In the US market alone, the consumption is more than 75% of its manufacturing market [32]. However, gas turbines can be modified to operate using hydrogen or hydrogen rich fuels to generate electricity [29, 31-33] and this will undoubtedly offer an expanded use of hydrogen in this sizeable end-use market.

In addition to hydrogen gas turbines, fuel cell systems can also be used for stationary power generation [32]. Fuel cells are modular design and can be used as single units, stacked together or they can be connected to other systems located all over the country to form a distributed network. By this way, they can form an easy to control network of decentralised power generation to supply power or to compensate load fluctuation in the grid [34]. Summarised below are examples of some current applications of hydrogen gas [21, 33]:

1. Transport sector: hydrogen fuelled IC engines or fuel cell power vehicles such as scooters, cars, buses, and possible future use in aviation and marine applications.
2. Industrial sector: ammonia production (fertilizers), high temperature industrial fuel, synthesis of methanol, ethanol, dimethyl ether (DME), hydrogenation of hazardous wastes (dioxins, PCBs), hydrogenation of oils in the food industry, reducing agent in electronic industry, and more.
3. Power sector: fuel cells, gas turbines, generators for on-site or distributed power generation.

2.1.8 Fuel Cells Technology

Fuel cell is based on a principle discovered long ago and it was known at that time that water can be separated into hydrogen and oxygen by using electricity (electrolysis) [26]. Hence, Sir William Grove believed that the principle might work in the opposite way instead, i.e. to produce electricity if hydrogen and oxygen are combined using the right infrastructure or technique. Thus, he successfully constructed the first cell in 1839 that was capable of producing electricity by using hydrogen and oxygen, which then known as fuel cell in a later date [35]. In general, fuel cell is an electrochemical energy conversion device that is capable of producing electricity at the point of use [36].

A typical fuel cell is a structure that consists of an electrolyte and two electrodes (anode and cathode) with catalysts. The reactions take place at the electrodes with the catalyst speeding up the reaction while the electrolyte acts as an ionic conductor which carries the electrically charged particles from one electrode to the other [38].

Currently, there are a variety of fuel cells and technologies available, which can be distinguished by their nature of ions transfer. Some types of fuel cells use combinations of fuel such as hydrocarbons and alcohols, while oxidants used include air and others [37]. However, their basic principle of operation remains the same. Generally, fuel cells are classified according to the operating temperature of the electrolytes used. Each type uses particular materials and fuels, and is usually applicable for a specific application [39]. Table 2.1 shows the types of fuel cell and their operating parameters while table 2.2 shows some of their advantages and disadvantages.

Type of Fuel Cell	Electrolyte	Operating Temperature	Efficiency	Power Output	Applications
Alkaline (AFC)	Aqueous alkaline solution (e.g. potassium hydroxide)	90 – 100 ^{o}C	60 %	10 – 100 kW	- Military - Space
Molten Carbonate (MCFC)	Molten alkaline carbonate (e.g. sodium bicarbonate	600 – 700 ^{o}C	45 – 47 %	1 kW – 1 MW	- Electric utility - Power station
Phosphoric Acid (PAFC)	Molten phosphoric acid	150 – 200 ^{o}C	32 – 38 %	50 kW – 1 MW	- Power station
Polymer Electrolyte Membrane (PEMFC)	Polymer membrane	50 – 100 ^{o}C	25 – 60 %	1 – 250 kW	- Backup power - Transportation
Solid Oxide (SOFC)	Ceramic oxide (e.g. zirconium dioxide)	650 – 1000 ^{o}C	35 – 43 %	5 kW – 3 MW	- Auxiliary power - Power station

*Table 2.1: Types of fuel cell and their applications**

(* *taken and modified from reference no. 39*)

Type of Fuel Cell	Advantages	Disadvantages
Alkaline (AFC)	- cathode reaction faster - higher performance	- expensive removal of CO_2 from fuel and air streams (CO_2 degrades electrolyte)
Molten Carbonate (MCFC)	- high efficiency - fuel flexibility - can use a variety of catalysts	- slow start-up - complex electrolyte management - high temperature speeds corrosion & breakdown of components
Phosphoric Acid (PAFC)	- higher overall efficiency - increased tolerance to impurities in H_2 stream	- requires expensive platinum catalysts - low current and power - large size/weight
Polymer Electrolyte Membrane (PEMFC)	- low temperature - quick start-up - less corrosion and electrolyte management problems	- requires expensive catalysts - high sensitivity to fuel impurities - low temperature waste heat
Solid Oxide (SOFC)	- high efficiency - fuel flexibility - can use a variety of catalysts - less corrosion and electrolyte management problems	- high temperature speeds corrosion & breakdown of components - slow start-up - brittleness of ceramic electrolyte with thermal cycling

*Table 2.2: Advantages and disadvantages of different types of fuel cells**

(* *taken and modified from reference no. 39*)

Because hydrogen and oxygen gases are electrochemically converted into water, fuel cells tend to have many advantages:

- high efficiency,
- silent operation,
- low level of pollutants,
- run on a wide range of fuels, ranging from gaseous fuels such as hydrogen and natural gas to liquid fuels (such as methanol and gasoline) [37].

If hydrogen fuel used is produced from renewable energy sources such electrolysis of water using solar energy, then the technology can be truly sustainable. Besides that, fuel cell has no major moving parts, thus having high reliability. Therefore fuel cell can be a very useful power source in remote locations and in space.

Although it has a lot of benefits, it is also associated with some challenges and uncertainties. Two of the main problems are the availability of infrastructure and the cost of balance-of-plant components it uses, including the precious metal catalysts (e.g. platinum). For that reason, researchers must find a way to reduce the amount of catalyst used or try to find an alternative replacement [36]. At present, there are no commercial infrastructures in place for the generation, delivery and storage of hydrogen fuel, as mentioned in previous subchapters. Therefore, in order for the technology to become viable and an attractive alternative for consumers, infrastructures such as fuelling stations have to be put in place.

2.2 Membrane Separation Process & Technology Review

The petrochemical and food processing industries typically consume or produce a vast variety of chemicals (feedstocks or by-products) that would either needs separation, concentration or purification [40]. Hence, separation application in the field of chemical engineering is important. These typically include reagents and chemicals used in manufacture, purification of product, and removing of contaminants or recovery of valuable component from waste streams.

In the context of chemistry, separation process is generally a method of transforming or dividing a mixture of substances into individual or compositional based components. Most elements or compounds found in nature are normally in an impure state as a mixture of two or more elements. For that reason, it has to be separated from the unwanted product before used. A general example is that of crude oil which in its natural form contains a mixture of hydrocarbons and other toxic gases. Crude oil has to go through the separation process in order to produce the end products such as gasoline, diesel, jet fuel, lubricating oils and etc.

Presently, there are a wide variety of separation processes that are being utilized in the industry and they can be classified by the physical or chemical properties of the components to be separated. Table 2.3 shows some of the many separation process utilized.

Physical/Chemical Property	Separation Process
Size	Filtration, microfiltration, ultrafiltration, dialysis, gas separation, gel permeation chromatography
Vapour pressure	Distillation, membrane distillation
Freezing point	Crystallisation
Affinity	Extraction, adsorption, absorption, reverse osmosis, gas separation, pervaporation, affinity chromatography
Charge	Ion exchange, electrodialysis, electrophoresis, diffusion dialysis
Density	Centrifugation
Chemical nature	Complexation, carrier mediated transport

Table 2.3: Separation processes based on physical/chemical properties [40].

2.2.1 Separation Process

The choice of separation process is influenced by a number of important factors such as economics, technical feasibility, advantages and disadvantages of the process and the type of application. However, depending on the desired end product, a combination of two or more processes might be needed for separation. Although these conventional processes have performed well in the industries for a long time, there are still a number of challenges that need to be addressed and improved, and this is where the membrane process comes in [42]. Over the last few decades, membrane separation processes has been widely adopted because they are often more economically viable and energy efficient [43].

2.2.2 Membrane Separation Process

As a method of separation, membrane processes are still considered relatively new when compared to other more conventional methods. It was not considered as a technically important and feasible separation process until about 25 years ago and has since undergone rapid growth in a wide range of applications [40]. The demand for membrane materials in the US market alone is forecasted to increase by 8.2% to $4.3 billion in 2012, contributed by the advances of membrane applications into key markets such as water and wastewater treatment, food and beverage processing, pharmaceuticals and medical product, and chemical and industrial gas production [41].

The one common factor that links every membrane separation system is the physical arrangement of the processes in which a membrane is utilised to perform a particular separation [43]. A general definition widely used for membrane separation process is "*A membrane is as a selective barrier that separates two phases, which will either restricts or allows the movement of certain species because of their differences in physical, chemical or other properties, and thus leads to a separation of components*" [42].

Over the years, membrane technologies are more preferred and extensively used in separation for wide variety of mixtures due to their advantages over the conventional processes [45 - 46]. Some of these advantages are:

- Flexibility:
  Membrane units are modular in design, thus they are compact and require less space. Besides that, modules can be added either to increase output or achieving the desired separation.

- Cost efficient:
  In addition to their compact size, it also has less moving parts and low specific power consumption, which in return will reduce the overall production cost.

- Simplicity:
  Simple, easy to operate and low maintenance process.

- Feasibility:
  Energy efficient and also cost saving as the separation process takes place without phase transition and generally carried out in atmospheric conditions.

- Cleaner technology:
  Considered as a clean technology since it only require the use of relatively simple and non-harmful materials.

Nevertheless, the membrane separation is also associated with some drawbacks such as; fouling of the membranes, durability of the membrane materials and availability of suitable membranes for specific operations [45]. This has no doubt prevented a wider application of the membrane-based technology. Nonetheless, several main membrane separation processes currently being utilized within the industries include microfiltration, ultrafiltration, nanofiltration, reverse osmosis, electrodialysis, pervaporation and gas separation.

All separation process using membranes are usually classified under the general title of membrane processes; however the fundamental principles governing each individual process are different. To date, a variety of membrane separation processes have been developed for specific industrial applications and the principal characteristics and properties of these commercialized membrane processes are determined by the:

- main objective of separation
- types and structure of membrane
- physical phase of the feed and permeates
- driving forces
- mechanism of transport

Some of the more widely used processes in the industries are shown in table 2.4, while a detailed explanation of each processes of each processes can be found in reference 42.

Process	Principle	Industrial Applications
Microfiltration	Separation or organic and polymeric compounds with micropore ranges of 0.1-10 µm.	Removal of suspended solids, bacteria in pharmaceutical,and electronic industries
Ultrafiltration	Separation of water and microsolutes from macromolecules and colloids.	Removal of colloidal material from wastewater, food process streams
Reverse Osmosis	Passage of solvents through a dense membrane that is permeable to solvents but not solutes	Drinking water from sea, brackish or groundwater; production of ultra-pure water for electronics and pharmaceutical industries
Electrodialysis	Ions are transported through a membrane from one solution to another under the influence of an electrical potential.	De-ionized water from conductive spacers, recovery of organic acids from salt, heavy metal recovery
Gas Separation	Component of mixture of gaseous is removed through a pressure gradient	Removal of nitrogen from air, hydrogen from petrochemical/refinery vents, carbon dioxide from natural gas, propylene and VOC removal petrochemical vents
Pervaporation	Component of a mixture diffuses through, evaporates under a low pressure and is removed by vacuum	Dehydration of solvents, separation of azeotropic mixtures

Table 2.4: Brief summary of the main membrane separation processes and their applications [47].

2.2.3 Driving Forces for Membrane Processes

Transport through a membrane generally takes place when there is a presence of driving force acting on the components either in the feed or permeate side. In most cases, the permeation rate through the membrane is proportional to the driving force [42]. The driving forces are the differences in terms of:

1. Concentration gradients,
2. Electrochemical gradients,
3. Pressure gradients, or
4. Temperature gradients

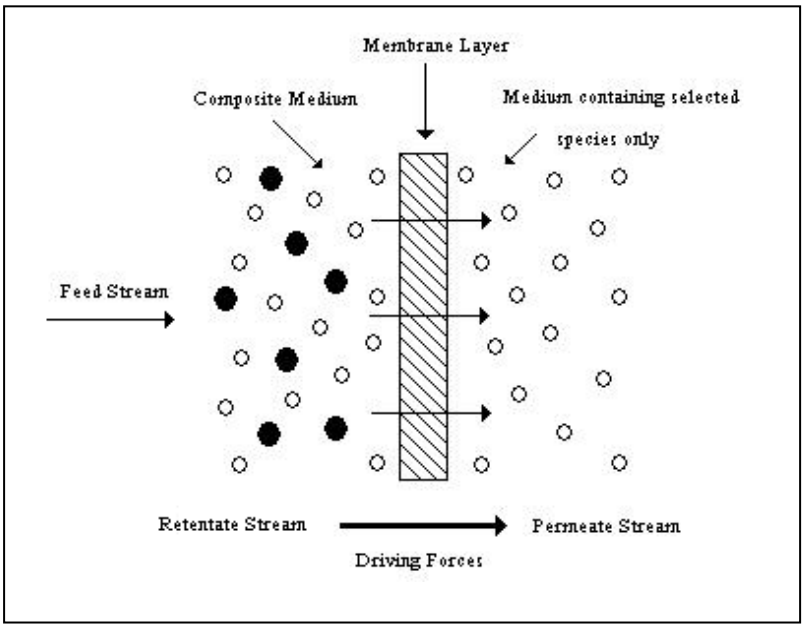

Figure 2.1: A simple diagram of a composite feed stream flowing past a membrane [42].

Figure 2.1 shows a simplified diagram of a composite feed stream containing a mixture of molecules flowing past a membrane based on size. The membrane layer then acts as barrier against the larger molecules, allowing only the smaller molecules to pass through it. The remaining feed stream is known as the retentate stream and the molecules that penetrate through the membrane is known as the permeate stream.

In addition to the molecule sizes, the physical and chemical structure of the membrane can also help to determine which driving force exist to separate the components, and hence determines which application will be most suitable for the membrane. Table 2.7 shows the driving forces for each membrane processes. Some of the membrane process will have more than one driving force which might affect the transport of molecules.

Driving forces	Membrane processes
Pressure difference	Microfiltration, Ultrafiltration, Nanofiltration, Reverse Osmosis
Concentration difference	Gas separation, Pervaporation, Dialysis, Diffusion dialysis
Temperature Difference	Membrane Distillation
Electrical Potential Difference	Electrodialysis

Table 2.5: Membrane processes and their driving forces [46].

2.2.4 Types of Membranes

Other than the driving forces, the membrane (structure and material) itself is the principal factor determining the selectivity and permeability, therefore it will also determine the most suitable type of application [42]. Progress made on material science over the years has enabled membranes to be produced using a variety of materials and with many different structures and properties [50]. This in turn has helped improve the performance and increase the amount of applications available for membrane separations.

Membranes are usually divided into different types and they are generally classified by two set of criteria. The initial classification is the nature or material used, whether it is natural or synthetic then whether it is organic or inorganic. Subsequently, they are further divided according to their configurations/structure such as porous/non-porous or symmetric/asymmetric. Figure 2.2 shows the simplified classification of membrane types.

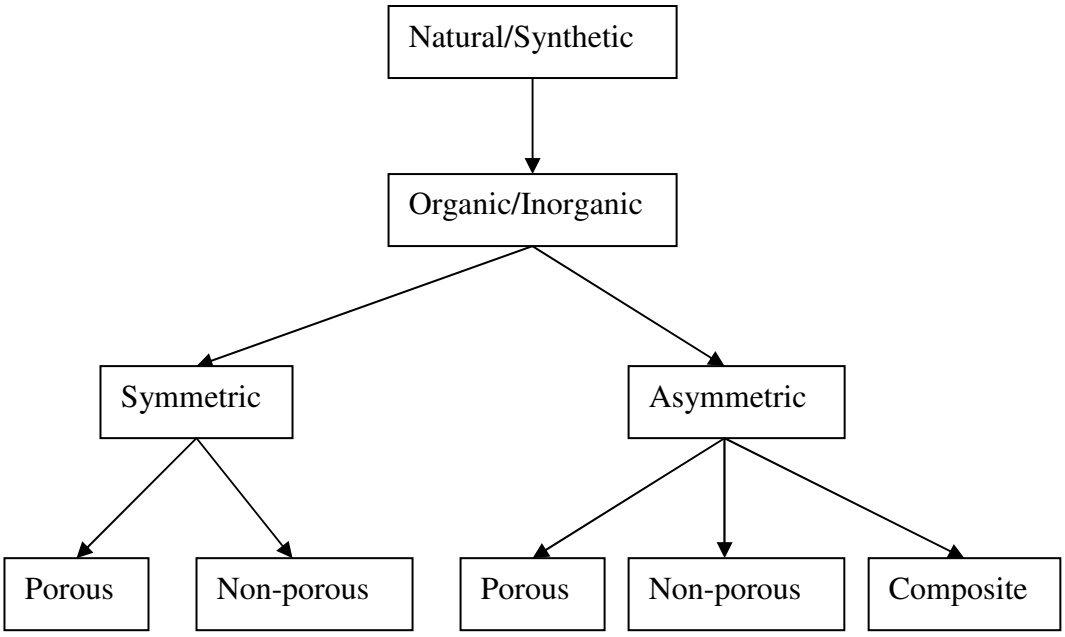

Figure 2.2: Simplified diagram of membrane classification.

There are two main structural configuration commonly found in membranes. These are symmetric or asymmetric configuration. Symmetric membranes are characterized by uniform structure and composition throughout the membrane, while asymmetric membranes are classified by non-uniform structures and composition.

A porous membrane is a highly permeable structure with randomly distributed interconnected network of pores, whereas the structure of a dense membrane are more compact or closely packed together making the structure difficult to penetrate [45].

Membranes are normally made as thin as possible because the resistance to mass transport is usually proportional to the thickness. The most common membrane configuration is a thin membrane layer on a mechanically strong support (porous support with dense or porous membrane on the top layer). These membranes are known as composite membranes (see figure 2.3). If the material used for the top layer is different from the support material, then it is known as asymmetric composite membrane [46].

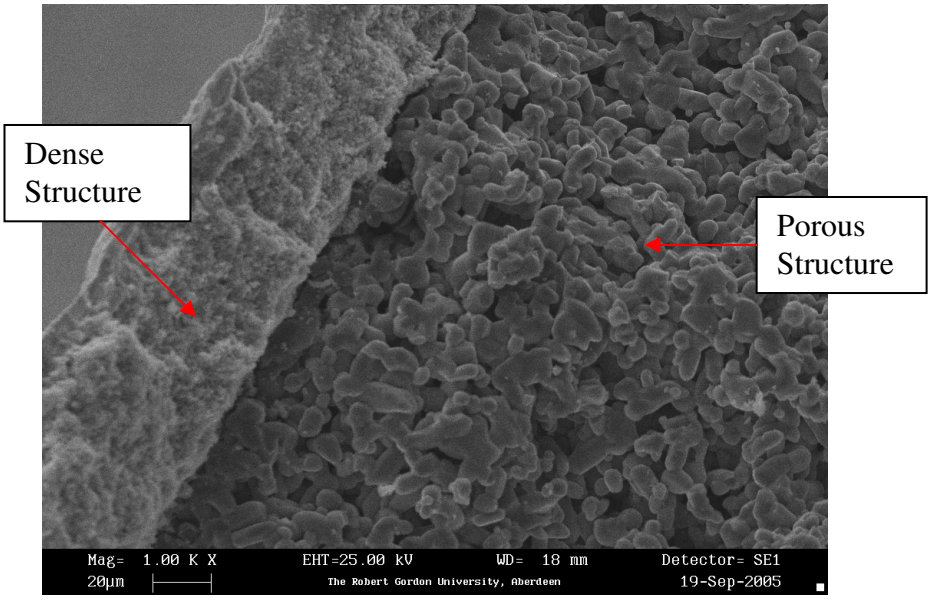

Figure 2.3: An example of a composite membrane (image obtained using the Scanning Electron Microscope).

2.2.5 Development of Membrane Gas Separation Process

In the context of this study which is focussed on membrane gas separation/purification, only the membrane gas separation process is detailed. More details on other membrane separation processes can be found in ref. 40 - 42.

The progress in the field of membrane gas separation has been growing progressively from the early basic concept of diffusion and permeation experiments in the 1800's by Thomas Graham and Fick, to industrially accepted products a century later [43 & 51]. Graham first observed the separation of gas mixtures by using a rubber membrane in the 1800's, but it was nearly a century later before commercial gas separation membranes became a reality [43].

Although there had been numerous early gas separation studies carried out, it was not until the pioneering work of Weller and Steiner that the potential of using polymeric membranes as a means of industrial gas separation was studied seriously [40]. Following the early studies on polymeric membranes, inorganic membranes were then developed for gas separation largely due to the need for separating gaseous Uranium isotopes in the 1940's to help the war effort [40]. However, due to its usage in military and nuclear applications, not much publicity was given during its early development.

By 1960, the elements of modern membrane science had developed sufficient knowledge on the relationships between structure and function in gas separation membranes. Unfortunately, the membranes at the time still suffered from problems such as low reliability, low selectivity and high fabrication cost [45, 50, 53].

Major milestone to the commercialisation came when Loeb-Sourirajan successfully developed an asymmetric reverse osmosis membrane [43]. The subsequent progress in the membrane science and technology was then concentrated on the development and refinement of these concepts. As a result, commercial processes for microfiltration, ultrafiltration and electrodialysis were all established [45, 51].

Further advances came with the development of composite membranes in the 1980's, and this had led to the production of membranes more suitable for commercial gas separation on a large scale and paved way for high performance reverse osmosis membranes [43]. Significant progress in every aspect of membrane technology was also made during this period including improvement in membrane processing, its chemical and physical structures, configurations and wider applications [45, 50].

By 1990s, the performance of polymeric membranes had reached its limit for many practical applications due to stability problems, low membrane efficiency with time caused by fouling, compaction, chemical degradation and thermal instability [50]. This has subsequently resulted in the shift toward the use of inorganic membranes to separate gas mixtures. Although the inorganic membranes are more costly, they offered the advantages of being more temperature and wear resistant, and most importantly being chemically inert. Subsequently, studies have since concentrated on the investigations of the separation properties of these membranes and their applications in membrane reactors [54].

Like polymeric membrane, inorganic membranes can either be porous or non-porous. Porous inorganic membranes are usually characterized by their high permeabilities but low selectivities and vice versa for the dense inorganic membrane. Therefore, composite membranes were produced in order to combine the high permeabilities of a porous membrane and high selectivities of a dense membrane by fabricating a thin layer of dense membrane on a porous support. An example used to illustrate this point would be the Palladium membrane used in this study.

2.2.6 Transport mechanisms for Gas Separation

The separation in membrane processes tends to take place through a variety of different transport mechanisms. The presence of any of these transport mechanisms is highly dependent on the physical and chemical properties of the membranes (ie. pore size, membrane material and structure, and pore size distribution) as well as the gases used (ie. molecular weight, affinity, and density of the gas). The type of transport through a membrane is generally categorized by the configuration or structure of the membrane used such as porous or non-porous as described in figure 2.4 below.

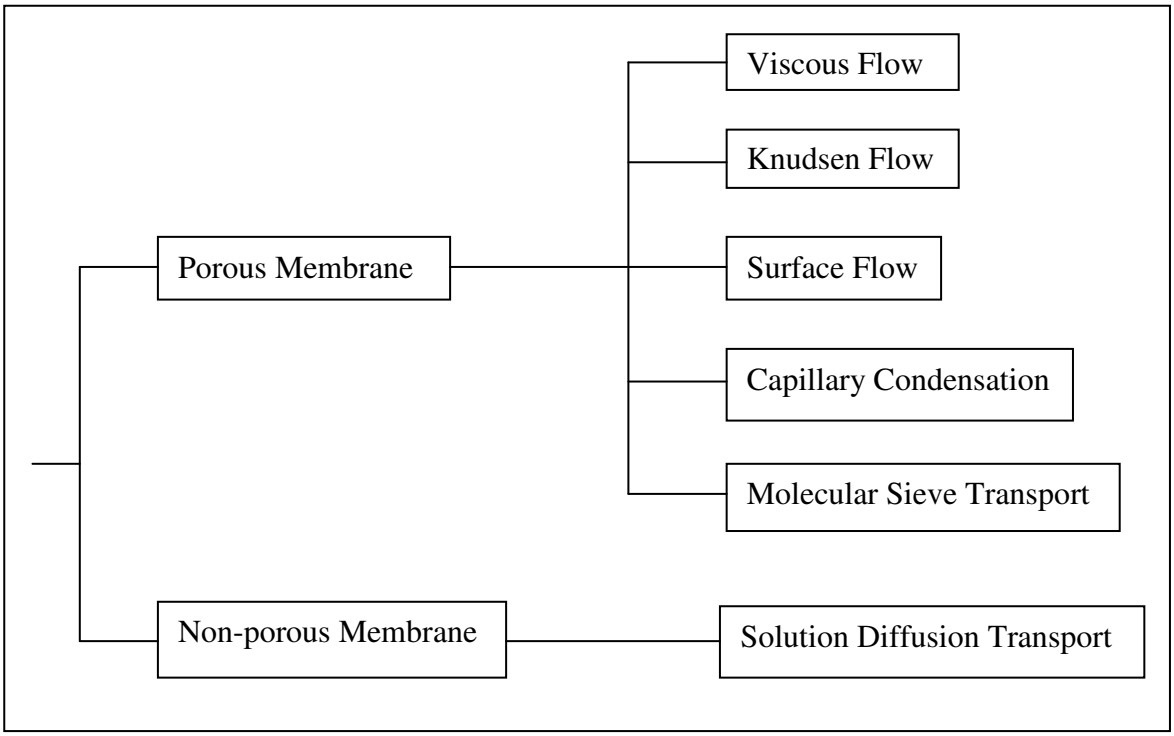

Figure 2.4: Diagram of membrane transport mechanisms associated with its structure.

2.2.6.1 Transport through Porous Membrane

The two predominant flow mechanisms that are usually present within a porous membrane are Knudsen or Viscous flow, and determination of which flow is in operation depends largely on both [40]:

- the pore radius of the membrane, and
- the mean free path of the gas molecules.

The mean free path is commonly expressed as the average distance travelled by the gas molecules between collisions of molecules [43].

Viscous flow prevails when the mean free path of the gas molecule is much smaller than the pore radius of the membrane (mean free path << pore radius). Under these conditions, the gas molecules collide more frequently with each other rather than with the walls of the membrane pores (see figure 2.5). Hence, the gases will flow easily through the pores, thus leaving very little or no gas separation.

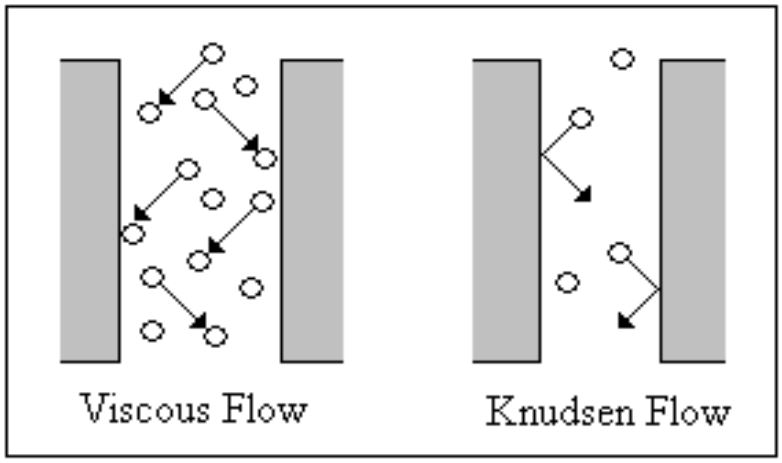

Figure 2.5: Schematic drawing showing Knudsen and Viscous Flow [42].

However, if the mean free path of the gas molecule is larger than the pore size of the membrane (mean free path >> pore radius), then Knudsen flow will predominate as the collisions of gas molecules with pore wall will be more frequent than collisions between gas molecules. As a result, the permeation will be lower and separation will be enhanced; since it will be harder for gases with larger molecular weight to pass through the membrane compared to the gases with smaller molecular weight. Hence, the separation of gas mixtures is achieved because gas species with different molecular weight will move at a different rate.

Surface flow/diffusion occurs when certain components within a gas mixture have a strong affinity (either chemically or physically) for the membrane surface (or material). The molecules will interact with the membrane, then adsorbs along the pore walls, and followed by diffusion across the pores [50]. Separation then occurs due to the permeability of the more adsorbed component from a mixture.

Capillary condensation is another form of surface diffusion, but with one of the components of the gas mixture now a condensable gas. At a certain pressure, the pores get filled by the condensed gas which will then evaporate at the permeate side; this will simultaneously prevent the flow of other gases through the pores [40] with the formation of a liquid layer [51].

Molecular sieving can occur if the pore size of the membrane is comparable to, or are in between those of the gas molecules to be separated [50]. If the membrane pore size is in between the smallest and largest molecules, then it will allow only smaller molecules to permeate while larger ones are retained from entering the pores. Thus, separation is achieved and the separation rate is dependent on the molecular shape and size, pore size, and interaction between the pore wall and gas molecules [51].

2.2.6.2 Transport through Non-porous Membrane

When the molecule size of the components within a gas mixture is more or less identical (eg. oxygen and nitrogen), the use of a porous membrane based on Knudsen mechanism will produce little or no separation and a non-porous membrane can be more useful [40]. The mechanism for transport through a non-porous membrane is different from that of a porous membrane and can be approximated by solution-diffusion mechanism.

The solution-diffusion mechanism is generally driven by the differences in the molecular interactions between the membrane material and the permeating species which will create a concentration difference between the upstream and downstream side. This will then lead the molecules to permeate and diffuse in the direction of the lower concentration.

In this mechanism, the permeants will dissolve in the membrane material and then diffuse through it, down the concentration gradient (from high to low concentration). The mechanism is commonly considered to occur in three steps [45, 51 - 52]:

1. Adsorption or absorption of gas molecules at membrane surface on the upstream side, followed by
2. Activated diffusion (solubility) of gas molecules through the membrane in the direction of lower concentration, and eventually
3. Evaporation or desorption of gas molecules on the other side of the membrane.

The rate determining factor which is the permeability coefficient (P) is considered to be a function of the product of solubility coefficient (S) and diffusion coefficient (D), as described by equation 1, where [40]:

$P = D \times S$ ..... Eq. 1

If the boundary condition on both side of the membrane is constantly maintained, then the diffusion of gas through the membrane can be described by Fick's First Law [52] as in equation 2 [48]:

$$J = -D\frac{dc}{dx}$$ ..... Eq. 2

Where: J = *Flux (rate of diffusion of the permeate gas per unit area)*

D = *Diffusion coefficient*

dc/dx = *Concentration gradient across the membrane*

Equation 2 can then be integrated to give the concentration decreases across the membrane [48].

$$J = \frac{D(c_r - c_p)}{l}$$ ..... Eq. 3

Where: c_r = *Retentate concentration on the upstream side of membrane*

c_p = *Permeant concentration on the downstream side of membrane*

l = *Membrane thickness*

The concentration of the permeating gas within a membrane cannot be measured; therefore the external pressure of the gas is used instead to express the concentration across the membrane. Thus, by using Henry's Law which states the linear relationship between the concentration inside the membrane and partial pressure of gas outside the membrane, the gas concentration can then be expressed as [43] described in equation 4 [48]:

$C = S \times p$ ..... Eq. 4

Where: S = *Solubility coefficient*

p = *partial pressure*

Substituting Eq. 4 into Eq. 3 gives [43]:

$$J = \frac{DS(p_r - p_p)}{l} \quad \text{..... Eq. 5}$$

Where: p_r = *partial pressure of the retentate side*

P_p = *partial pressure of the permeant side*

Then, by substituting Eq. 1 into Eq.5, we have [43]:

$$J = \frac{P(p_r - p_p)}{l} = P\frac{\Delta p}{l} \quad \text{..... Eq. 6}$$

Where: P = *Permeability coefficient*

Δp = *Difference in partial pressure*

Finally, the separating ability or selectivity (α) of a membrane can be defined by using the ratio of individual gas permeabilities. The equation can be written based on single gas permeability of species A and B [43]:

$$\alpha_{A/B} = \frac{P_A}{P_B} = \frac{D_A \times S_A}{D_B \times S_B} \quad \text{..... Eq. 7}$$

2.3 Palladium Based Membrane Review

Palladium (Pd) based membranes have long been widely used for the purpose of hydrogen gas separation and purification due to high hydrogen permeability and selectivity [54-64]. Due to the market demand for hydrogen in recent years in the petroleum refining, petrochemical industries, in semiconductor processing, and fuel cell applications, there is currently a renewed and growing interest in Pd based membranes [54]. Besides that, Pd based membranes are now used in a variety of processes such as membrane reactors for hydrogen related reactions including hydrogenations, dehydrogenations and methane reforming [55].

Nevertheless, a practical limit in the use of these membranes is restricted by the high cost of precious metal. In the early days of research and applications, bulk Pd and Pd-alloy film of high thickness (50 - 200 µm) were used in order to achieve the mechanical strength required to withstand the pressure differentials of up to 15 bars during operation [55-56]. However, since hydrogen flux is inversely proportional to thickness, the technology is prone to two limitation namely low hydrogen permeability and high cost of Pd metal [56].

Hence, film thickness is the main factor which controls the membrane performance and cost. These limitations have provided incentives and motivation toward more research and development of thinner Pd membranes. A variety of techniques have since been studied and research conducted to reduce the amount of Pd metal used [59]. Current development of Pd membranes are mostly composite based in which the Pd or Pd-alloy is deposited as a thin film onto a porous support [54-56, 58-60, 63-64, 68-69]. The more commonly used supports being ceramic and stainless steel porous supports.

2.3.1 Palladium and Palladium-Alloy Composite Membrane

The successful industrial application of Pd membranes depends largely on the ability to produce them cost effectively, at the same time having high H_2 permeability, good mechanical strength and thermal properties [55]. The optimal thickness of Pd film in a composite membrane will depend on a number of factors such as:

- method of fabrication,
- mechanical stability of the layer,
- dense Pd film formation,
- surface defects of the support, and
- the type and quality of support used.

Therefore, in the subsequent phase of research, development and applications, has concentrated on the preparation and utilisation of composite membranes due to the fact that successful deposition of thin Pd layer has the potential to overcome the limitation of using higher thickness [55, 58, 68].

These composite membranes (consisting of a thin Pd or Pd-alloy layer on a porous support) provide the membrane with high hydrogen permeability and selectivity without compromising its mechanical strength. This will then significantly reduce its fabrication cost. Porous inorganic support such as Vycor glass, ceramic and stainless steel are commonly used for this purpose. In addition, recent improvements in membrane fabrication have created new opportunities for preparing thinner supported Pd metal films of 4 – 15 μm [58].

However, very thin Pd composite membranes are associated with the major drawback of hydrogen embrittlement and cracking. Hydrogen embrittlement is a phenomenon in which dissolved hydrogen tends to cause lattice expansions in the metal on repeated pressure and temperature cycling, which will eventually cause it to rupture [60]. Therefore pure Pd membranes cannot be used below 250 - 300 ^{0}C. In addition, the membrane is prone to deactivation by carbon compounds at temperatures above 450 ^{0}C and will suffer irreversible poisoning (Pd catalyst cannot be regenerated) in the presence of sulphur compounds [61].

These issues can be reduced or addressed by alloying Pd with group 1b metals [62]. Besides that, Pd is also a very expensive metal and by alloying it with other metal, would help reduce the amount of Pd needed thus reducing the cost of production. The more commonly used metallic elements for alloying with Pd are silver (Ag), gold (Au), copper (Cu), iron (Fe), nickel (Ni), platinum (Pt) and yttrium (Y) [61].

2.3.2 Membrane Support

As mentioned earlier, dense thick membranes are characteristically associated with low permeability but with high selectivity. The high selectivity being associated with the absence of any pinholes. Although permeability can be increased by reducing the thickness of the Pd metal, there is a critical thickness below which the mechanical strength begins to be affected. In order to improve its permeability while maintaining the high selectivity and structural integrity, thin Pd or Pd-alloy layer are usually deposited on the outer surface or inside the pores of a porous support. The new configuration is then known as composite membrane.

2.3.2.1 Inorganic support

Porous inorganic supports are typically utilised for gas separation purposes due to their thermal stability, mechanical strength and chemically inertness. Furthermore, the surface of the support also has to be smooth and defect free [61]. Uemiya [64] reported that the quality of the support used such as the pore size distribution and defects on the surface will have an influence on the minimum thickness of the Pd layer.

Among the inorganic supports, non-metals such as ceramic and glass are usually associated with weak adhesion to the deposited metallic thin film. Besides that, different thermal expansion coefficients between the materials during operation may cause stability problems [63]. Thermal cycling and hydrogen loading during operation at temperature will cause the Pd layer to expand/elongate at different rate with respect to the ceramic support, and this increases stress to the adhesion layer and will eventually cause it to rupture or peel off [59]. On the other hand, porous stainless steel support also has its share of problems at high temperature with atomic inter-diffusion of metals between thin Pd/Pd-alloy layer and the support (e.g. stainless steel components).

2.3.3 Pd Based Membrane Fabrication Method

Recently, much effort has been focussed in preparing not only thinner, but also pinhole or defect free membranes with high permeability and selectivity for hydrogen from a variety of methods. Amongst them, the more common and widespread use methods are magnetron sputtering, electroless plating and chemical vapour deposition.

2.3.3.1 Magnetron Sputtering

Magnetron sputtering is a very powerful and flexible technique which can be used to coat any type of support with a wide range of materials and a variety of compounds [65] and is usually used for thin film deposition. Sputtering is a physical process whereby atoms in a solid target material (Pd) are evicted into the gas phase due to bombardment by energetic ion [64]. The process can be summarised as the ion striking a large cluster of closed-packed atoms and the rate of deposition is largely driven by the energetic ion collision with the target atoms [67]. One major drawback is the process is unable to deposit long or large supports due to the facts that a vacuum has to be created during deposition.

The sputtering process takes place in a vacuum chamber which contains the target of material to be sputtered and the support for deposition (see figure 2.6). For this case, the target material is Pd metal and the support is ceramic. The Pd metal is maintained at a negative potential and, when Argon is introduced into the chamber, it will be ionized into positively charged atoms. The positive ion will subsequently accelerate toward the negative charge metal and hitting it with enough energy to remove the material. The materials that are removed will then settle on the support.

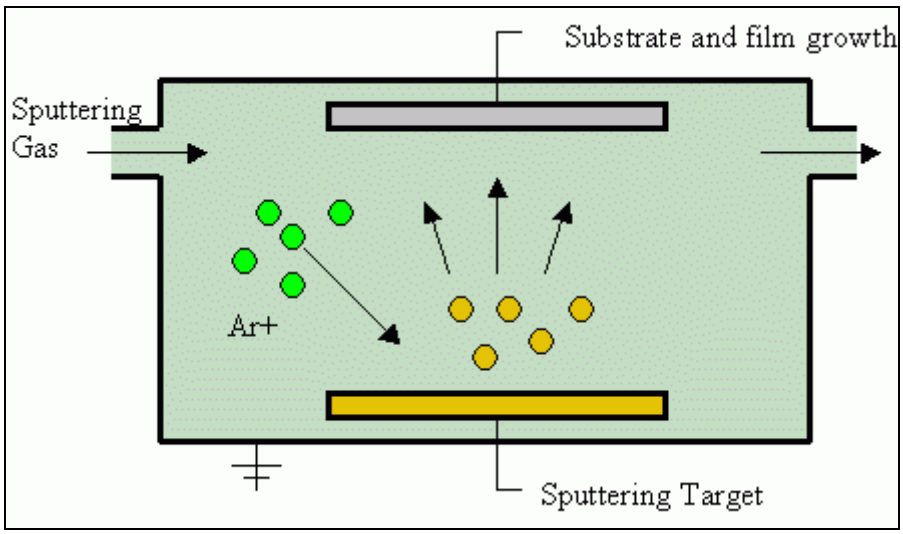

Figure 2.6: Schematic drawing of a sputtering process (taken from ref. 56).

2.3.3.2 Chemical Vapour Deposition (CVD)

CVD is a chemical process often used in the semiconductor industry for the deposition of thin film of various materials. In this process the support is exposed to one or more volatile precursors which will react and/or decompose on the support surface to produce the desired deposit [70]. In this process, the precursor gases (often diluted in carrier gases) are delivered into the reaction chamber at ambient temperature. As they pass over or come into contact with a heated substrate, they react or decompose forming a solid phase and are deposited onto the support [71].

In the case of Pd metal deposition, a chemical reaction associated with the generation of the palladium vapour will occur at high temperature. The vapour is then condensed on the support to obtain the dense palladium film. The deposition apparatus consists of a central reactor, hydrogen and metal chloride vapour delivery system and vacuum system as shown in figure 2.7.

Palladium chloride vapour generated by heating the solid was carried by N_2 stream towards the face of the support while a H_2/N_2 mixture is introduced from the other side (to control vacuum pressure). The deposition can then be started or stopped by adjusting the hydrogen feed into the reactor (more detailed information about CVD process can be found in reference 72).

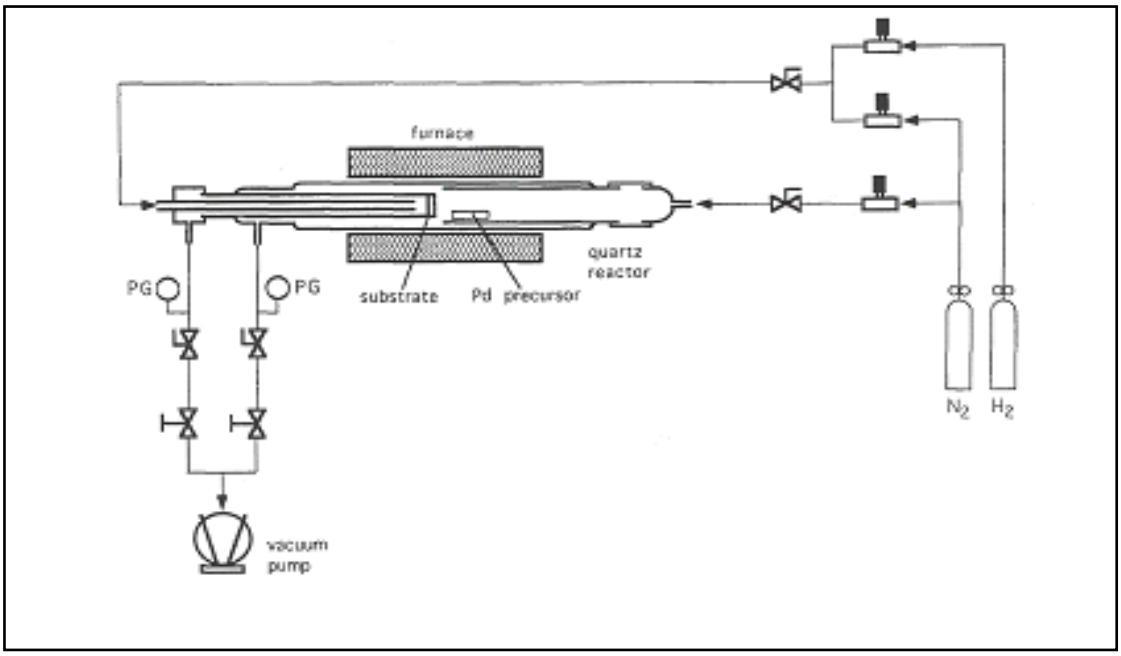

Figure 2.7: Schematic drawing of a chemical vapour deposition process (taken from ref. 61).

2.3.3.3 Electroless Plating (ELP)

Electroless plating is a method that involves deposition of metals on a catalytic surface from solution without an external source of current (Pd ions present in a solution are transfered to the surface of the support as palladium metal). Since it allows the metal ion concentration to cover all parts of the substrate, it deposits metal evenly along edges, inside holes, and over irregularly shaped objects which are often difficult to plate evenly with electroplating and other methods [73].

The electroless plating technique comprises of three steps, namely sensitization, activation and finally the actual plating [74]. Sensitization step is performed to sensitize the support surface initially with tin ions, while activation step involves the displacement and replacement of tin ions on the support surface with Pd nuclei. These steps are crucial for the initiation of electroless plating of Pd on the membrane surface. Sensitization and activation processes have to be performed in a cyclic fashion for a number of times in order to obtain a fully activated membrane support. Figure 4.3 shows the schematic drawing of the electroless plating process.

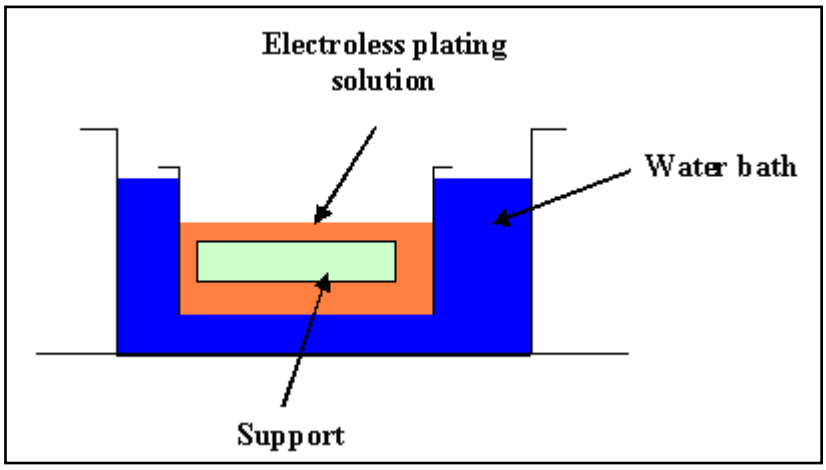

Figure 2.8: Schematic drawing of the electroless plating process.

Subsequently, the porous support that has been uniformly activated with Pd nuclei is then subjected to plating in a tank filled with plating solution for a set period of time (e.g. 30 mins or 60 mins). The tank is placed/heated in a water bath for controlled/constant plating temperature. The plating step is also repeated a few times depending on the film thickness required.

The rate of metal deposition is slower compared to other methods but, the main advantage of using this method is that the process is equally effective, inexpensive and far simpler to set-up compared to other methods. However, a major drawback with the existing electroless plating technique is the inability to control the rate of deposition of the metal onto the substrate. Therefore, advanced technique are required if this process is to be commercialized.

2.3.4 Review of Pd-based Membrane Applications

Collins and Way [75] presented a detailed fabrication procedure for Pd composite membrane. For the first time, the authors have indicated in their work, a factor termed as plating surface area. It is defined as the membrane surface area that is exposed to the quantity of plating solution used. The authors used asymmetric alumina supports with skin layer pore size varying from 10 nm to 200 nm. The bath composition constituted $PdCl_2$ of about 5.4 g/l and eight successive depositions for one hour each were conducted. The Pd metal plated was at a rate of about 2 – 2.5 microns/hour under those conditions.

The membrane thickness obtained varied from 11.4 – 20 microns on the composite supports resulting in a hydrogen permeability of about 3.23 x 10^{-9} mol.m/m^2.s.$Pa^{0.62}$. The H_2/N_2 selectivity of the membrane was about 380 at 823 K. Although the membrane has a high selectivity toward H_2, it is at the expense of H_2 flux due to its thickness. However, conventional electroless plating is known to have difficulties in fabricating thinner defect free Pd membranes.

Li et. al. [76] claimed fabrication of defect free Pd composites using osmosis technique for repairing the original membranes prepared using conventional plating method. The plating solution composition corresponded to about 4 g/l of tetraammonium palladium chloride, $(NH_4)_4.PdCl_2$. Asymmetric porous supports with the skin layer pore size of about 160 nm were used for the fabrication. The original membrane produced using the conventional method was then repaired using osmosis process with the circulation of 3M NaCl solution through the bore of the membrane tube during electroless plating.

The original deposition time was 7 hours which was extended to a total of 25 hours (18 hours for osmosis) after the repairing process. The original H_2/N_2 selectivity of the membrane was about 10, which increased to a value of about 970 after repairing and the corresponding membrane thickness of 10.3 microns. Here, the authors have improved the membrane performance by repairing it osmosis after electroless plating to reduce the amount of pinholes. However, osmosis is a very slow process (which has shown by the authors) and it takes 18 hours to repair the membrane. At the same time, it will also indirectly increase the overall thickness of the deposited Pd layer

Hollein et. al. [77] prepared Pd composite membranes using both stainless steel and alumina supports with the average skin layer pore size of about 500 nm and 100 nm respectively. The composition of the plating solution used was about 5 g/l of $PdCl_2$. Defect free films have been synthesized by having a minimum film thickness of about 3 microns. However, these membranes offered pinholes during performance at higher temperatures and a film thickness of about 7 microns or more is observed to provide a better separation factor (100 – 1000 for H_2/N_2 system). Although both membranes showed good performance, the membrane produced with electroless plating has to be well above 7 microns in order to obtain a satisfactory separation factor. The final membrane has a thickness of 14 microns.

Souleimanova et. al. [78] prepared dense Pd membranes using vycor glass supports with skin layer pore size of about 4 nm. The authors have concluded that the use of osmosis allows for the preparation of a thinner and dense Pd films in a shorter period of time. The plating time is shown by the authors to have reduced from 8 hours (for conventional plating) to 3.5 hours with the use of 9M sucrose solution. The authors argued that the metal penetrates much deeper into the pores of the support during electroless plating under osmosis compared to the conventional plating, thus enhancing interaction between film and support.

The authors also successfully reduce the amount of plating time by coupling the osmosis technique with electroless plating. However, the use of salt will sometime present another set of problem during drying of the membrane. During osmosis, some salt will eventually occupied the pinholes of the membrane and it would have been very difficult to remove all the salt solution before drying it. Therefore, the trapped salt can cause additional stresses during the evaporation of water, which will eventually crack the Pd layer

Mardilovch et. al. [79-80] studied the permeation characteristics of electroless plated Pd composite membranes prepared using 316 L sintered stainless steel supports with the average skin layer pore size of about 100, 200 and 500 nm respectively. Mercury intrusion experiments were conducted by the authors to evaluate the actual pore size distribution of these supports. It was observed that the maximum pore size of the supports were about 4 – 5 microns (100 nm skin layer), 6 – 7 microns (200 nm skin layer) and 11 – 12 microns (500 nm skin layer).

From their research findings, the authors concluded that the thickness of the palladium film should be at least three times the maximum pore size of the supports in order to exhibit hydrogen permeation according to Sieverts law (suggesting the formation of a dense palladium film). However, no selectivity values have been presented with respect to permeation of other gases in these research findings.

Roa et. al. [81] have fabricated Pd-Cu composite membranes on different types of supports with the average skin layer pore size of about 200 nm (symmetric alumina), 50 nm (asymmetric zirconia) and 5 nm (asymmetric alumina). The composition of $PdCl_2$ electroless bath was about 5.45 g/l and copper bath was about 6.225 g/l $CuSO_4.5H_2O$. The plating time was not provided by the authors. The authors obtain the following set of permeation characterstics:

Membrane	Support	H_2/N_2 Selectivity
27.6 µm thick Pd(72%)-Cu	200 nm symmetric alumina	14 at 723 K, 6.895 bar pressure differential
11 µm thick Pd(80%)-Cu	200 nm symmetric alumina	270 at 723 K, 3.447 bar pressure differential
12 µm thick Pd(91%)-Cu	50 nm asymmetric zirconia	1400 at 723 K, 3.447 bar pressure differential
1.5 µm thick Pd(70%)-Cu	50 nm asymmetric zirconia	47 at 723 K, 3.447 bar pressure differential
10 µm thick Pd film	5 nm asymmetric alumina	Very high N_2 flow rate, even at room temperature

Table 2.8: Permeation results and membrane characteristics obtained by the authors [81].

The authors finally concluded that asymmetric supports with smaller skin layer pore sizes (between 5 – 50 nm) were ideal for deposition of thin palladium films that can offer membranes with good selectivity at high temperatures.

Huang et al. [82] fabricated Pd membranes on alumina supports with an average skin layer pore size of about 190 nm and 10 nm. The authors used a $PdCl_2$ composition of 0.297 g/l with a plating surface area factor of about 60 cm^2/l and conducted the plating at 333 K. The thickness of the Pd-Ag metal deposited after 8 hours is evaluated to be about 20 microns. The H_2/N_2 separation factor is evaluated and varied from 30 – 178 for a temperature variation of about 473 – 616 K and pressure differential of about 0.8 – 2.5 bar. The authors concluded that the membrane has some pinholes on the skin layer and thus, provided a low selectivity.

D. A. P. Tanaka et al. [83] fabricated Pd-alloy membrane on a porous tube by simultaneous deposition of Pd and Ag (silver) using electroless plating. The authors used a 99.99% pure α-alumina tube with the average pore size of 150 nm and outer diameter of 2.0 mm and internal diameter of 1.6 mm. Electroless plating is then carried out (with plating solution containing a 9:1 ratio of Pd acetate to silver nitrate) and the solution stirred magnetically to homogenize the solution. The membrane produced is then heat treated with flowing hydrogen at 500 ^{0}C for 4 hours resulting in the formation of a Pd-Ag layer with a thickness of 5.12 μm.

From the permeation tests and analysis conducted, the authors concluded that the use of palladium acetate in the plating solution instead of the more commonly used palladium chloride can eliminate tin contamination during the activation stage and simultaneously also enhance the plating rate of Pd. Besides that, careful control of the chemical composition of the plating solution against the given amount of Pd and Ag can realize the simultaneous deposition of the two metals.

P. M. Thoen et al. [84] fabricated Pd-Cu composite membrane using sequential electroless plating of Pd and Cu on a 20 nm pore sizes zirconia coated α-alumina tubes. The thickness of the Pd-Cu layer is reported to be about 1.3 µm consisting of 95% Pd and 5% Cu. The thin membrane layer translate to a significant step change in mass transfer reduction and cost saving. This was done by modifying the chemical composition of the plating solution. The authors removed EDTA (Disodium salt hydrate) from the plating solution in order to reduce or eliminate carbon contamination during plating, and concluded that the membrane fabricated using the new plating solution exhibit higher hydrogen permeability than those fabricated using conventional plating solution containing EDTA. They have concluded that membrane fabricated using the new plating solution exhibit higher hydrogen permeability than those fabricated using conventional plating solution containing EDTA

Yan Huang et al. [85] studied the effect of coating thin composite palladium membranes on supports with rough surfaces. The supports used were made of SS310L with an outer diameter of 10 mm and inner diameter of 6 mm with average top layer pore size of 500 nm (asymmetric structure with finer pores on the outside surface). The supports are then coated with a porous layer of yttria-stabilized zirconia (YSZ) to serve as a layer to prevent against intermetallic diffusion. Three membranes were then produced using:

- Magnetron sputtering – did not manage to produce a dense film
- Atmospheric plasma spraying – produce a relatively thick film but contain pinholes
- Electroless plating – produce the densest layer but a rather thick layer was required to reduce the defects

The authors concluded that a defect free thin membrane layer can be produced by modifying the activation method, instead of using the conventional sensitization and activation pre-treatment of supports. The activation can be performed by using metal organic chemical vapour deposition of palladium. The resulting membrane showed a significantly higher selectivity but at the same time, it lowers the hydrogen permeability. However, the authors did point out that further researches are still required to confirm the effects of modification.

D. Pizzi et al. [86] received a Pd-Cu membrane (Cu 20 wt%) on an asymmetric porous ceramic support from NGK Insulators Ltd., Nagoya, Japan for their work. The support used is alumina with average top layer pore sizes of 100 nm and the Pd-Cu layer is reported to be about 2.5 µm thick. Pd was deposited by electroless plating onto the support, and then Ag (silver) is layered on by electroplating using the Pd layer as electrode. The membrane is then subjected to permeation tests at 300, 400 and 500 ^{0}C with trans-membrane pressure of between 0.2 – 6 bars using:

- Pure H_2 and N_2
- H_2/N_2 mixture
- H_2/CO mixture

The membranes showed high selectivity for H_2 with respect to N_2 and CO, which indicate that the alloy layer formed is free from pin holes and is also defect free. The authors also reported that a significant decrease in permeability was observed when nitrogen mixture were used and concluded that was due to the non-negligible transport resistances in the gas phase. Furthermore, CO poisoning was also observed with feed gas containing 12% CO with the significant decrease in H_2 permeability, 75% lower than the value observed using N_2 mixture. However, the effect of poisoning was found to be reversible after flowing air at 400 ^{0}C.

2.4 References:

1. University of Birmingham. **The Hydrogen Economy**. Available from: http://www.fuelcells.bham.ac.uk/documents/Hydrogen_and_Fuel_Cell_-_The_University_of_Birmingham.pdf [Accessed 03 August 2010].
2. The National Hydrogen Association. **The Hydrogen Economy**, Fact Sheet Series. Available from: http://www.hydrogenassociation.org/general/factSheets.asp [Accessed 03 August 2010].
3. International Energy Agency**. Moving To A Hydrogen Economy: Dreams And Realities**, *Standing Group on Long-Term Co-Operation, IEA/SLT (2003)5.*
4. LOVINS, AMORY, ADAMS and ELAINE. **Hydrogen: The Future of Energy**, *Rocky Mountain Institute*. Available from: http://www.rmi.org/rmi/Library/E03-15_HydrogenFutureEnergy [Accessed 03 August 2010].
5. PHILIP TSENG, JOHN LEE and PAUL FRILEY, 2005. **Hydrogen Economy: Opportunities and Challenges**, *The International Journal of Energy, Volume 30, Issue 14, (November 2005), International Energy Workshop, pg 2703-2720.*
6. The National Hydrogen Association. **Hydrogen's Properties**, The Basics. Available from: http://www.hydrogenassociation.org/general/basics.asp [Accessed 03 August 2010].
7. Hydrogen Storage Research Network. **Hydrogen Energy Technologies**. Available from: http://www.imr.salford.ac.uk/hytrain/energy/index.html [Accessed 03 August 2010].
8. Air Products. **Hydrogen Safety Data Sheet**, MSDS No. 300000000074. Available from: https://apdirect.airproducts.com/msds/DisplayPDF.aspx?docid=68763 [Accessed 03 August 2010].
9. The National Hydrogen Association. **The Hydrogen Production Overview**, *Fact Sheet Series.* Available from: http://www.hydrogenassociation.org/general/factSheets.asp [Accessed 03 August 2010].
10. TRYGVE RISS, ELISABET F. HAGEN, PREBEN J. S. VIE and OYSTEIN ULLEBERG, 2005. **Hydrogen Production – Gaps and Priorities**, *Hydrogen*

Implementing Agreement, International Energy Agency. Available from: http://www.ieahia.org/page.php?s=d&p=special [Accessed 03 August 2010].

11. KATHLEEN MCHUGH, 2005. **Hydrogen Production Methods**, *MPR Associates, Inc*.
12. US Department of Energy (DOE). **Natural Gas Reforming – How Does it Work?** *Hydrogen, Fuel Cells & Infrastructure Technologies Program, Energy Efficiency and Renewable Energy (EERE).* Available from: http://www1.eere.energy.gov/hydrogenandfuelcells/production/natural_gas.html [Accessed 03 August 2010].
13. National Renewable Energy Laboratory. **Hydrogen Production and Delivery**, *Hydrogen and Fuel Cells Research*. Available from: http://www.nrel.gov/hydrogen/proj_production_delivery.html [Accessed 03 August 2010].
14. US Department of Energy (DOE). **Hydrogen Production**. *Hydrogen Program*. Available from: http://www.hydrogen.energy.gov/pdfs/doe_h2_production.pdf [Accessed 03 August 2010].
15. US Department of Energy (DOE). **High-Temperature Water Splitting**. *Hydrogen Production*, *Hydrogen, Fuel Cells & Infrastructure Technologies Program, Energy Efficiency and Renewable Energy (EERE).* Available from: http://www1.eere.energy.gov/hydrogenandfuelcells/production/water_splitting.html [Accessed 03 August 2010].
16. US Department of Energy (DOE). **Photo-chemical Water Splitting.** *Hydrogen Production*, *Hydrogen, Fuel Cells & Infrastructure Technologies Program, Energy Efficiency and Renewable Energy (EERE).* Available from: http://www1.eere.energy.gov/hydrogenandfuelcells/production/photoelectrochemical.html [Accessed 03 August 2010].
17. JAMES A. RITTER, ARMIN D. EBNER, JUN WANG and RAGAIY ZIDAN, Sept 2003. **Implementing a Hydrogen Economy**, *Materials Today, 6(9),* pg 18-23.
18. US Department of Energy (DOE). **Photobiological Water Splitting**. *Hydrogen Production*, *Hydrogen, Fuel Cells & Infrastructure Technologies Program, Energy Efficiency and Renewable Energy (EERE).* Available from:

http://www1.eere.energy.gov/hydrogenandfuelcells/production/photobiological.html [Accessed 12 August 2010].

19. Agriculture and Consumer Protection Department. **Chapter 5 – Hydrogen Production**. *Renewable Biological Systems for Alternative Sustainable Energy Production, Food and Agriculture Organization of the United Nations (FAO) Corporate Document Repository*. Available from: http://www.fao.org/docrep/w7241e/w7241e0g.htm [Accessed 12 August 2010].
20. CAROLYN C. ELAM, CATHERINE E. GREGOIRE PADRO, Gary SANDROCK, ANDREAS LUZZI, PETER LINBALD and ELISABET F. HAGEN, 2003. **Realizing The Hydrogen Future: The International Energy Agency's Effort To Advance Hydrogen Energy Technologies**, *International Journal of Hydrogen Energy 28*, pg 601-607.
21. University of Strathclyde, Glasgow. **Hydrogen Storage**. Available from: http://www.esru.strath.ac.uk/EandE/Web_sites/99-00/hybrid_PV_FC/hydrogenstorage.html [Accessed 03 August 2010].
22. Wired Digital, Inc. **How Hydrogen Can Save America**. *On Newsstand Now, Issue 11.04 (Apr 2003).* Available from: http://www.wired.com/wired/archive/11.04/hydrogen.html [Accessed 03 August 2010].
23. University of Birmingham. **Hydrogen Storage and Purification Research Metallurgy and Materials**. http://www.ierp.bham.ac.uk/documents/res_MMH2.pdf [Accessed 03 August 2010].
24. HydrogenTrade.com. **Hydrogen Distribution**. Available from: http://www.hydrogentrade.com/distribution/ [Accessed 03 August 2010].
25. US Department of Energy (DOE). **Hydrogen Distribution and Delivery Infrastructure**, Oct 2006. *Hydrogen Program.* Available from: http://www1.eere.energy.gov/hydrogenandfuelcells/pdfs/doe_h2_delivery.pdf [Accessed 03 August 2010].
26. CLEFS CEA (French Atomic Energy Commission). **Challenges of a Hydrogen Distribution Infrastructure**. *The Hydrogen Pathway,* No. 50/51, winter 2004-2005. Available from:

http://www.cea.fr/var/cea/storage/static/gb/library/Clefs50/pdf/052a055hagen-gb.pdf [Accessed 03 August 2010].

27. Roads2HyCom. **Hydrogen Transport by Pipelines**. Available from: http://www.ika.rwth-aachen.de/r2h/index.php/Hydrogen_Transport_by_Pipeline [Accessed 03 August 2010].
28. ROBERT K. DIXON, 2005. **Advancing Towards a Hydrogen Energy Economy: Status, Opportunities and Barriers**, *US Department of Energy (DOE), USA*. DOI: 10.1007/s11027-006-2328-0.
29. A. BAYANO, A. FERNANDEZ, and P. DE LA VEGA, 2009. **Hydrogen Internal Combustion Engine for Stationary Applications**, *Journal of Applied Energy*, DOI: 10.1016/j.apenergy.2009.01.007.
30. MUSTAFA BALAT, 2008. **Potential Importance of Hydrogen As A Future Solution to Environmental and Transportation Problems**, *International Journal of Hydrogen Energy 33*, pg. 4013-4029.
31. **The Hydrogen Economy: Opportunities, Costs, Barriers and R&D Needs**, *National Academy of Engineering, Board on Energy and Environmental Systems*, (2004), ISBN – 10: 0-309-09163-2. Available from: http://positiontoknow.com/S-11/doc/www.house.gov/science/hearings/full04/mar03/ramage.pdf [Accessed 03 August 2010].
32. U.S. Climate Change Technology Program. **Chapter 2.2.5: Hydrogen Use,** *Technology Options for the Near and Long Term*, Nov 2003, pg. 79-81. Available from: http://www.climatetechnology.gov/library/2003/tech-options/tech-options-2-2-5.pdf [Accessed 03 August 2010].
33. CORNELIA R. KARGER, and RICHARD BONGARTZ, 2008. **External Determinants for the Adoption of Stationary Fuel Cells – Infrastructure and Policy Issues**, *Journal of Energy Policy 36*, pg. 798-810.
34. FuelCellStore.com. **Fuel Cell Education**. Available from: http://www.fuelcellstore.com/education.asp [Accessed 03 August 2010].
35. KARIM NICE and JONATHAN STRICKLAND. **Introduction To How Fuel Cells Work**. *Alternative Fuel, HowStuffWorks, Inc*. Available from: http://www.howstuffworks.com/fuel-cell.htm [Accessed 03 August 2010].
36. NIGEL BRANDON and DAVID HART, July 1999. **An Introduction to Fuel Cell Technology and Economics**, *Occasional Paper 1*, *Centre For Energy*

Policy And Technology, Imperial College Of Science, Technology And Medicine, London.

37. Smithsonian Institution. **What Is A Fuel Cell?** *Fuel Cell Basics. National Museum of American History*. Available from: http://americanhistory.si.edu/fuelcells/basics.htm [Accessed 03 August 2010].
38. Fuel Cell Today.com. **The Technology**. *Education Kit, General Fuel Cell Information.* Available from: http://www.fuelcelltoday.com/media/pdf/education-kit/The-Technology.pdf [Accessed 03 August 2010].
39. US Department of Energy (DOE). **Comparison of Fuel Cell Technologies**. *Types of fuel Cells*, *Hydrogen, Fuel Cells & Infrastructure Technologies Program, Energy Efficiency and Renewable Energy (EERE).* Available from: http://www1.eere.energy.gov/hydrogenandfuelcells/fuelcells/pdfs/fc_comparison_chart.pdf [Accessed 03 August 2010].
40. KEITH SCOTT and RONALD HUGHES, 1996. **Industrial Membrane Separation Technology**. *Blackie Academic and Professional, Glasgow*, ISBN 0-7514-0338-5.
41. Press Release - Reuters.com**. Learn About the US Membrane Separation Technologies Market**, 11th Mar 2008. Available from: http://www.reuters.com/article/pressRelease/idUS161789+11-Mar-2008+MW20080311 [Accessed 03 August 2010].
42. MARCEL MULDER, 2000. **Basic Principles of Membrane Technology**. *Kluwer Academic Publishers, Netherland*, ISBN 0-7923-4248-8.
43. R. B. COUSINS. **Membrane Technology**. *M.Eng 2003-4 Lecture Notes*, *University of Strathclyde, Glasgow*.
44. W. S. WINSTON HO and KAMALESH K. SIRKAR, 1992. **Membrane Handbook**. *Chapman and Hall, London*, ISBN 0-412-98871-2.
45. V. SONI, J. ABILDSKOV, G. JONSSON, and R. GANI, 2009. **A General Model for Membrane-based Separation Process**, *Computers and Chemical Engineering 33*, pg. 644-659.
46. MARYAM TAKHT RAVANCHI, TAHERAH KAGHAZCHI, and ALI KARGARI, 2009. **Application of Membrane Separation Processes in Petrochemical Industry: A Review**, *Journal of Desalination 235*, pg. 199-244.

47. SHIN-LING WEE, CHING-THIAN TYE, and SUBHASH BHATIA, 2008. **Membrane Separation Process – Pervaporation Through Zeolite Membrane**, *Separation and Purification Technology 63*, pg. 500-516.
48. RICHARD W. BAKER, 2004. **Membrane Technology and Applications**, 2nd Edition, John Wiley & Sons, ISBN 0-4708-5445-6.
49. PRATIBHA PANDEY and R. S. CHAUHAN, 2001. **Membranes for Gas Separation**, *Progress in Polymer Science 26*, pg. 853-893.
50. ASAD JAVAID, 2005. **Membranes for Solubility-based Gas Separations**. *Chemical Engineering Journal 112*, pg. 219-226.
51. T. D. STARK and H. CHOI, 2005. **Methane Gas Migration through Geomembranes**, *Geosynthetics International 12 No.2*, pg. 120-126.
52. A. K. JAIN et al., 2008. **Study of Hydrogen Transport through Porous Aluminium and Composites Membranes**, *International Journal of Hydrogen Energy 33*, pg. 346-349.
53. A. F. Ismail and L. I. B. David, 2001. **A Review on the Latest Development of Carbon Membranes for Gas Separation**, *Journal of Membrane Science 193*, pg. 1-18.
54. ANWU LI, WEIQIANG LIANG and RONALD HUGHES, 2000. **Fabrication of Dense Palladium Composite Membranes for Hydrogen Separation**, *Catalysis Today 56 (1-3)*, pg. 45-51.
55. S. SOULEIMANOVA, ALEXANDER S. MUKASYAN and ARVIND VARMA, 2000. **Effects of Osmosis on Microstructure of Pd-Composite Membranes Synthesized By Electroless Plating Technique**, *Journal of Membrane Science 166 (2)* pg. 249-257.
56. ITOH N., 1987. **A Membrane Reactor Using Palladium**, *AIChE Journal, 33(9)*, pg. 1576-1578.
57. M. OERTEL, J. SCHMITZ, W.WEIRICH, D. JENDRYSSEK-NEUMANN and R.SCHULTEN, 1987. **Steam Reforming of Natural Gas with Integrated Hydrogen Separation for Hydrogen Production**, *Chemical Engineering and Technology, 10,* pg. 248-255.
58. J. N. KEULER, L. LORENZEN and S. MIACHON, 2002. **Preparing and Testing Pd Films of Thickness 1-2 µm with High Selectivity and High Hydrogen Permeance**, *Separation Science and Technology, 37(2)*, pg. 379-401.

59. S. TOSTI, 2003. **Supported and Laminated Pd-based Metallic Membranes**, *International Journal of Hydrogen Energy 28*, pg. 1445-1454.
60. V. JAYAMARAN and Y.S. LIN, 1995. **Synthesis and Hydrogen Permeation Properties of Ultrathin Palladium-Silver Alloy Membranes**, *Journal of Membrane Science 104*, pg. 251-262.
61. SABINA K. GADE, PAUL M. THOEN, J. DOUGLAS WAY, 2007. **Unsupported Palladium Alloy Foil Membranes Fabricated by Electroless Plating**, *Journal of Membrane Science 316*, pg. 112-118.
62. GRASHOFF, G.J.; PILKINGTON, C.E.; CORTI, C.W., 1983. **The Purification of Hydrogen – A Review of the Technology Emphasizing the Current Status of Palladium Membrane Diffusion**, *Platinum Metal Reviews*, *27 (4),* pg. 157-169.
63. S.-K. RYI et al., 2006. **Development of a New Porous Metal Support of Metallic Dense Membrane for Hydrogen Separation**, *Journal of Membrane Science 279*, pg. 439-445.
64. S. UEMIYA, 1999. **State of the Art of Supported Metal Membrane for Gas Separation**, *Separation and Purifications Review 28*, pg. 51-85.
65. PVD-coatings.co.uk. Available from: http://www.pvd-coatings.co.uk/theory-of-pvd-coatings-magnetron.htm [Accessed 12 August 2010].
66. YUANFANG, GAO, 2006. **Microfabricated Devices for Single Cell Analysis**, *PhD Dissertation, Faculty of Graduate School, University of Missouri-Columbia, US*, pg. 42.
67. READE. **Sputtering Targets**. Available from: http://www.reade.com/index.php?option=com_content&task=view&id=740&Itemid=10 [Accessed 12 August 2010].
68. JAYAMARAN V., LIN Y.S., PAKALA M. and LIN R.Y., 1993. **Fabrication of Ultrathin Metallic Membranes on Ceramic Supports by Sputter Deposition**, *Journal of Membrane Science, 99*, pg. 89-100
69. ZHANG Y., OZAKI T., KOMAKI M. and NISHIMURA C., 2003. **Hydrogen Permeation Characteristics of V-15Ni Membrane with Pd/Ag Overlayer by Sputtering**, *Journal of Alloys and Compounds, 356-357*, pg. 553-556.

70. Engineer's Handbook. **Manufacturing Processes – Coatings Surface Finishing**. Available from: http://www.engineershandbook.com/MfgMethods/cvd.htm [Accessed 12 August 2010].
71. Azom.com. **Chemical Vapour Deposition (CVD) – An Introduction**. Available from: http://www.azom.com/details.asp?ArticleID=1552#_Background [Accessed 12 August 2010].
72. XOMERATIAKIS G and LIN Y.S., 1996. **Fabrication of a Thin Palladium Membrane Supported in a Porous Ceramic Substrate by Chemical Vapour Deposition**, *Journal of Membrane Science, 120*, pg. 261-272.
73. FRED SENESSE. **What is Electroless Plating ?**. *General Chemistry Online*. Available from: http://antoine.frostburg.edu/chem/senese/101/redox/faq/electroless-plating.shtml [Accessed 12 August 2010].
74. CHENG Y. S., PENA M. A., FIERRO J. L., HUI D. C. W. and YEUNG K. L., 2002. **Performance of Alumina, Zeolite, Palladium, Pd–Ag alloy Membranes for Hydrogen Separation from Towngas Mixture**, *Journal of Membrane Science 204(1-20),* pg. 329-340.
75. JOHN P. COLLINS and J. DOUGLAS WAY, 1993. **Preparation and Characterization of a Composite Palladium-Ceramic Membrane**, *Industrial and Engineering Chemistry Research 32*, pg. 3006-3013.
76. LI A., LIANG W., HUGHES R., 1999. **Fabrication of Defect Free Pd/α-alumina Composite Membranes for Hydrogen Separation,** *Thin Solid Films 350 (1-2)*, pg. 106 – 112.
77. HOLLEIN V., THORNTON M., QUICKER P., DITTMEYER R., 2001. **Preparation and Characterization of Palladium Composite Membranes for Hydrogen Removal in Hydrocarbon Dehydrogenation Membrane Reactors,** *Catalysis Today 67 (1-3)*, pg. 33 – 42.
78. RAZIMA S. SOULEIMANOVA, ALEXANDER S. MUKASYAN and ARVIND VARMA, 2001. **Pd-Composite Membranes Prepared by Electroless Plating and Osmosis: Synthesis, Characterization and Properties**, *Separation and Purification Technology 25*, pg. 79-86.

79. MARDILOYCH I.P., SHE Y., and MA Y.H., 1998. **Defect Free Palladium Membranes on Porous Stainless Steel Support**, *AIChE Journal 44 (2)*, pg. 310 – 322.
80. MARDILOYCH I.P., SHE Y., and MA Y.H., 2002. **Dependence of Hydrogen Flux on the Pore size and Plating Surface Topology of Asymmetric Pd-porous Stainless Steel Membranes,** *Desalination 144 (1-3)*, pg. 85 – 89.
81. ROA F., WAY J.D., MCCORMICK R.L., PAGLIERI S.N., 2003. **Preparation and Characterization of Pd–Cu Composite Membranes for Hydrogen Separation**, *Chemical Engineering Journal 93 (1),* pg. 11 – 22.
82. HUANG T., WEI M., CHEN H., 2003. **Preparation of Hydrogen Permselective Palladium-Silver Alloy Composite Membranes by Electroless Deposition**, *Separation and Purification Technology 32 (1-3)*, pg. 239 – 245.
83. DAVID A. PACHECO TANAKA et Al., 2005. **Preparation of Palladium and Silver Alloy Membrane on a Porous α-alumina Tube via Simultaneous Electroless Plating**, *Journal of Membrane Science 247*, pg. 21-27.
84. PAUL M. THOEN, FERNANDO ROA and J. DOUGLAS WAY, 2006. **High Flux Palladium-Copper Composite Membranes for Hydrogen Separations**, *Desalination 193*, pg. 224-229.
85. YAN HUANG and ROLAND DITTMEYER, 2007. **Preparation of Thin Palladium Membranes on a Porous Support with Rough Surface**, *Journal of Membrane Science 302*, pg. 160-170.
86. DIEGO PIZZI et Al., 2008. **Hydrogen Permeability of 2.5 µm Palladium-Silver Membranes Deposited on Ceramic Supports**, *Journal of Membrane Science 325*, pg. 446-453.

CHAPTER 3

3.0 Experimental Work

Following the findings from literatures review, the experimental work for this study was structured to fill in the gap in the production of pure hydrogen for fuel cell application. The experiments were designed in order to study the effects of:

- Type of Pd precursor used for plating (nitrate or chloride based)
- Effect of composition of the plating solution
- Effect of the number of plating deposition
- Pore size of the ceramic support used

After that, the subsequent set of experiments was designed in order to fabricate a dense pinhole free membrane using the advanced electroless plating (ELP) technique:

- ELP under osmosis
- ELP with water circulation
- ELP under partial vacuum
- ELP under total suction
- ELP under partial suction

These effects and results obtained are further discussed in chapter 4.

3.1 Apparatus/Experimental Set-up

The experimental set-up use for this work consists of three major sections, which are:

a) Feed delivery system
b) Membrane reactor
c) Analytical system

The simplified schematic diagram of the whole experimental set-up is shown in figure 3.1.

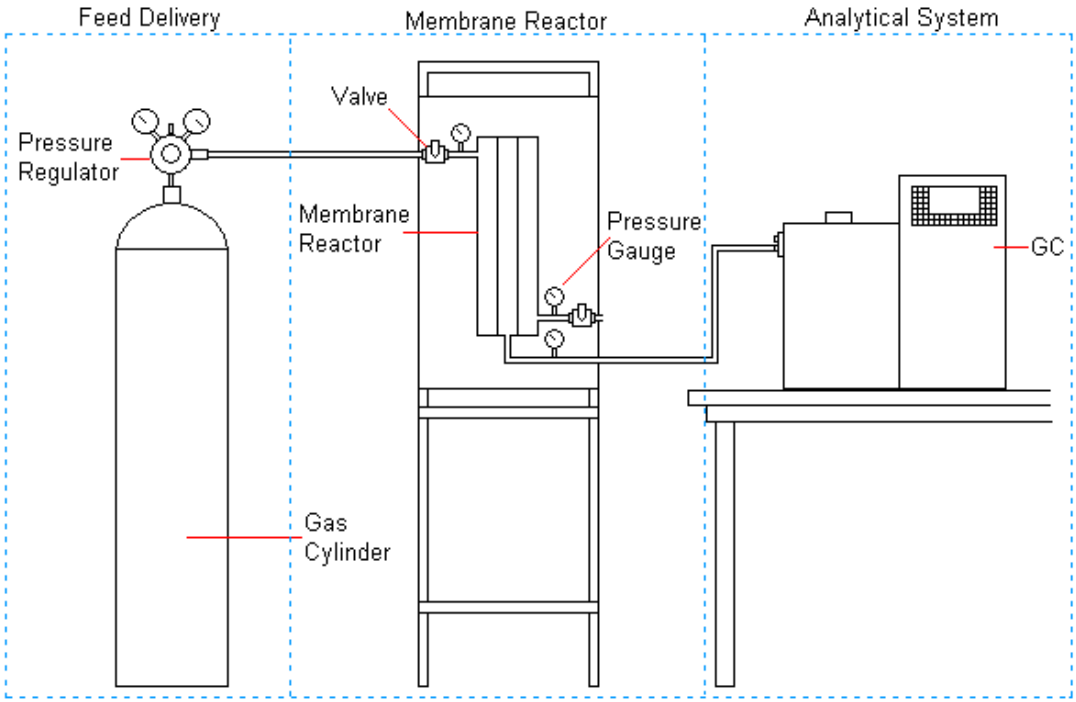

Figure 3.1: Simplified schematic diagram of the experimental set-up.

3.1.1 Feed Delivery System

The feed delivery system comprises a gas cylinder and the corresponding pressure regulator, both supplied by BOC Limited. The delivered pressure from the cylinder is kept constant and monitored using the pressure regulator. The pressure and flow rate of the feed gas entering the reactor is then fine-tuned using the needle valve. The differential pressures across the membrane are monitored by using the digital pressure gauge (by measuring the membrane shell inlet and membrane bore outlet pressure).

3.1.2 Membrane Reactor

The membrane reactor used for this work was constructed in-house (technical department of the university) using stainless steel 316L and the schematic of the reactor layout is shown in figure 3.2 below.

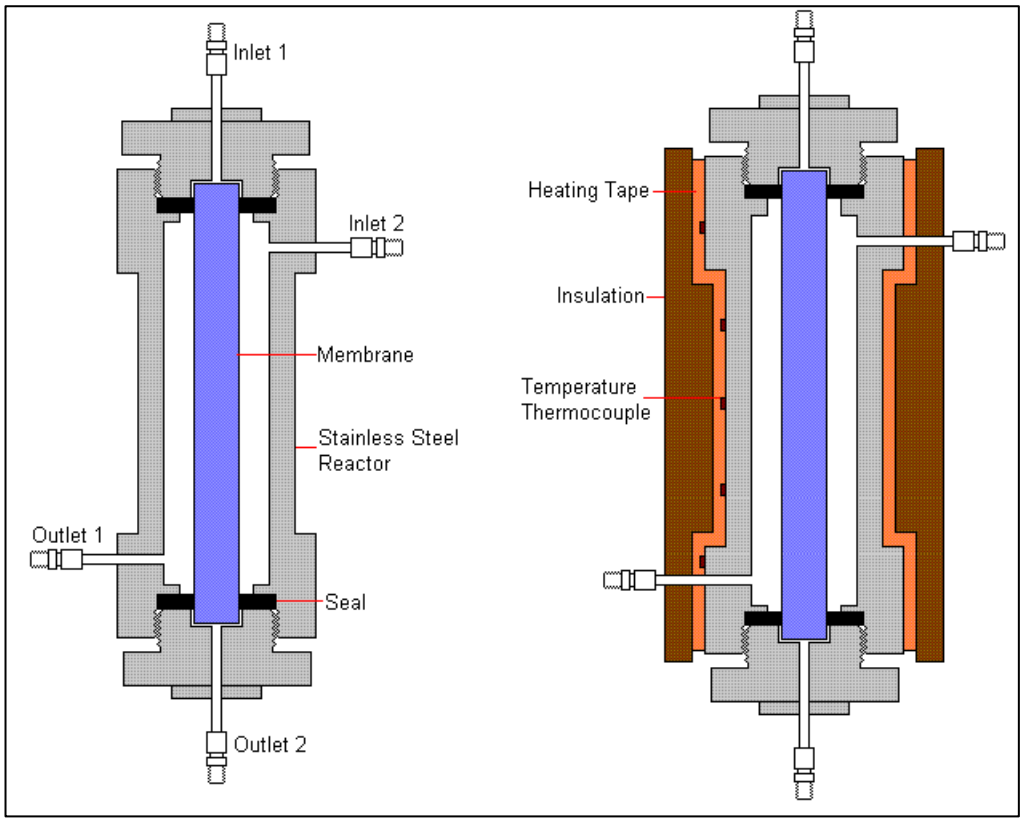

Figure 3.2: Schematic diagram of the membrane reactor without (left) and with heating (right) system.

The reactor assembly consists of a stainless steel shell with two inlets and two outlets. The membrane is placed in the centre of the shell and sealed at both ends using graphite seal. The reactor is designed to seal and hold the membrane in place by compressing the graphite seal around the membrane when the top and bottom bolt of the reactor is tightened.

Thermocouples are then placed on strategic locations for the entire length of the exterior of the shell to provide readings of the reactor temperature. A heating tape is then used to wound around the shell and the shell assembly is subsequently insulated to minimise heat losses and to maintain a uniform temperature along the reactor. The heating tape is connected to an adjustable temperature controller, thermocouple selector and digital thermometer to provide the temperature reading for each section (see figure 3.3).

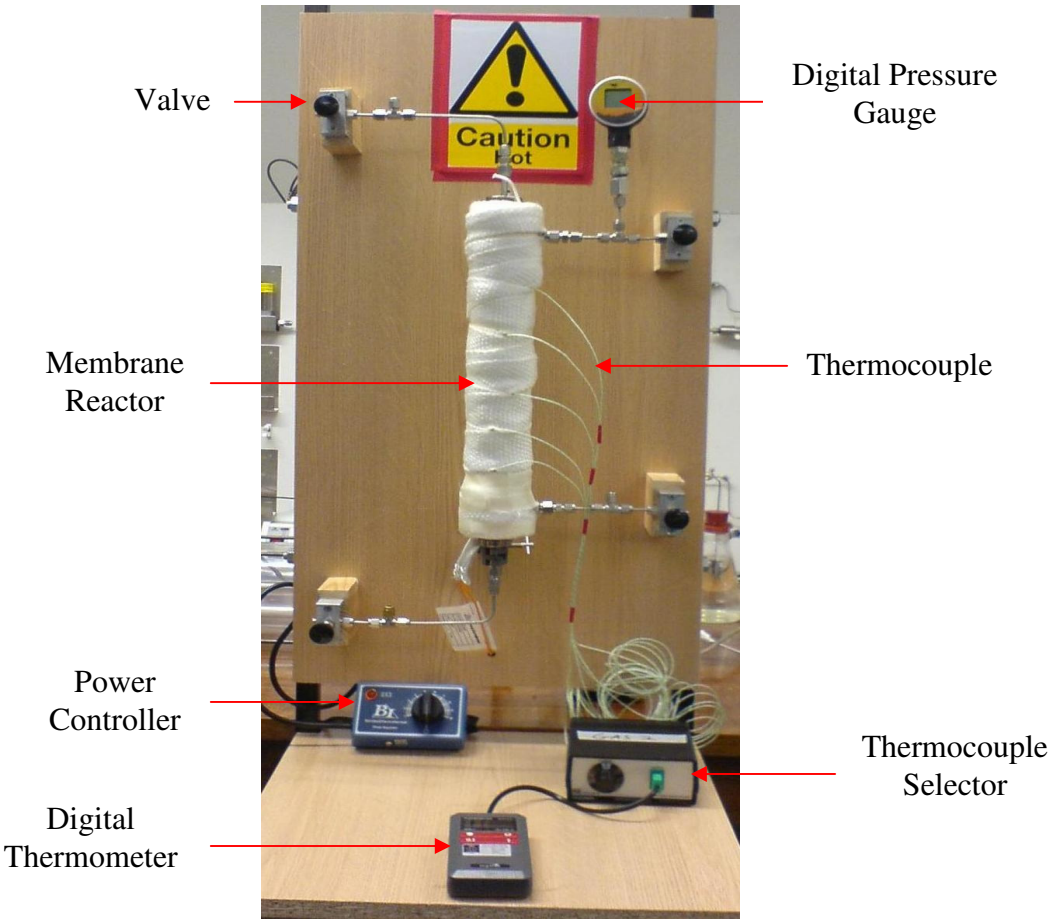

Figure 3.3: Picture showing the membrane reactor assembly.

3.1.3 Analytical System (Gas Chromatograph)

The gas chromatograph (GC) is the single most important analytical equipment for his work and is used to identify and quantify the gas compositions going in and coming out from the membrane reactor. In general, chromatography is a method for the separation of a mixture of compounds into their separate individual components. By separating into components, it is therefore easier to identify and measure their relative amount.

The GC used for analysing the feed and product for this work is a Varian, Inc. Model CP3800 (see figure 3.4).This GC model is capable of supporting up to four columns and two detectors. However, there are only two columns and a TCD detector installed on this GC. Both are packed columns and are connected to the TCD detector. The specifications for the columns are:

- Molecular sieve 5A, 60-80 mesh, 2m x 1/8" x 2mm stainless steel column
- Haysep Q, 80-100 mesh, 2m x 1/8" x 2mm stainless steel column

The GC is operated with two gases, Argon or Helium gas (depending on the test sample) is used as carrier gas and a cylinder of air is used to activate (open) the sampling valves during injection.

However, in order to verify the reproducibility of the result and to ensure that the result obtained were accurate, a second GC was utilised. The second GC (see figure 3.5) used is a compact Varian Micro-GC model 4900 (modular system, where the column and oven is built into a single unit) and is equipped with two capillary columns connected to the TCD detector:

- Molecular sieve 5A, 20m (CP740129)
- PoraPlot Q, 10 m (CP740124)

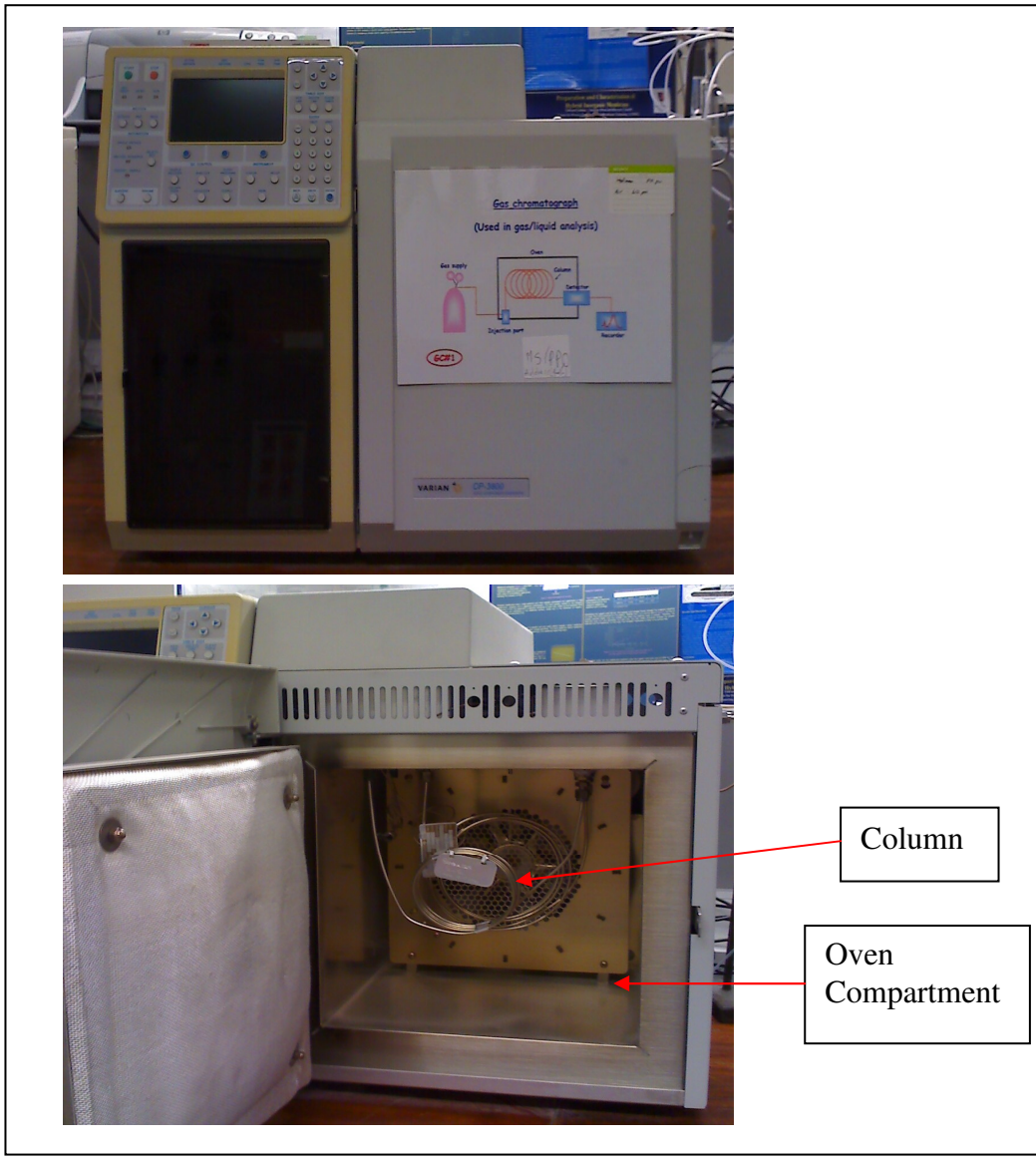

Figure 3.4: Picture of the GC used including view of the two columns inside the GC oven.

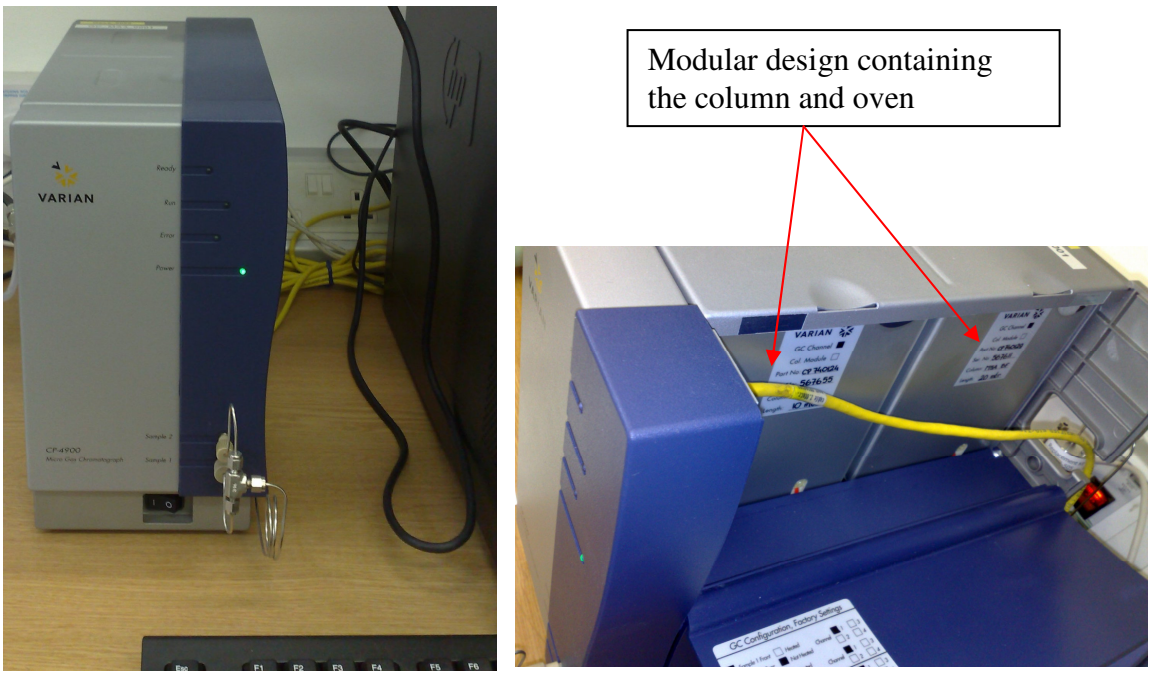

Figure 3.5: Picture of the second GC used including the inside view showing the modular unit containing the oven and column.

3.2 Materials

A list of materials used for this project includes gases, chemicals and ceramic supports. However, the majority of the project cost is on the palladium metal, which is why the main target of this work is to produce a thin but dense palladium membrane to reduce the cost of membrane fabrication.

3.2.1 Gases

All the gases used in this work are supplied by BOC-Gases, which comprised of the gas cylinders, their corresponding pressure regulators and delivery hoses. The gases used include:

i. Argon Cylinder
ii. Compressed Air Cylinder
iii. Nitrogen Cylinder
iv. Helium Cylinder
v. Hydrogen Cylinder
vi. Cylinders of Mixed Gas (containing Hydrogen, Nitrogen, Methane, Carbon Monoxide and Carbon Dioxide)

3.2.2 Chemicals

The chemicals used for this work include:

i. Palladium Chloride ($PdCl_2$) (99.9+ %)
   CAS 7647-10-1
ii. EDTA Disodium Salt Dihydrate (99 %)
   $C_{10}H_{14}N_2O_8Na_2.2H_2O$
   CAS 6381-92-6

iii. Ammonia Solution SG 0.91 (25 %)
NH_3
CAS 1336-21-6

iv. Hydrochloric Acid
HCl
CAS 7647-01-0

v. Stannous Chloride (99 %)
$SnCl_2$
CAS 7772-99-8

vi. Hydrazine Hydrate (35 %)
H_4N_2.H2O
CAS 10217-52-4

3.2.3 Ceramic Support

The ceramic supports used for the project are obtained from CTI SA (Ceramiques Techniques & Industrielles SA, France).

3.2.3.1 Description

All support used in this work have a base material of α-alumina with titania wash coat. Their average pore size ranges from 30, 80, 200, and 6000 nm respectively. The supports are in tubular configuration and the dimensions are as follows:

Outer diameter: *10 mm*
Inner diameter: *7.6 mm*
Wall thickness: *1.2 mm*
Length: *37 mm* (20 mm glazed at each end for membrane seal incorporation and handling purpose).

An example of the support used is shown in figure 3.6.

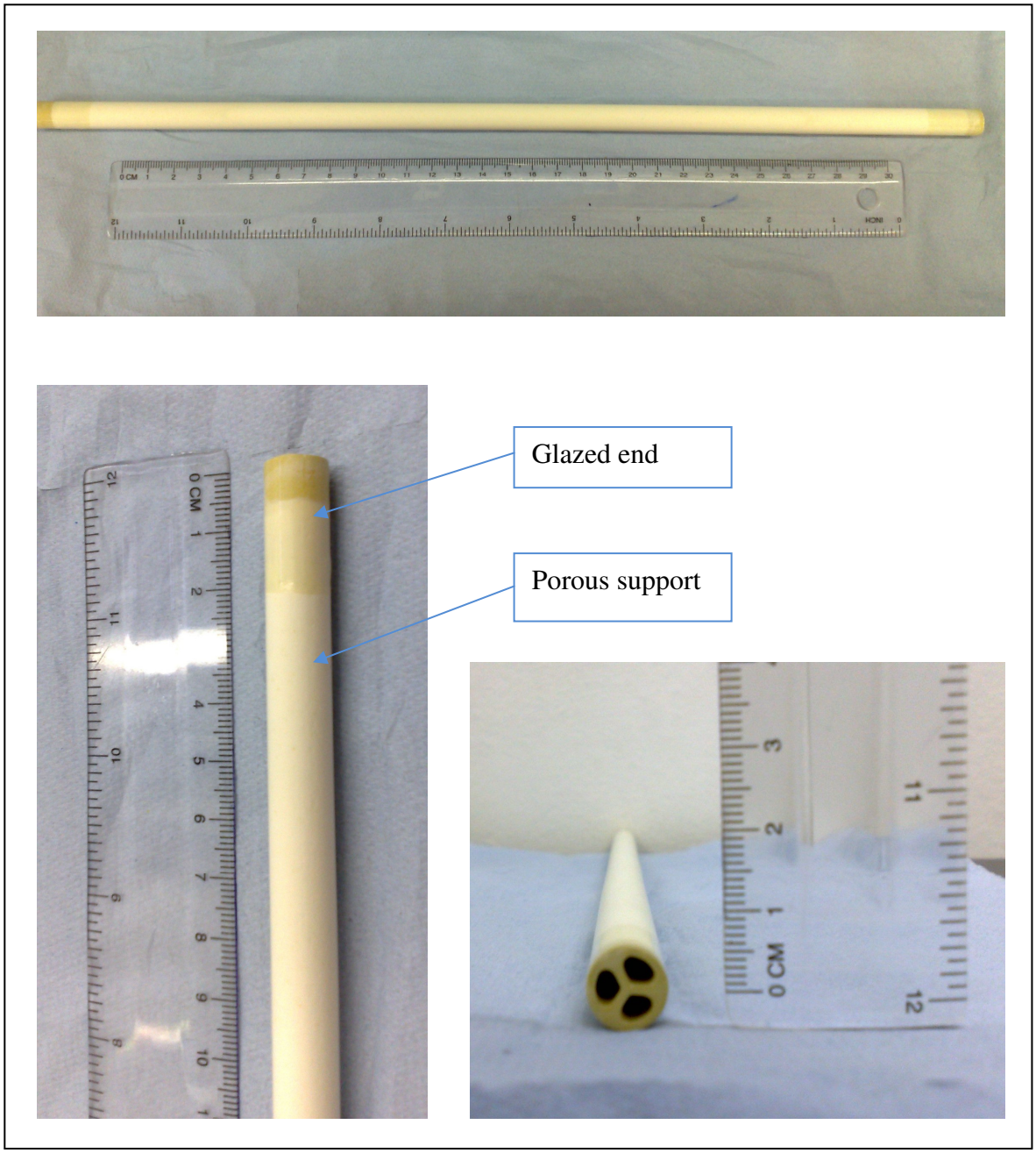

Figure 3.6: Pictures showing the full support (top), glazed end (left) and internal support structure (right).

3.2.3.2 Support Characterization

For characterization purpose, one of the supports of each pore size is broken into small pieces and analysed by scanning electron microscopy. The equipment used is the Leo model S430 scanning electron microscope and an example of the cross-section image taken is shown in figure 3.7. Images of the inner and outer surfaces are also shown.

From all the images taken, it could be seen that the supports are asymmetric. An example would be the 30 nm pore size membrane, whereby the outer layer is 30 nm with a thickness of about 30 µm deposited on a layer of 6000 nm (figure 3.7). Therefore, it is concluded that the pore size quoted by the ceramic supplier are actually the pore size of the outer layer (titania wash coat layer) which is supported by the 6000 nm α-alumina layer. The only exception would be the 6000 nm pore size supports which symmetric.

The SEM machine is also linked with electron dispersive X-ray (EDXA). Therefore it was utilised to determine the composition (elements) of each of the support surface. Results obtained for the 30nm support surface shows the presence of titania and also other different elements and is summarises in table 3.1. An example of the results generated by an EDXA analysis can be seen in appendix B.

Element	Composition (%)
Al	5.0104
Si	2.1938
P	0.76
Ca	0.3632
Ti	91.673

Table 3.1: EDXA analysis of the 30 nm support

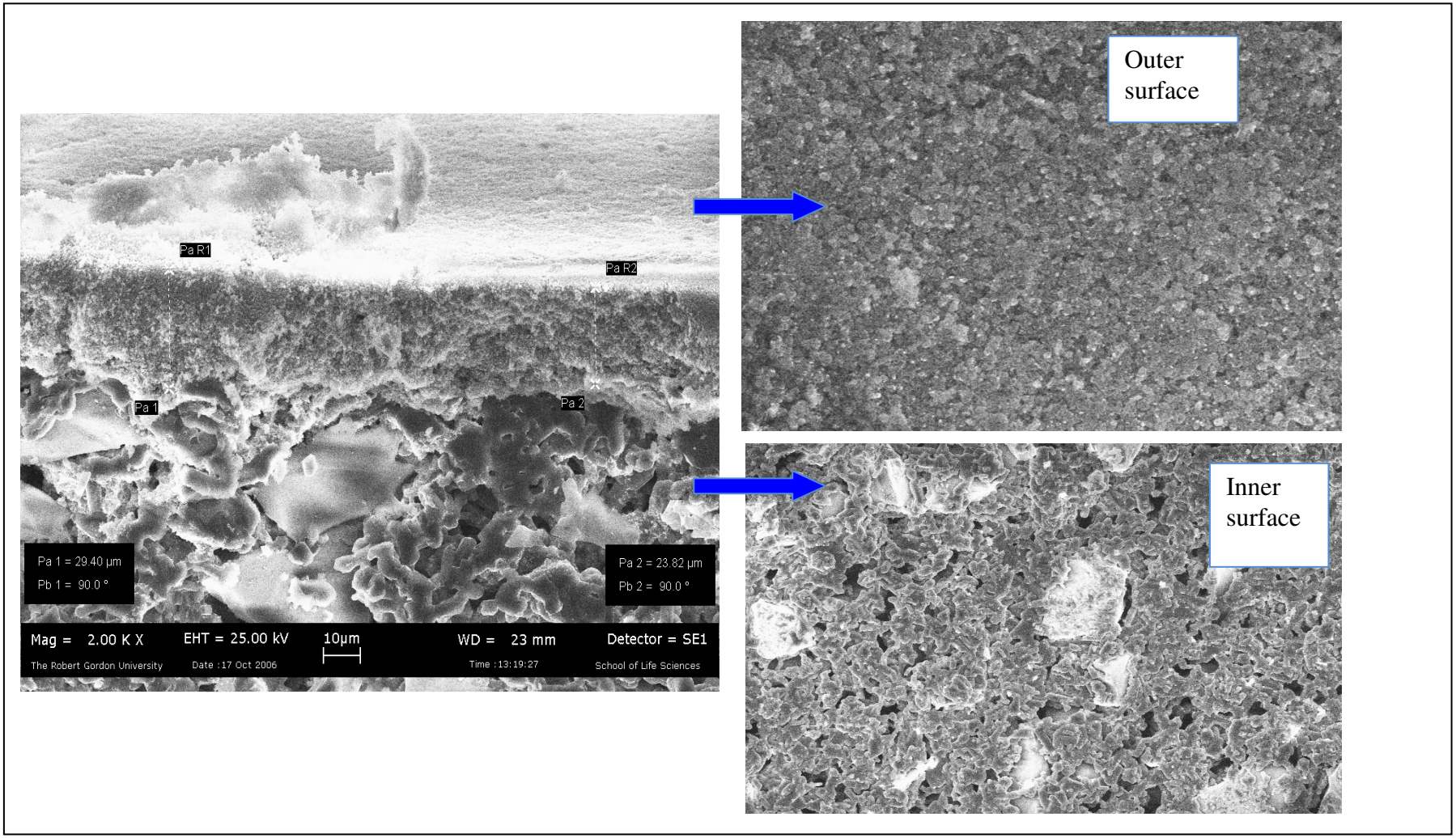

Figure 3.7: SEM images for a 30 nm support (2000X magnification).

3.3 Health and Safety

Safety is paramount when working inside the lab with high pressure gas cylinders and chemicals, therefore COSHH and risk assessments were conducted for all the materials used for this project which included gases, chemicals, coated ceramic supports and the safe operation of membrane reactor. A brief description of the safety characteristics of some of the materials used is discussed.

3.3.1 Gases

Safety characteristics of Argon*

- Inert under most conditions and it is colourless, odourless, tasteless and non-toxic. In high concentration will cause asphyxiation by depleting/displacing oxygen.

Safety characteristic of Compressed air*

- Not classified as dangerous

Safety characteristics of Nitrogen*

- Non-toxic and non-reactive except at high temperature. In high concentration will cause asphyxiation.

Safety characteristics of Helium*

- Inert gas and in high concentration will cause asphyxiation, however due to its low density it will rise upward and dissipate rapidly. Therefore lessening the danger.

Safety characteristics of Hydrogen*

- Non-toxic, colourless, odourless, tasteless and lighter than air, so it will dissipate rapidly when released or leak. It's highly flammable and has lower ignition energy than natural gas. Thus it can ignite easily and burns with an almost invisible flame.

Safety characteristics of Carbon Dioxide*

- Non-flammable, colourless, odourless, tasteless and heavier than air, thus the risk of asphyxiation is higher.

(**Safety information and data sheet about gases can be found on the supplier's (BOC) website: http://www1.boc.com/uk/sds/*)

3.3.2 Chemicals

i. Palladium Chloride† ($PdCl_2$) (99.9+ %)

Hazard	Risk	Safety
Very toxic	• Toxic if swallowed • Cause burns • May cause sensitisation by skin contact	• If contact with eye, rinse immediately with water and seek medical advice • Wear suitable PPE's (personal protective equipment)

ii. EDTA Disodium Salt Dihydrate† (99 %)

Hazard	Risk	Safety
Irritant	• Irritating to eyes and skin	• If contact with eye, rinse immediately with water and seek medical advice • Wear suitable PPE's

iii. Ammonia Solution† SG 0.91 (25 %)

Hazard	Risk	Safety
Corrosive and dangerous for the environment	• Cause burns • Very toxic to aquatic organisms	• If contact with eye, rinse immediately with water and seek medical advice • Wear suitable PPE's • Avoid release to environment

iv. Hydrochloric Acid†

Hazard	Risk	Safety
Corrosive	• Cause burns • Irritating to respiratory system	• If contact with eye, rinse immediately with water and seek medical advice • Wear suitable PPE's

v. Stannous Chloride† (99 %)

Hazard	Risk	Safety
Corrosive	• Harmful if swallowed • Cause burns • May cause sensitisation by skin contact	• If contact with eye, rinse immediately with water and seek medical advice • Wear suitable PPE's

vi. Hydrazine Hydrate† (35 %)

Hazard	Risk	Safety
Toxic and dangerous for the environment	• May cause cancer • Toxic by inhalation, in contact with skin or swallowed • May cause sensitisation by skin contact • Very toxic to aquatic organisms	• Avoid exposure and obtain special instructions before use • In case of accident or feeling unwell, seek medical advice immediately • Avoid release to environment • Material and container must be disposed of as hazardous waste

(†*Safety information's are obtained from the supplier's website: http://www.acros.com by entering the CAS number in to the search function*)

3.4 Membrane Fabrication

Electroless plating (ELP) is the method chosen for this work for membrane fabrication and it is also one of the most commonly used methods. As mentioned earlier, several methods have been proposed and developed for the preparation of Palladium (Pd) based membranes, including magnetron sputtering, electroless plating and chemical vapour deposition.

However, in general the ELP technique is by far the simplest and more effective method of membrane fabrication. In comparison with other methods, a number of advantages exist for electroless plating technique such as the uniformity of deposits on complex shapes, adherence of deposits, low cost and very simple equipment set-up. One of the most important advantages of this technique is its ability to handle huge surface areas for plating; therefore the process is easy to scale up for commercialisation purpose.

However, the main reason for using ELP method within the university is due to its equally effective and relatively inexpensive process compared to other preparation methods; whereby the equipment or plating setups required are not complex compared to other methods. These features are very attractive for the development of the experimental setup, equipments and expertise (how to produce/coat other metallic layer using electroless plating) in the metallic coating/plating field within the university's Centre for Process Integration and Membrane Technology (CPIMT).

3.4.1 Conventional Electroless Plating Technique

The conventional electroless plating technique comprises two main stages; namely sensitisation plus activation, and then metal deposition.

a) Sensitisation and Activation

During conventional ELP process, the initial step is to seed the ceramic support surface with Pd nuclei, which will then initiate the autocatalytic reaction of the palladium complex in the subsequent plating step. Therefore, a surface activation process is carried out, consisting of successive immersion in an acidic $SnCl_2$ (stannous chloride) bath (sensitizing) followed by an acidic Pd bath. After immersing the support in the $SnCl_2$ bath, a gentle rinsing with deionised water is then performed. During this rinsing step, partial hydrolysis of Sn^{+2} takes place to form little (poorly) soluble product $Sn(OH)_{1.5}Cl_{0.5}$ and other more complicated hydroxy-chlorides [1].

Tin hydroxy-chlorides is strongly attached to the surface of the support as a layer with a thickness of a thousandth-tenth of a micron. The support is then immersed in the acidic Pd bath, and excess Sn^{+2} is then displaced and replaced by Pd^{+2}. After that, a gentle rinsing with deionised water is performed to remove any excess Pd^{+2} that has not attached to the surface of the support.

The distribution of Pd nuclei during this seeding process has to be dense and uniform. To achieve this goal, the two step immersion sequence in $SnCl_2$ and Pd solutions is generally repeated 4 – 8 times, depending on the intensity of the activation. A perfectly activated layer has a smooth surface with a uniform dark brown colour.

The thickness of the activated layer is observed to be about 1.5 – 2 microns after about 10 cycles. A thicker activated layer results in a higher density of Pd nuclei on the support surface, but will lower the adhesion of further additional Pd layers during plating to the support surface. In many cases, the thickness of the activated layer will depend on the composition of the activation solution and the amount of repeated cycles. Figure 3.8 shows the schematic diagram of the simplified plating procedure and figure 3.9 shows the picture showing the different stages of the support during plating process.

b) Metal deposition

The pre-seeded Pd nuclei from activation stage will then initiate the autocatalytic process for the Pd metal deposition. The metal plating step is carried out at 60 ^{o}C in a plating bath containing a Pd precursor as palladium source, hydrazine as reducer and EDTA (disodium salt dehydrate) as stabilising agent for a set amount of time (exp. half an hour or 1 hour coating). After immersion in the plating solution, a gentle rinsing with deionized water is then performed to remove any Pd metals that has not attached to the surface before the next plating.

Simultaneously, a new plating solution is prepared for the second plating step. New solutions are prepared for each coating due to the mass transfer resistance for the deposition, as over time the amount of Pd metal available in the solution will be the same as the amount of Pd deposited on the ceramic support. Therefore, no further deposition will occur. The thickness and density of the membrane produced will depend on the amount of Pd used in the solution and the amount of plating steps used. This can be measured by using gas permeation test (for density) and SEM analysis (for thickness).

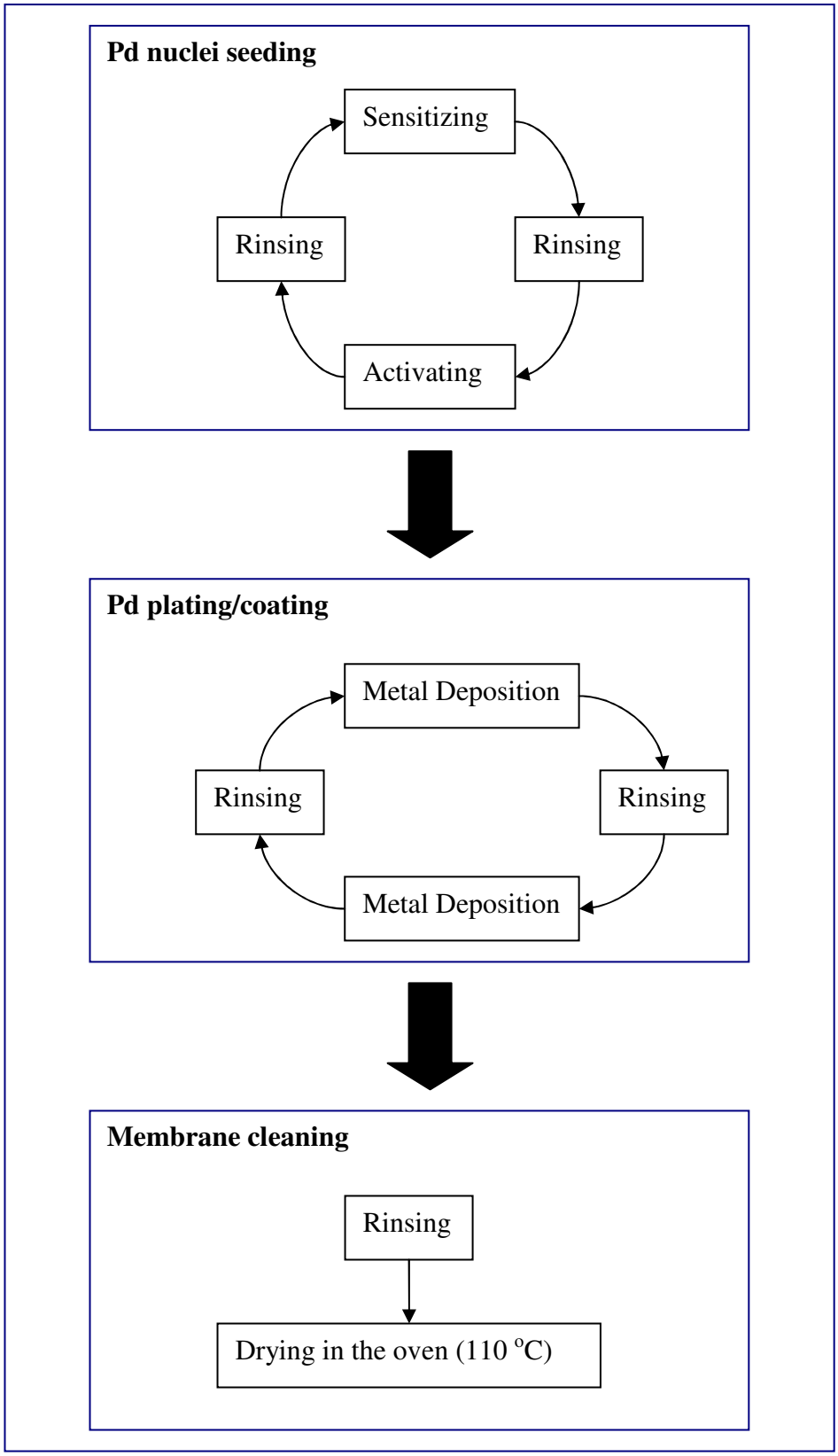

Figure 3.8: Schematic diagram showing the simplified electroless plating procedure.

Ceramic support

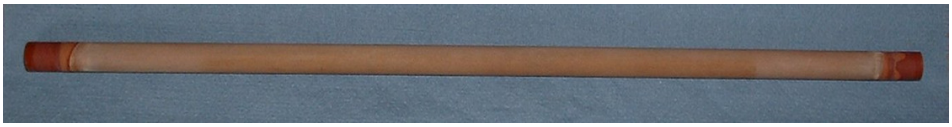

Seeded support

Pd membrane

Figure 3.9: Picture showing the different stages of the ceramic support during plating process.

3.4.2 Advanced Electroless Plating Technique

As mentioned in previous subchapter 2.3.3.3, there are some drawbacks associated with the original ELP technique. These drawbacks are the metal deposition rate is slower compared to other techniques and most importantly, the inability to control the deposition rate as well. However, it is still the most cost effective and by far the simplest technique compare to sputtering and vapour deposition. Therefore, the technique has to be modified in order to be a feasible membrane fabrication method.

Initial experimental result has also showed the evidence of these drawbacks where the original technique would require 16 hours to produce a Pd membrane, while the modified method would only require half that amount of time and Pd metal used. There were also signs of Pd metal peeling off from the membrane layer, which in turn indicates that the reaction is rate is now too high. These issues were addressed by further modification to the technique and coupling it with a peristaltic pump to generate a slight pressure drop. The reasons and benefits of using this advanced technique are further discussed in the detail in chapter 4.

3.5 References:

1. PETER P. MARDILOVICH, YING SHE, YI HUA MA, MIN-HON REI, 2004. **Defect-Free Palladium Membranes on Porous Stainless-Steel Support**, *AIChE Journal, 44 (2), pg. 310-322.*

CHAPTER 4

4.0 Results

4.1 Initial Investigation

A significant part of this research project involves experimental work and analysis of results, therefore the procedure for coating, composition of bath solution and the type of support used to fabricate the membrane is extremely crucial. As a result, the initial approach to this work is to identify the suitable type of ceramic support and also to determine the plating procedure.

Due to the high cost of Pd, all the membranes fabricated at this stage were of shorter length (of around 6 cm long). The reason for doing this is to reduce the amount of Pd used for coating, thus reducing the cost. Besides that, once the coating process and procedure have been determined and verified, it can then be scaled-up. At the same time, it was useful to determine if the process is feasible before scaling-up to a longer membrane (37 cm long).

For the initial investigation, the membrane leak tests (gas permeation test) were conducted using Helium (He) and Nitrogen (N_2) to examine if there are any pinholes present on the membrane layer. The stainless steel reactor was originally constructed for use with the long ceramic support (which is 37 cm). Therefore, for the purpose of leak tests, a new permeation cell has been designed for use with shorter membrane length and at room temperature. Figure 4.1 shows the picture of the Perspex cell used for leak tests. The Perspex cell is pressure rated to 0.5 bars.

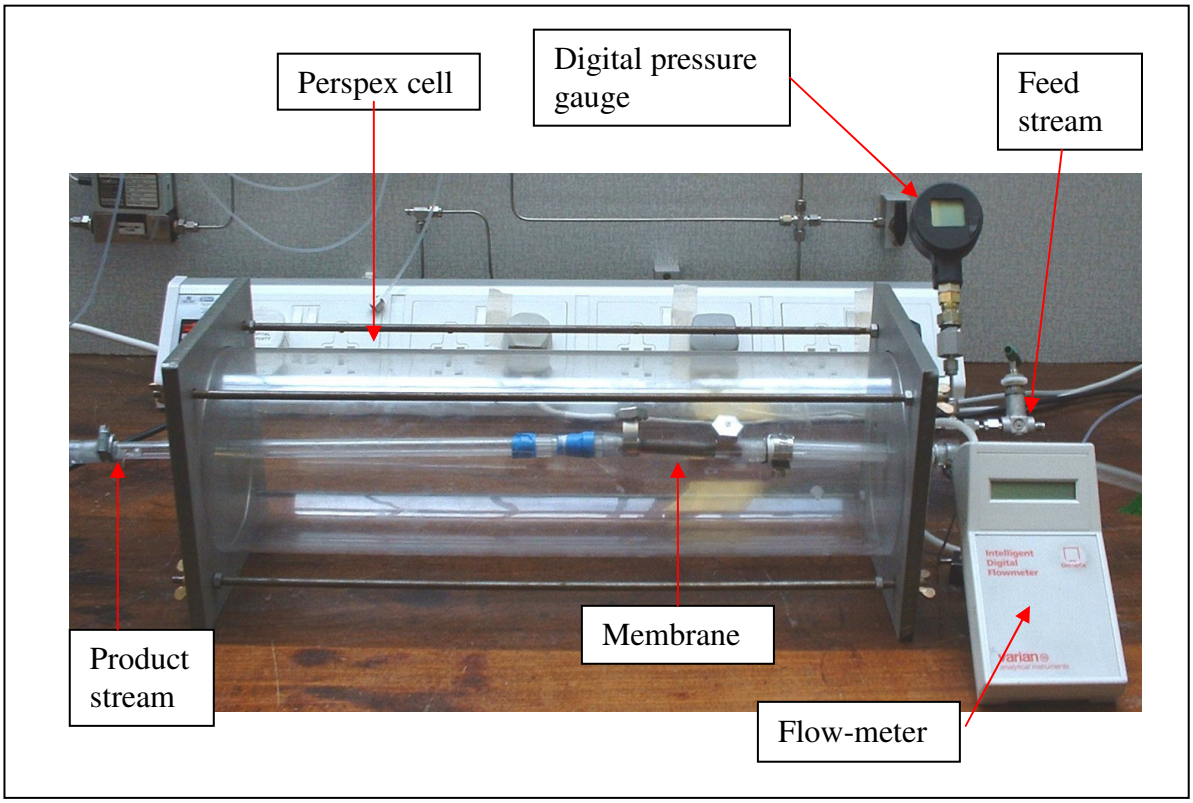

Figure 4.1: Picture of the perspex permeator cell.

4.1.1 Preliminary Experimental Work

In the early stage of this work, 6000 nm supports were used for coatings as these are readily available in the lab at the time. A brief description of the experiment conducted is as follow:

- A 6000 nm support were prepared for the experiment
- The electroless plating are conducted using nitrate precursor (tetraamonium palladium nitrate 10% in water)
- The plating bath composition used (table 6.1) is taken from Keuler et. al. [1999]
- The supports are coated only once in the solution for 4 hours

From the initial observation, the support does not show a metallic surface finish which was the expected indication for successful deposition of Pd metal. In addition, the performance of the membrane is extremely poor based on the leak test results obtained (the presence of pinholes due to the high flow rate of N_2 gas passing through the membrane). Therefore, results from the experiment have led to the following observations:

a) The plating time (dipping time) and the amount of plating solution used need to be varied and studied in order to obtain a better surface finish.
b) A different Pd precursor which can offer a higher concentration has to be investigated.
c) Developing a suitable plating procedure.
d) Varying the pore size of the support used, as the 6000 nm pore size might be too high.

With the above observations, the next phase of the experimental work was strictly devoted to the successful fabrication of a membrane with uniform metallic surface finish. In order to do that, a method developed by Collins and Way [1993] was adapted and applied. The reason in doing so is that the authors gave detailed information of the plating procedure with respect to support cleaning, plating process, composition of the solution used and membrane drying process.

Therefore, four sets of systematic experiments were then carefully executed for the purpose of understanding the whole plating process, which includes:

1. *Type of Pd precursor used for plating*
2. *Effect of composition of the plating solution*
3. *Effect of the number of plating deposition*
4. *Pore size of the ceramic support used*

4.1.1.1 Type of Pd Precursor Used

In order to study the effect of using different Pd precursors, two plating compositions were taken from literature for experimentation (table 4.1). The plating procedure used is briefly described as follows:

- Two 6000 nm supports were used for comparison purposes
- One of the supports is electroless plated using nitrate precursor while the second uses chloride precursor.
- Both are coated for one hour for 16 times and new solutions are prepared for each coating.
- The composition of the plating bath used is shown in table 4.1:

Nitrate Precursor [*Keuler et. al. 1999*]	**Chloride Precursor** [*Collins & Way 1993*]
27.5 g of 10 % $(NH_3)_4Pd(NO_3)_2$ solution	5.4 g $PdCl_2$
200 ml of 25 % ammonia solution	440 ml of 25 % ammonia solution
137 g of Na_2EDTA	70 g Na_2EDTA
345 ml of 0.02 M N_2H_4	10 ml of 1 M N_2H_4
100 ml of Buffer (pH = 11)	

Table 4.1: Plating bath composition per litre of solution for nitrate and chloride precursor.

The membranes obtained with both the nitrate and chloride precursors are shown in Figure 4.2 and 4.3 respectively. It can be observed from those figures that the palladium deposition has been much better with the chloride precursor as it provides a more silvery finish (indicating the presence of Pd metal) as opposed to the brown finish provided by the nitrate precursor. The reason stems from the fact that the chloride bath offers a higher Pd concentration in the plating solution (0.6 g of Pd metal from 1 g of $PdCl_2$) than the nitrate precursor (0.035 g of Pd per 1 g of solution used), thus offering a significant mass transfer of Pd to the membrane surface.

The palladium film thickness is estimated to be about 8.5 microns (μm) for nitrate precursor and 12.0 microns for the chloride precursor based on the estimated weight gain measurements (sample of weight gain calculation can be seen in appendix D). The variation in the metal film thickness also confirms that a higher solution concentration of Pd allows for a thicker and denser film of Pd to be deposited.

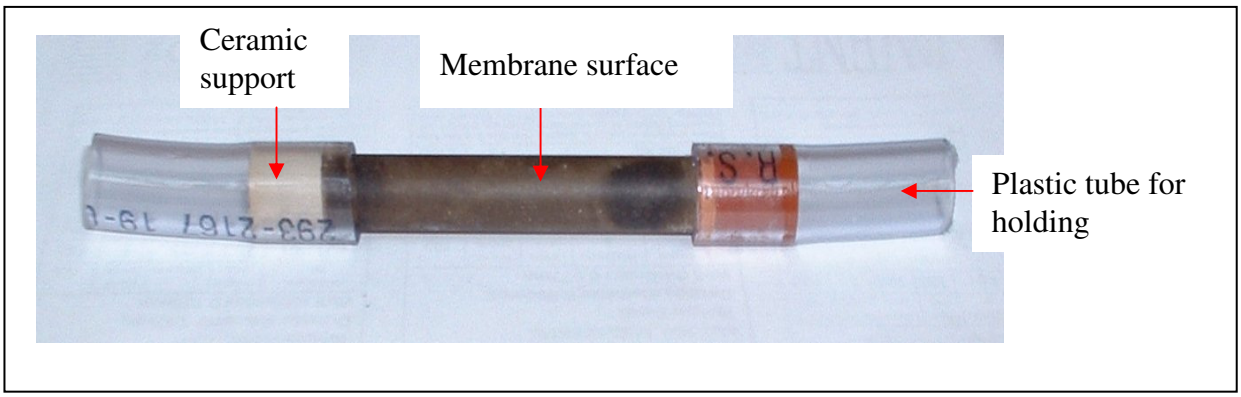

Figure 4.2: Membrane prepared using the nitrate precursor.

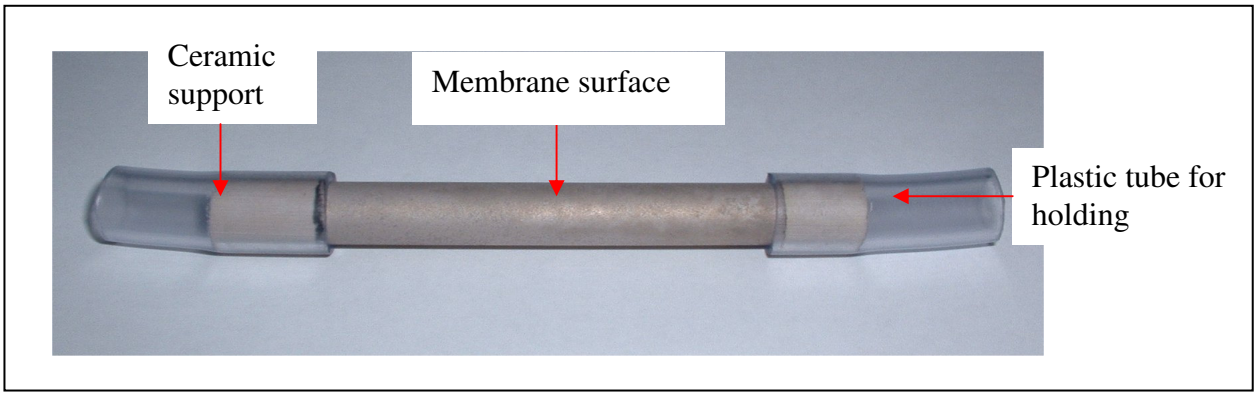

Figure 4.3: Membrane prepared using the chloride precursor.

Although the chloride precursor provides the metallic surface finish required, the surface finish is non-uniform and rough. This is due to the very high reaction rate during plating which causes the Pd metal to be deposited at a very high rate. Figure 4.4 shows the He gas leak test results for the support before coating and after coating for the membrane prepared using chloride precursor. The result shows that the He gas fluxes through the Pd deposited composite (membrane) are much lower than the support due to the successful deposition of a thin Pd film on the support surface.

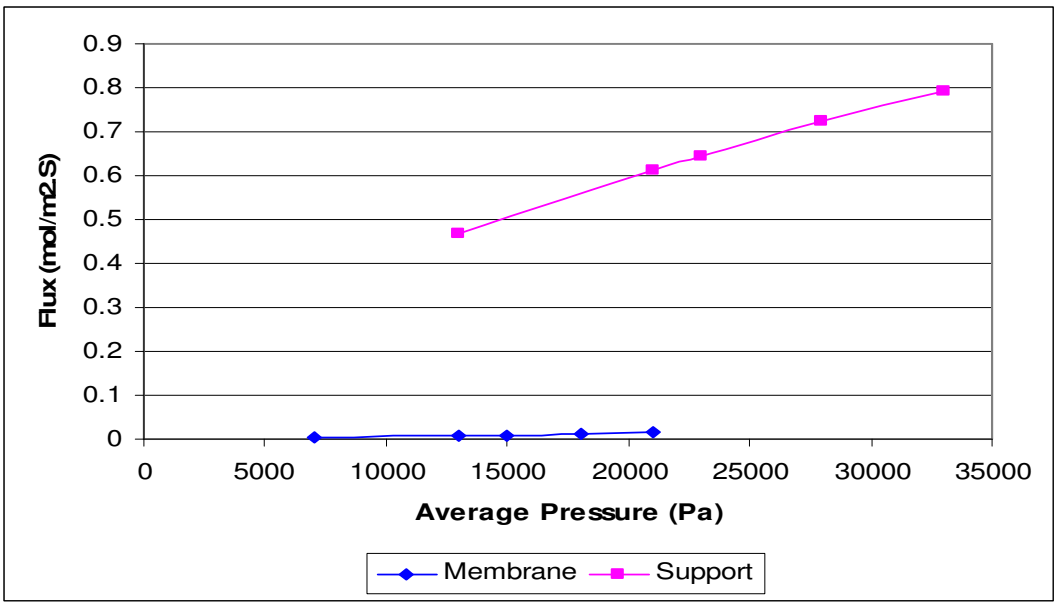

Figure 4.4: Helium fluxes for the support and membrane with average pressure across membrane.

The main observations from these membranes are as follows:

- The membrane produced using the chloride precursor shows a metallic surface finish while the membrane produced using the nitrate precursor does not.
- The number of steps required for the nitrate precursor to develop a Pd membrane would be significantly higher due to its lower Pd metal concentration in solution.
- The surface texture of the chloride based membrane is rough and has pinholes. This is due to the high reaction rate of the solution; therefore modification to the solution composition is required.
- The α-alumina support is suitable to be used for Pd deposition.

Hence, the next stage of the experimental work was focused on producing a membrane with a smoother surface finish and with little or no pinholes by using the chloride precursor but with a modified composition to control the rate of deposition.

4.1.1.2 Composition of the Plating Solution

From the previous result obtained, it is known that the reaction rate was too fast and the glass cylinder used for plating is also coated with some Pd metal. Therefore, the composition of the bath solution need to be modified. The amount of $PdCl_2$ and hydrazine used is then halved for this set of test.

Chloride Precursor (*taken from Collins & Way [1993] and modified*)
2.7 g $PdCl_2$
440 ml of 25 % ammonia solution
70 g Na_2EDTA
5 ml of 1 M N_2H_4

Table 4.2: New plating bath composition (using chloride precursor).

The plating procedure used is exactly the same as previous test whereby it was also coated 16 times for one hour each coat. The surface of the membrane is now smoother (see figure 4.5) and the reaction rate is more controllable as compared to the previous membrane, and the thickness is estimated to be at 12.3 microns.

This experimental set has resulted in the understanding of the effect on changing the compositions of solution on the rate of deposition, which will eventually influence the membrane thickness and surface texture. The leak test result obtained is then used for further comparison with the next set of experiment planned, which entail the effect of number of plating steps.

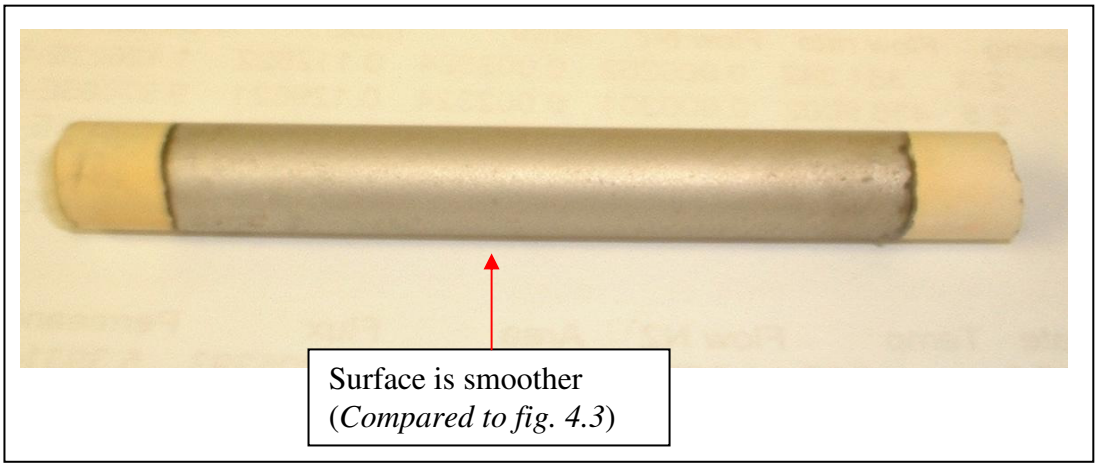

Figure 4.5: Picture showing the membrane produced using the new plating bath composition.

4.1.1.3 Numbers of Plating Steps

The main objective for this set of experiment is to confirm the impact of the numbers of depositions on the membrane performance. Thus, another membrane was produced using the same method as the membrane produced previously (subchapter 4.1.1.2) but with a lower amount of steps (9 plating steps) for comparison.

The Pd film thickness estimated from the weight gain measurements is about 8.3 microns for 9 plating steps compared to 12.3 microns for the 16 plating steps (see page 139 & 176 for thickness calculation estimated by weight gained and the associate accuracy/error with this process).

Figure 4.6 presents the helium leak tests of the membranes prepared using nine and 16 successive one hour plating steps. It can be observed at the pressure of 20,000 Pa, the helium permeance reduced from a value of 9.1 x 10^{-7} mol/m^2.s.Pa to 7.6 x 10^{-7} mol/m^2.s.Pa. This corresponds to a reduction of 16.4 % for an additional seven plating steps.

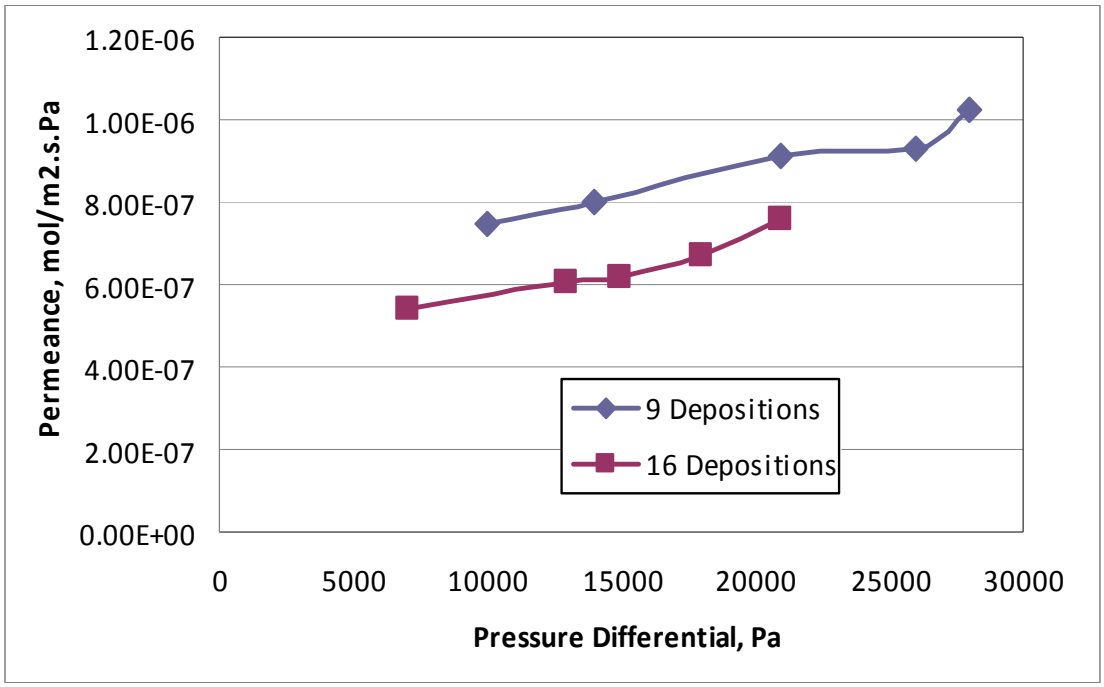

Figure 4.6: Helium permeances of palladium membranes prepared using 9 and 16 successive plating steps.

The result shows that higher number of plating steps is required to improve the performance (reducing the amount of pinholes present). However, one of the main objectives of this project is to reduce the thickness of the Pd film thus reducing the amount of Pd use. Hence, more experimental work was performed in order to evaluate the underlying phenomena which can reduce the pinholes successfully.

4.1.1.4 Pore Sizes of Support

Since by increasing the amount of plating steps does not necessary produce a denser membrane, it was necessary and important to verify the posibility that a smaller pore size support would require a lower number of plating steps to produce a dense membrane film.

Beside that, the new ceramic supports with the pore size of 30, 80, and 200 nm were now available. Hence, a support with the lowest pore size of 30 nm and support with the highest pore size of 6000 nm were used for plating. The plating procedure was maintained so that the two new membranes produced could be compared to the membrane produced in subchapter 4.1.1.2 (6000 nm – 16 plating steps). A total of three membranes are used for comparison and a brief description of these is presented in table 4.3:

Membrane	Pore size of support	Number of plating steps
1	6000 nm	16
2	6000 nm	32
3	30 nm	16

Table 4.3: Membranes used for comparison purpose.

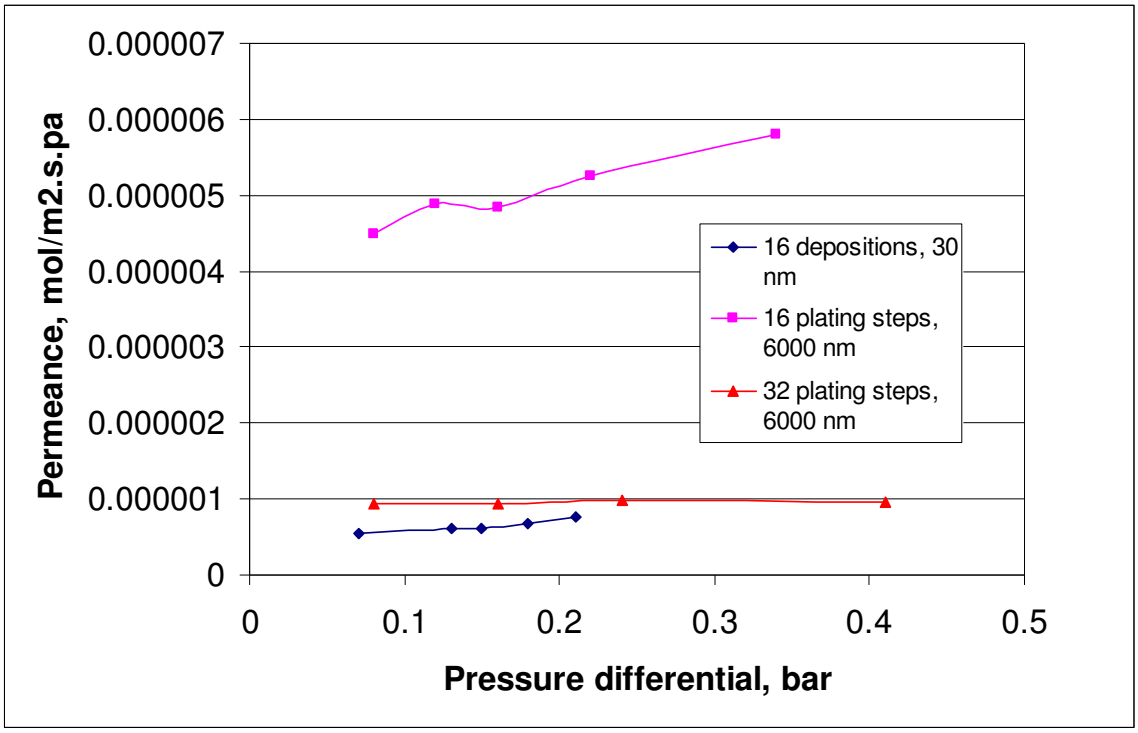

Figure 4.7: Helium leak tests of the 3 membranes compared with differential pressure across membrane.

Figure 4.7 shows the helium gas leak test for the three membranes for comparison. Although it uses the same or less number of plating steps, it can be seen clearly that the He leak for the 30 nm support membrane is lower than that both of the 6000 nm support membranes. Therefore, it can be concluded that the 6000 nm support pore size is definitely not suitable for the development of cost effective palladium membranes as more Pd metal is required to coat the bigger pores.

This is because in order to form a dense film on the 6000 nm support, the large pores have to be filled first and this entails large penetration of palladium in the support matrix. Even then, densification cannot be achieved at the similar number of coatings as the 30 nm pore size support.

4.2 Pinhole Reduction Methodologies

As discussed in the previous subchapter, from all the preliminary work conducted, the most important investigation still un-attempted is modifying the ELP method. It would be more beneficial to attempt to develop/optimise the current process as it has the potential for improvement since other researchers in this area has tried the same approach and managed to obtain some good result (see literature review in subchapter 2.3.4). Thus, one idea that came to mind involves the application of different types of pressures (suction, osmosis, etc.) under different conditions during plating.

This is because while ELP occurs on the membrane surface, the suction pressures will be applied along the bore side of the ceramic support. This will then create a pressure difference between the bore and tube side of the support. The pressure in the bore side will be slightly lower than the tube side and this will eventually encourage mass transfer of the solution carrying the Pd metal to travel from the solution to the support and eventually depositing the metal on the support surface as it travels across the support wall.

A set of advanced experiments were then designed and executed by utilising the equipment and materials already available in the lab (such as the peristaltic pump). Figure 4.8 shows a picture of the peristaltic pump in use. All the membrane produced in this section will then be compared against the membrane produced using the conventional method in subchapter 4.1.1.2.

4.2.1 Electroless Plating under Osmosis (ELP under osmosis)

The objective of these of experiments is to obtain a dense pinhole free membrane using electroless plating in conjunction with osmosis. The underlying principle of osmosis involves the circulation of salt solution through the bore side of the tube to allow the transport of water from the pinholes on the external surface of the support thus exposing the surface pinholes to reaction solution for densification. The exact procedure is as follows:

a. The membrane is initially subjected to eight depositions without osmosis using the procedure presented earlier (see subchapter 4.1.1.2).
b. Subsequently, eight more successive depositions are performed by circulating 3M NaCl solution through the bore side of the membrane tube. Total of 16 depositions.
c. The membranes are thoroughly washed in hot water after the final plating step.
d. The membranes are finally dried in the oven at 110 ^{o}C overnight.

The palladium composite membrane prepared using ELP under osmosis conditions is presented in figure 4.9. It can be observed that the membrane surface is rough with further membrane peeling effects. This is attributed by the fact that salt eventually occupied the pinholes of the membrane and it would have been very difficult to remove the salt solution before drying. Consequently, this caused additional stresses during the evaporation of water and the peeling of the membrane.

Given that the membrane clearly shows the peeling effects and does not provide the surface finish as required, a further gas leak test was not considered necessary and was therefore not carried out.

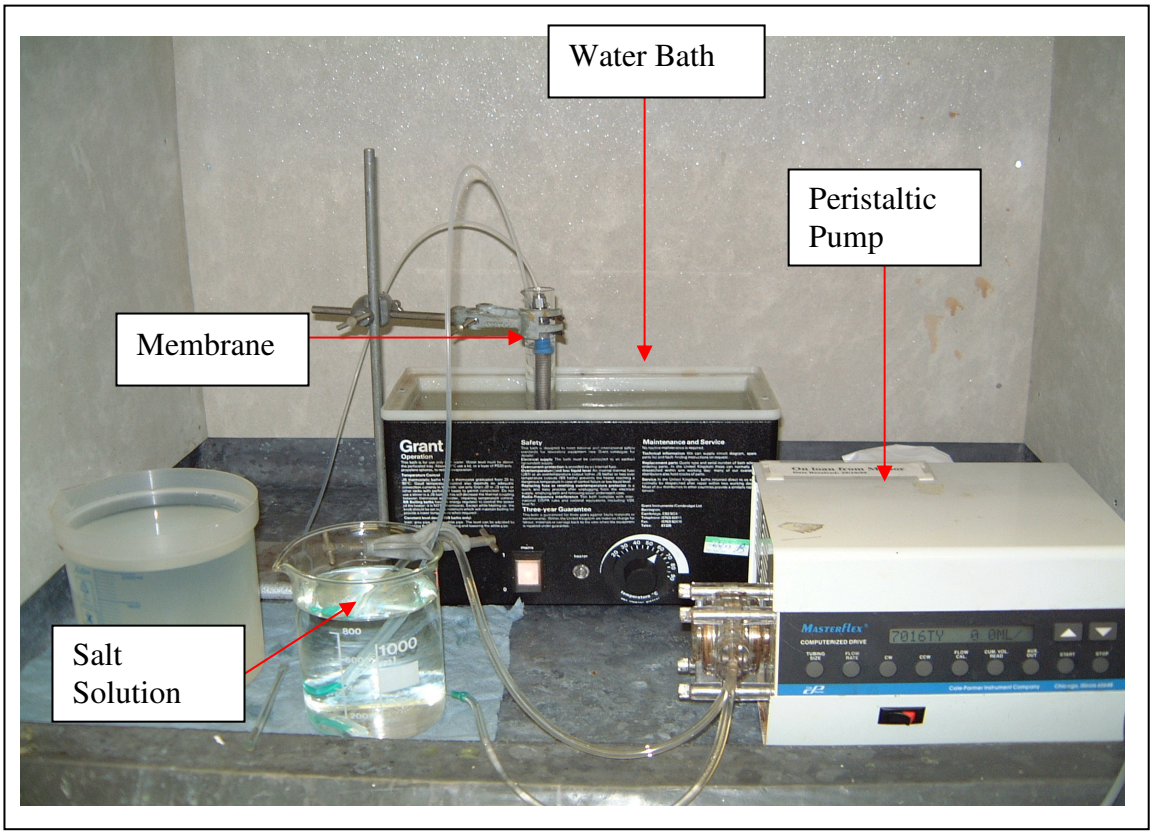

Figure 4.8: Experimental set-up for electroless plating under osmosis.

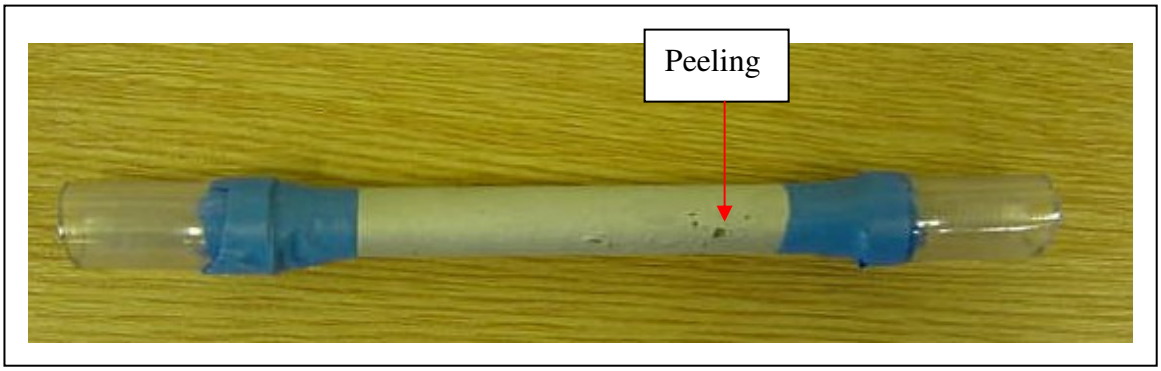

Figure 4.9: Membrane produced using ELP under osmosis.

4.2.2 Electroless Plating with Water Circulation (ELP with water circulation)

The hypothesis for water circulation comes from the presumption that the circulation of water would provide agitation on the bore side of the membrane, thereby increasing the ionic concentration gradient (concentration difference between both sides) across the membrane wall. This can then assist the reaction rate for densification. The experimental set up for the membrane fabrication is similar to that presented in subchapter 6.3.1. The procedures for membrane fabrication using electroless plating coupled with water circulation are presented as follows:

a. The initial deposition of a membrane with conventional electroless plating for eight successive plating steps using the procedure summarised earlier.
b. The membrane is then subjected to electroless plating under similar bath and operating conditions for eight more consecutive one hour plating steps with water circulated through the bore of the tube at a flow rate of about 30 ml/min. A total of 16 depositions were carried out.
c. The final composite membrane obtained is then cleaned and dried. The membrane gas leak tests are then measured in a permeation cell.

The composite membrane obtained after ELP with water circulation is presented in figure 4.10. The thickness of the Pd film estimated from the weight gain measurement is about 11.6 microns. The membrane surface appears to be silvery, which indicates successful deposition of Pd. However, the membrane surface is rough. Leak test results obtained is shown in figure 4.11.

Figure 4.10: Membrane produced using ELP with water circulation.

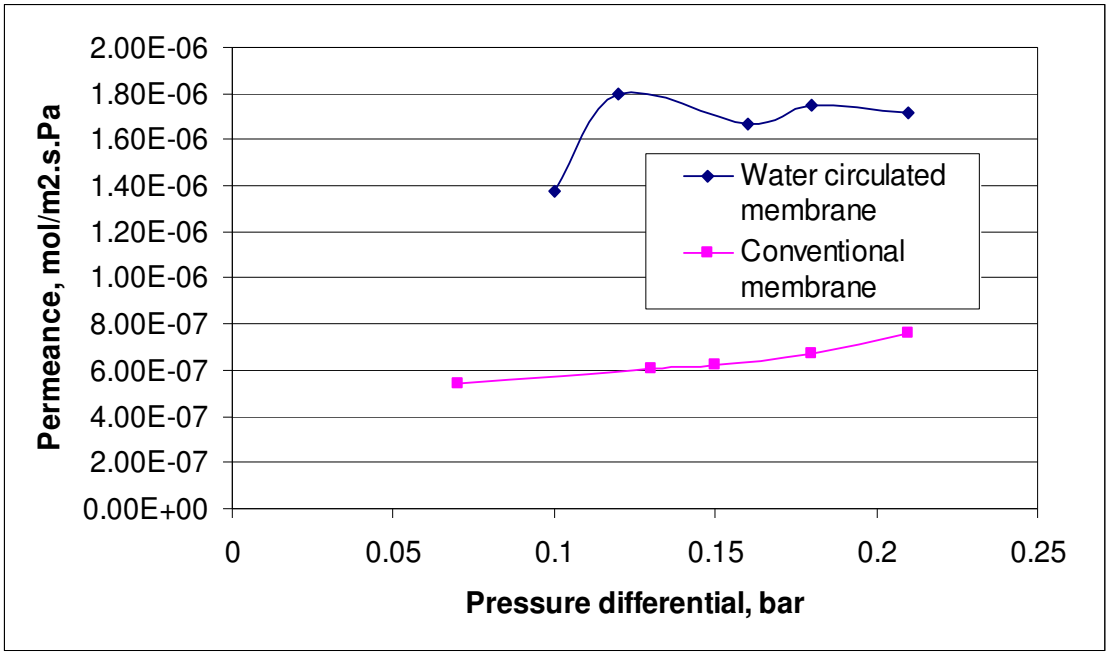

Figure 4.11: Graph showing the Helium leak test for the membrane produced using ELP with water circulation in comparison with membrane produced using conventional ELP process.

Figure 4.11 shows the helium leak for the membrane prepared with and without water circulation technique. The membrane without water circulation used for comparison purpose was the membrane produced previously in subchapter 4.1.1.2. From the plot, it is observed that the water circulation technique did not perform well, as the He gas leak is higher. Furthermore, the rate of Pd metal deposition is also lower in comparison to the membrane produced in subchapter 4.1.1.2. In other words, the water circulation technique has not solved the problem of densifying the membrane. Instead, the greater turbulence possibly hinders or obstructs the deposition of Pd film. Hence, it is also considered as a non-viable technique.

4.2.3 Electroless Plating under Partial Vacuum

The main objective of this test is to successfully fabricate a dense membrane using the partial vacuum application during ELP. The partial vacuum application involves the suction of air from the bore of the membrane (the tube is exposed to atmosphere via a small aperture using a T joint, as shown in figure 4.12). The application of partial vacuum was planned with the hypothesis that, partial vacuum can provide additional suction effects which can then pull the reaction solution into the membrane pinholes. It involves the bottom end of the T joint connected to the membrane bore and one of the side ends connected to the peristaltic pump, while the other connected to an aperture for controlled suction of air.

The experimental procedure for the fabrication is presented as follows:

a. The initial deposition of a membrane with conventional ELP for eight successive plating steps and then eight more plating steps under partial vacuum application (with a suction flow rate of 30 ml/min of air).
b. The final composite membrane obtained is then cleaned and dried. The membrane gas permeances are then measured in a permeation cell.

The Pd composite membrane prepared from this method is presented in figure 4.13. From visual observation, the membrane surface is found to be rough and did not display the silvery finish, which indicates the lack of deposited Pd metal. Therefore, in this case there was no formation of Pd film on the support. Hence, gas leak test was not carried out as it was considered unnecessary since there is no formation of Pd film and the membrane will have significant amount of pinholes.

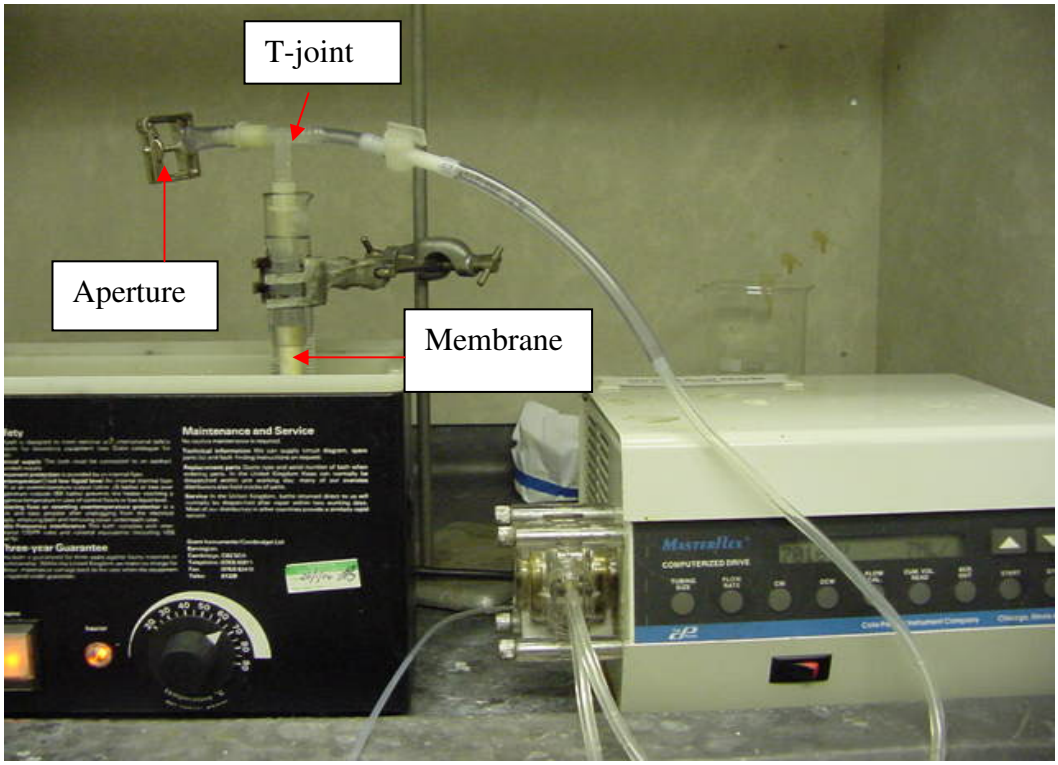

Figure 4.12: Experimental set-up for ELP under partial vacuum.

Figure 4.13: Membrane produced using ELP under partial vacuum.

4.2.4 Electroless Plating under Total Suction

The experimental set-up for this section involves the blocking of one end of the ceramic support while the other end is connected to the peristaltic pump. The hypothesis involved is the same as other modified methods; the suction created by the pump will drive the reaction solution through the membrane wall and fill up the pores with Pd metal in the process, thus reducing the amount of pinholes. The steps involved in the total suction technique are as follows:

a. The initial deposition of a membrane with conventional electroless plating for eight successive plating steps.
b. Then subjected to eight more plating steps with the top end of the membrane connected to the peristaltic pump and the flow rate set to 10 ml/min. The bottom end of the membrane is blocked using a plastic cap.
c. The final composite membrane obtained is then cleaned and dried. The membrane gas leak is then measured in a permeation cell.

The membrane obtained is shown in figure 4.14. The silvery appearance on the support surface conveys the successful deposition of Pd layer. The thickness of the palladium film evaluated from the estimated weight gain calculations to be 4 microns, which is extremely low compared to previous membranes. The surface deposition is also observed to be not as rough as previous membranes.

Figure 4.14: Membrane produced using ELP under total suction.

Figure 4.15 compares the He gas leak of the membrane fabricated under total suction with the conventional plated membrane, and it can be observed that the helium leak is higher than the conventional membrane. This indicates that there are pinholes still present.

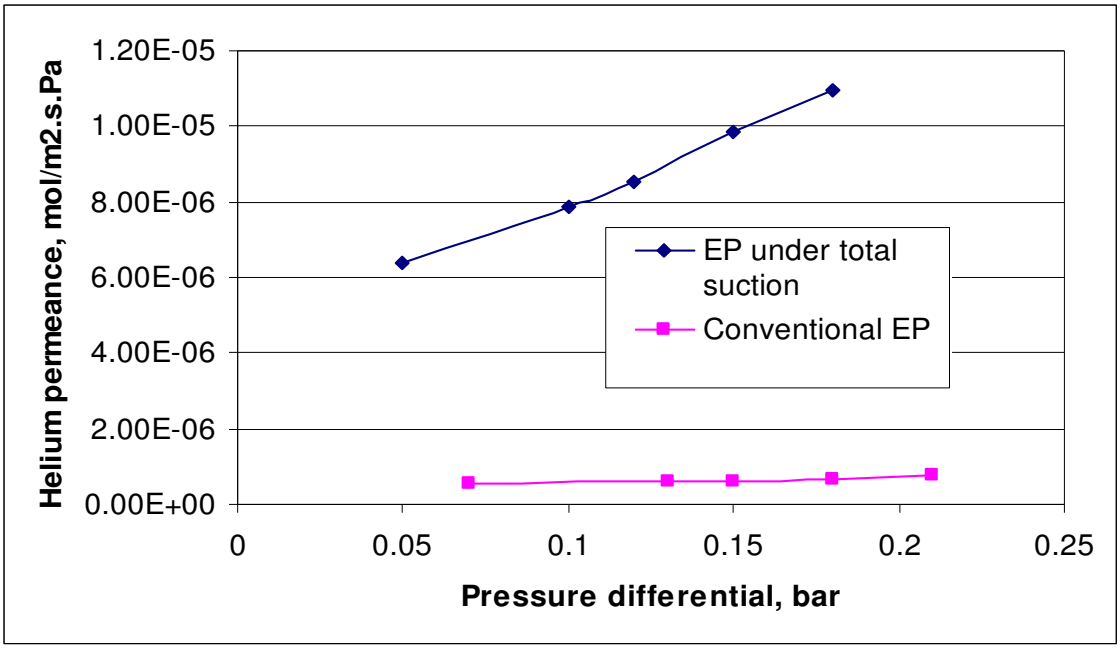

Figure 4.15: Graph showing the Helium gas permeance for the membrane produced using ELP under total suction in comparison with membrane produced using conventional ELP process.

The modified method did not provide the desired result due to the removal or peeling of the deposited Pd observed during plating. The pressure generated from suction not only acted on the membrane pinhole, but also on the stable Pd film and meta-stable Pd film forming on the surface. The effect of pressures has lead to the removal of palladium from the surface due to interfacial stresses.

The setback associated with the concept of total suction is the ability to provide a suction flow rate that is suitable during the course of deposition. During the initial stage of deposition, higher suction flow rates can encourage more deposition when there are still many uncoated pores available. Subsequently, the suction flow rate has to be reduced in order to relieve the stresses applied across the deposited palladium film for the densification process to work properly.

Therefore, it is felt that some improvement can still be sought in this technique by reducing the pressure effect on the membrane layer (by using partial suction instead). By doing so, the suction force applied will be split between the surface pores and membrane bore. The interfacial stresses would therefore not be too significant at later stages when Pd film is formed. Thus, the final set of test is conducted to verify this hypothesis.

4.2.5 Electroless Plating under Partial Suction

The experimental set-up here is exactly the same as total suction. The only difference this time is the bottom end of the bore side of the support tube is not completely blocked. A small apparture is made through the plastic cap using a needle. The procedure used is as follow:

a. The initial deposition with conventional ELP for eight successive plating steps.
b. Then subjected to eight more plating steps under partial suction with the flow rate of the peristaltic pump set to 30 ml/min.
c. The final composite membrane obtained is then cleaned and dried. The membrane gas permeances are then measured in a permeation cell.

Figure 4.16 shows the membrane under partial suction. The surface finish of the membrane is silvery (which conveys the successful deposition of Pd layer) and the texture of the surface is smoother than previously produced membranes. The thickness of the Pd film is estimated to be 16 microns.

Figure 4.16: Membrane produced using ELP under partial suction.

The result obtained from the He gas leak test of the membrane is shown in figure 4.17. It can be observed that the permeances is at a much lower value of 10^{-9} mol/m^2.s.Pa as opposed to the value of about 10^{-7} mol/m^2.s.Pa for the conventional fabricated membrane.

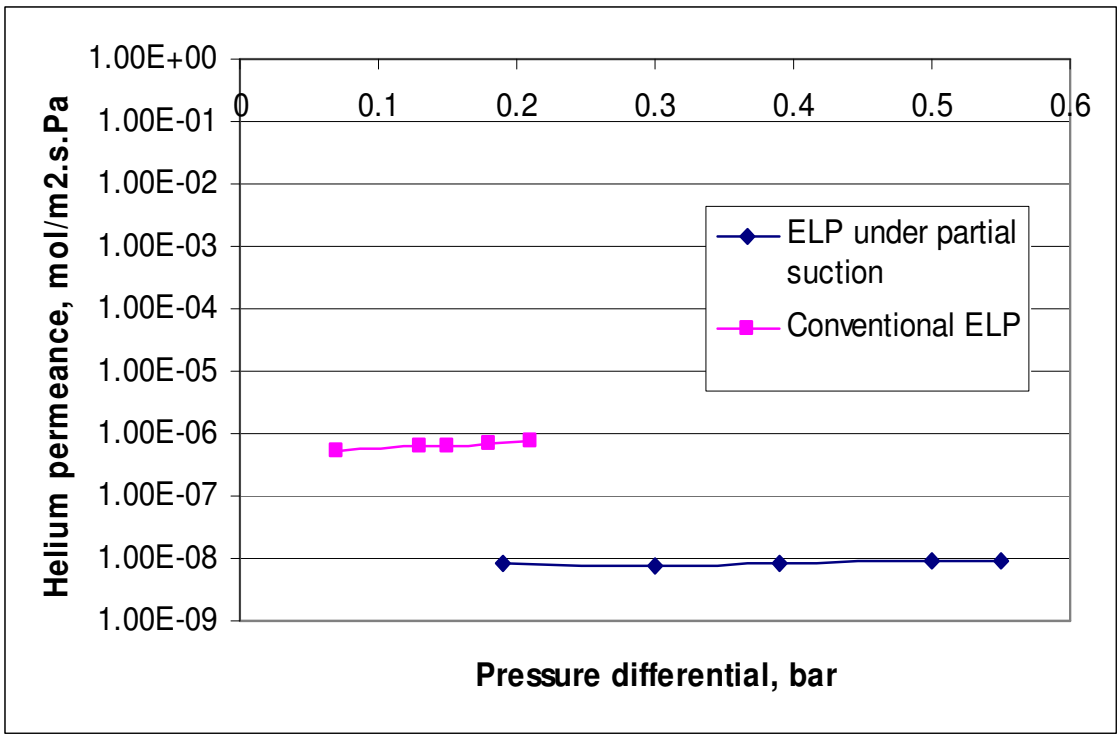

Figure 4.17: Graph showing the Helium gas leak for the membrane produced using ELP under partial suction in comparison with membrane produced using conventional ELP process.

However, during plating some Pd metal was observed to have fallen off from the membrane surface toward the fourth plating step under partial suction (plating step 10). This has indicated that the pressure acting on the membrane surface after the 9th step might be too high. These results obtained are extremely encouraging and it shows that the theory of modifying the conventional method does work. The following discussions were generated from the results obtained:

a. The partial suction allows the natural distribution of suction forces along the surface pinholes and through the bore side of the membrane simultaneously. In other words, additional interfacial stresses on the deposited layer are eliminated.

b. The circulation of the solution enhances the reaction rate and increases the rate of palladium deposition.

c. The Pd peeling effect at later stages during plating is also likely due to the high deposition rate provided by the partial suction whereby the Pd metal are being quickly formed and do not have sufficient time to adhere to the surface.

d. As each deposition leads to membrane densification, the suction effect has to be lowered gradually by reducing the pump flow rate in order to reduce the stresses induced.

e. The partial suction technique might have eliminated the entrapped air in the pinholes which is not possible with any other methods other than total suction technique. However, in total suction method there is a possibility of re-introducing pinholes due to subsequent higher vacuum application. Partial suction involves distribution of vacuum effects on the membrane surface and bore, thus bringing wider application of suction force.

f. The partial suction technique involves the subtle distribution of vacuum in the membrane bore as opposed to the gross distribution of vacuum with total suction technique. Besides that, the method used still has sufficient room for process optimisation by varying the pump flow rates.

4.3 Further Investigation

This stage of the project has identified the suitable fabrication procedure, composition of plating solution, and finally a suitable pore size of supports. Subsequent stages involve the scale up of the fabrication of membranes. In previous sub-chapters, membranes having the length of 6 cm while the length of the ceramic support used were 8 cm (1 cm from each ends are not plated for handling purposes). However, the actual length of the ceramic support obtained from the manufacturer is 37 cm, therefore the aim is to be able to produce a Pd membrane of this length.

Besides that, the membranes produced previously were not tested with H_2 gas. This is due to the fact that H_2 embrittlement will occur on Pd membranes at room temperature. The shorter membranes produced could not be tested at temperature. Therefore, in order to test the membrane at high temperature, the stainless steel reactor has to be utilised since it was designed to only accommodate the full length support. Producing a long Pd membrane would enable tests for H_2 permeability and selectivity to be carried out at high temperature.

Furthermore, it will be interesting if the method used to produce the shorter membrane can be utilised for scaling-up. Besides that, it will also be attractive for future commercialization purpose as more gas can be separated (higher output) with the large surface area of the longer membranes.

4.3.1 Experimental Work for 368 mm Long Membrane

From previous investigations, it is known that smaller pore size supports are more suitable for the separation process and henceforth the support used will be 30 nm. The main objective of this stage is to validate that the plating process finalised in previous chapter is still applicable for scaling up purposes. Hence, the first long membrane was produced using ELP with partial suction technique mentioned in subchapter 4.2.5 with the same flow rate of 30ml\min. Figure 4.20 shows the set-ups for the plating of the longer support.

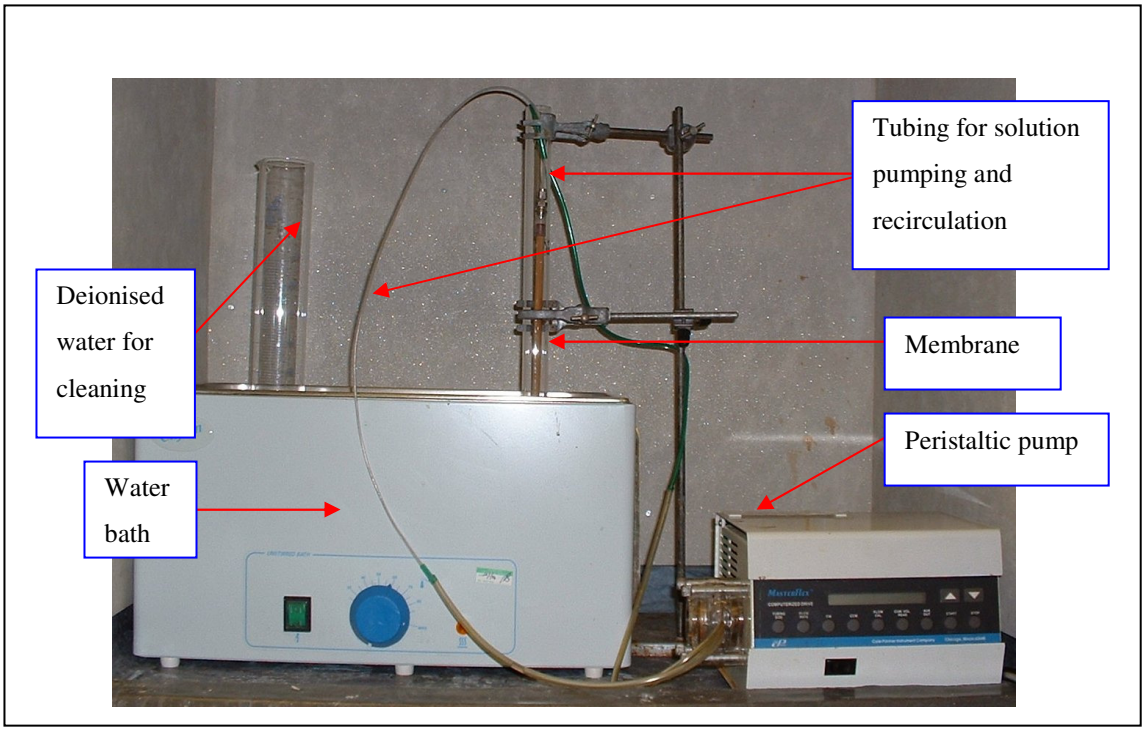

Figure 4.18: Picture showing the set-up for ELP with partial suction.

After cleaning and drying, the membrane is then subjected to permeation test at 400 ^{0}C using N_2 and H_2 gas. The result obtained from the gas permeability test was then summarised in table 4.4, figure 4.19 and 4.20.

Pressure Differential (bar)	Hydrogen Gas		Nitrogen Gas	
	Flow rate (ml\min)	Permeance (mol\m2.s.Pa)	Flow rate (ml\min)	Permeance (mol\m2.s.Pa)
0.1	720.5	4.60E-06	25.7	1.6E-07
0.2	1390.0	4.68E-06	56.1	1.8E-07
0.25	1581.1	4.04E-06	86.9	1.8E-07
0.3	1882.8	4.01E-06	120.0	1.9E-07
0.5	3599.4	4.60E-06	155.0	2.0E-07

Table 4.4: Membrane permeation result at 400 ^{0}C.

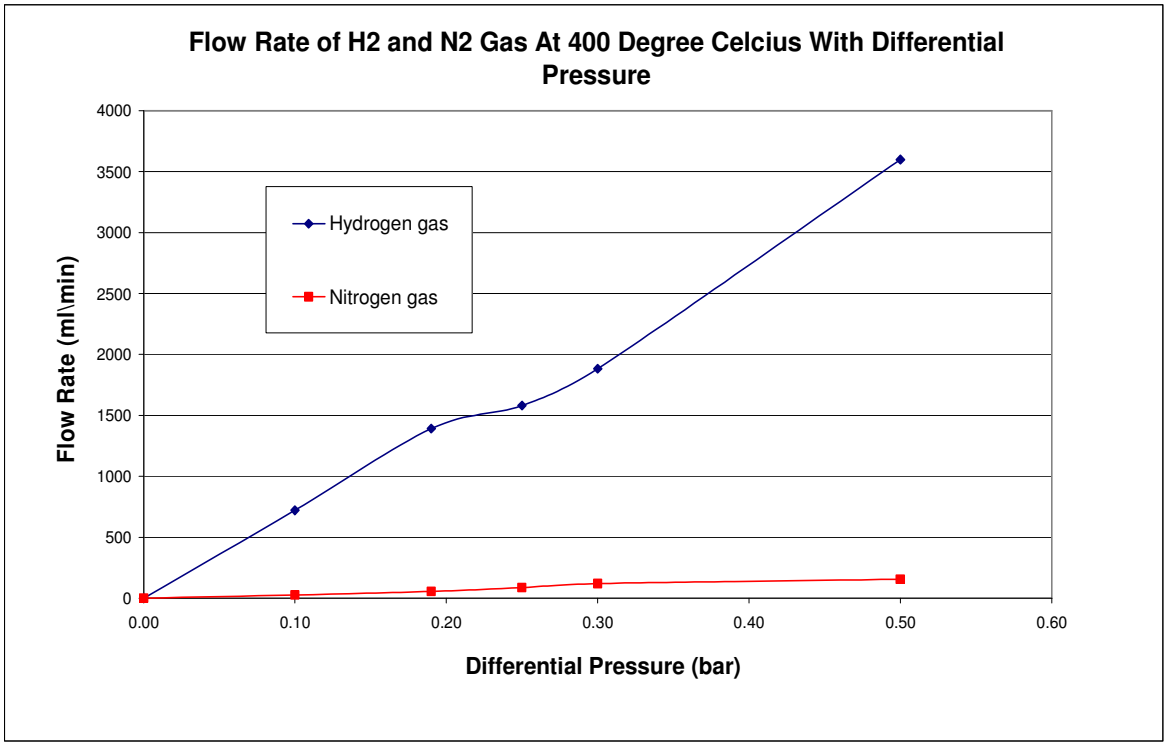

Figure 4.19: Graph showing flow rate of H_2 and N_2 gas at 400 ^{0}C with the pressure differential across membrane.

Visual inspection of the membrane produced showed a uniform coating of Pd metal for the entire length and the thickness estimated from weight gain measurements is about *20.1* microns. However, the surface is not as smooth as the shorter membrane produced previously, indicating a possibility of the membrane surface having high amount of pinholes. This was then reflected in the permeation results obtained, where N_2 gas was present in the product stream.

Nevertheless, from figure 4.19 it can be seen that the flow rate of H_2 gas for the similar pressure differential is significantly higher compared to N_2 gas. This is due to the properties of Pd metal, as once it is activated at temperature, only H_2 gas is allowed to pass through the membrane while N_2 gas can only pass through the pinholes or through the leaks from the membrane seal.

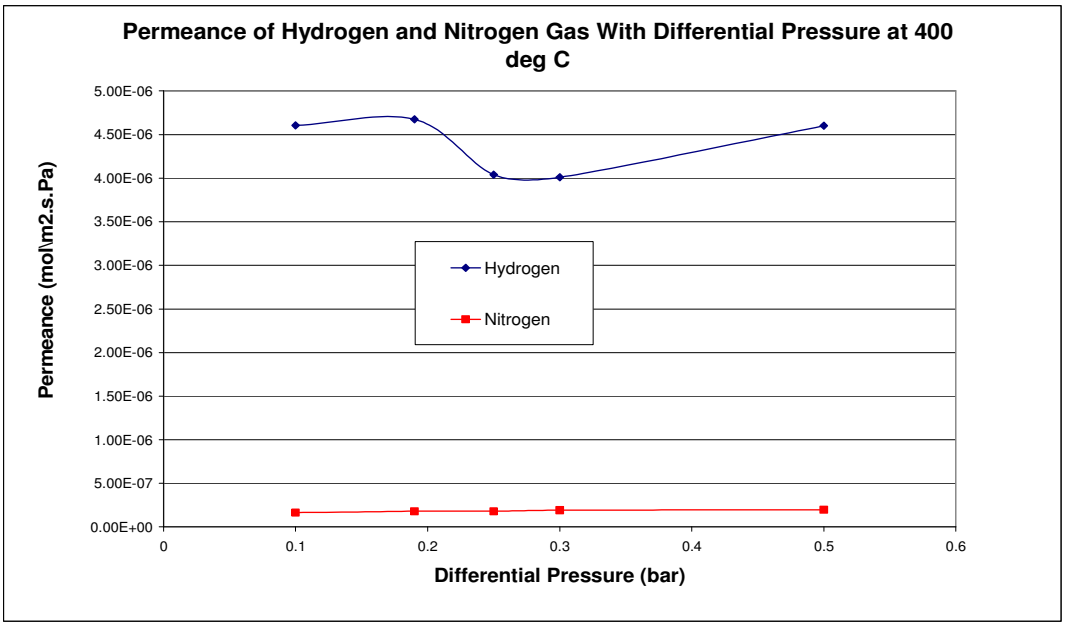

Figure 4.20: Graph showing the permeance of H_2 and N_2 gas at 400 ^{0}C with pressure differential across membrane.

The H_2/N_2 selectivity of the membrane is low, only 23 at 0.5 bars. Therefore, from the understandings gained from previous work on shorter membranes, the next step is to modify the fabrication method further in order to make it suitable for the production of a long membrane with a lesser amount of pinholes and a smoother surface finish.

4.3.2 Modification of 368 mm Long Membrane

It was known from the conclusion drawn in subchapter 4.2.6 that the plating procedure has a significant impact on the quality of the Pd layer produced. The membrane layer produced by the original ELP under partial suction for the shorter membrane tends to be thicker but less dense. Thus, the plating process has to be refined to make it more applicable for the deposition on the longer support. Besides that, the flow rate of the peristaltic pump has to be controlled such that the Pd metal deposited during plating can be compressed onto the formed layer by the pressure applied to provide a denser layer.

For the ease of identification and comparison purpose, the first long membrane produced (see section 4.3.1) is named as membrane A. It was produced using 16 plating steps consisting of eight conventional platings followed by eight steps with partial suction (with the flow rate of 30ml/min). However, the results obtained shows a poor membrane performance with high presence of N_2 gas.

The plating steps have therefore been reduced this time and the ceramic support plated only for a total of eight steps instead of the usual 16. Besides that, all eight plating steps are conducted under partial suction. A brief description of the procedure used is as follows:

1. Composition of the plating solution used will remain the same
2. Plating time remains the same, at one hour for each plating step
3. Pd deposition using ELP under partial suction for eight successive steps with the flow rate of 30 ml\min.
4. The membrane is eventually cleaned in hot water and then dried overnight in the oven.
5. The weight of the membrane was taken before it is subjected to permeation test at 400 ^{0}C using N_2 and H_2 gas.

The membrane (named as membrane B) display a smoother surface finish and the results obtained from the permeation tests are summarised in table 4.5. The H_2 gas permeance is almost the same as membrane A but the N_2 gas permeance is lower. Therefore, the average selectivity of the membrane for H_2/N_2 is moderately better at ~82.39 and the membrane thickness estimated from weight gain measurements is about *12.6* microns.

A major breakthrough has been achieved. This time, the Pd layer produced is thinner and has lesser amount of pinholes compared to membrane A. Furthermore, the membrane was produced using eight plating steps instead of 16, thus reducing considerably the time and amount of Pd metal used for membrane fabrication.

Pressure Differential (bar)	Hydrogen Gas		Nitrogen Gas	
	Flow rate (ml\min)	Permeance (mol\m2.s.Pa)	Flow rate (ml\min)	Permeance (mol\m2.s.Pa)
0.05	338.16	5.4024E-06	5.43	6.9398E-08
0.10	720.50	4.6041E-06	7.96	5.0866E-08
0.15	1207.75	5.1452E-06	12.60	5.3678E-08
0.20	1390.05	4.6751E-06	16.80	5.3678E-08
0.25	1581.14	4.0415E-06	20.53	5.2476E-08
0.30	2200.89	4.6881E-06	25.60	5.453E-08

Table 4.5: Membrane permeation result at 400 ^{0}C (membrane B).

While the amount of plating steps has been successfully reduced, the membrane performance still has to be improved. Therefore, the plating procedure has to be further refined to reduce the presence of pinholes.

4.3.3 Membrane Optimisation

Membrane B was produced using eight plating steps under partial suction at 30 ml\min flow for each step. The flow rate used for partial suction is crucial as it controls the pressure applied on the membrane layer, thus controlling the reaction rate as well. Hence, in order to produce a dense Pd layer, the flow rate used has to be varied for each of the plating steps.

The reason being that the flow rate of 30 ml/min during initial plating (1st and 2nd plating step) is deemed too high, and therefore the Pd deposition rate was too fast as observed from the intensity of the reaction during plating. Thus, the deposited Pd does not have enough time to adhere and densify onto the support. In addition, some small amount of Pd metal was observed to have coated onto the glass beaker instead of the ceramic support. Therefore, it was concluded that deposition rate has to be controlled by varying the flow rate of the pump.

After some trial and error and observing the reaction rate, the membrane was finally produced using the following procedure:

1. Composition of the plating solution used will remain the same
2. Plating time remains the same
3. Deposition using EP under partial suction for eight successive steps, with the following flow rate:

Plating steps	Suction flow rate
1 & 2	10 ml/min
3 & 4	15 ml/min
5 & 6	20 ml/min
7 & 8	30 ml/min

4. The membrane is eventually cleaned in hot water and then dried overnight in the oven.
5. The weight of the membrane was taken before it is subjected to permeation test at 400 ^{0}C using N_2 and H_2 gas.

The membrane (named as membrane C) produced exhibit a Pd layer with smooth surface finish and the results obtained from the permeation tests are summarised in table 4.6. The estimated membrane thickness from weight gain is about *8.67* microns, which is the lowest as compared to membrane A and B (see table 4.7 & figure 4.21). The nitrogen permeance obtained is also lower than membrane B, which is a good indication that the amount of pinholes has been reduced.

Pressure Differential (bar)	Hydrogen Gas		Nitrogen Gas	
	Flow rate (ml\min)	Permeance (mol\m2.s.Pa)	Flow rate (ml\min)	Permeance (mol\m2.s.Pa)
0.05	247.65	3.1567E-06	1.96	2.5049E-08
0.1	414.34	2.6455E-06	3.78	2.415E-08
0.15	538.29	2.2919E-06	6.89	2.9352E-08
0.2	680.77	2.1726E-06	8.47	2.7062E-08
0.3	-	-	12.00	2.5560E-08
0.4	-	-	15.80	2.5241E-08

Table 4.6: Membrane permeation result at 400 ^{0}C (membrane C).

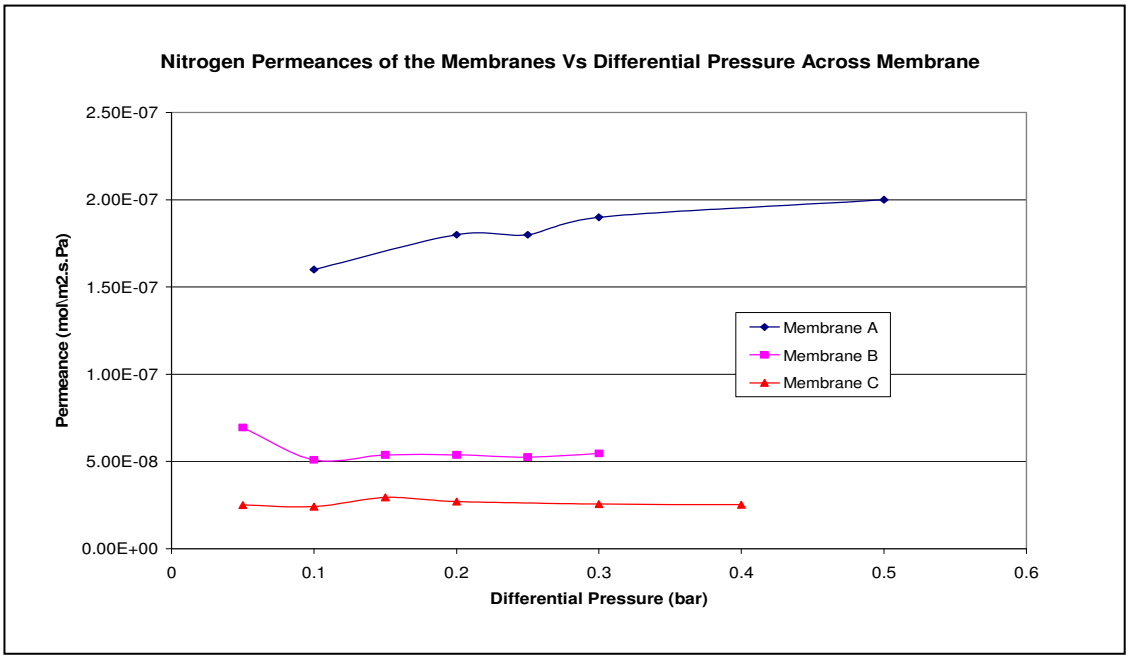

Figure 4.21: Graph showing the comparison of nitrogen permeance for all 3 membranes.

Membrane	Procedure Used	Thickness (µm)
Membrane A	8 EP conventional step + 8 EP with partial suction at 30 ml\min	20.10
Membrane B	8 EP with partial suction at 30 ml\min	12.60
Membrane C	8 EP with partial suction at variable flow rate	8.67

Table 4.7: Procedure used for membrane fabrication and their thickness.

However, at one point during the permeation test with H_2 gas when the differential pressure was slowly increased to 0.3 bar, the membrane suddenly failed and there was a huge amount of H_2 coming out from the reactor. The experiment was immediately stopped and the reactor was left cooling down before taken apart the next day for investigation. That is why there was no values obatined for H_2 permeance after differential pressure of 0.2 bar.Upon removing the membrane, it was confirmed that hydrogen embrittlement had cause the failure (see figure 4.24).

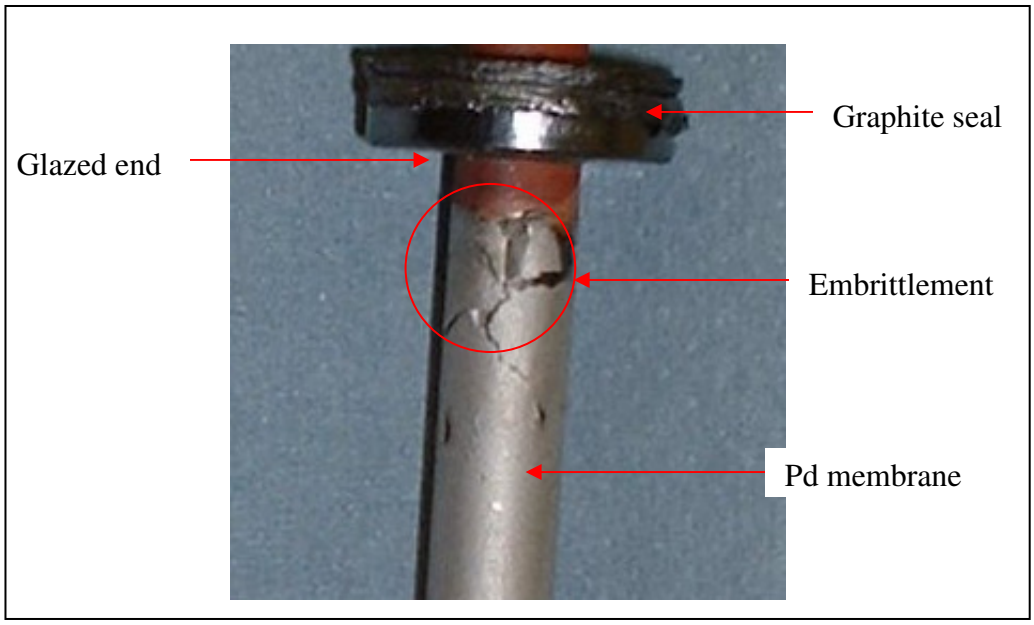

Figure 4.22: Picture of membrane C removed from the reactor.

The reason for embrittlement occurring at that particular part of the membrane is due the location of the entrance of feed gas. The high flow rate of feed gas flowing into the reactor is actually cooling down that part of the membrane. Therefore, the actual temperature for that particular zone will be significantly lower than the 400 ^{O}C set for the reactor and was also made worse with the lower thickness of Pd layer this time. As a result, the entrance of feed gas was modified in order to protect the membrane.

4.3.4 Reactor Modification

The membrane reactor design was modified to allow the feed gas to enter the reactor hot. Therefore, a pre-heater capable of heating the feed gas was incorporated to the reactor. This was done using a $^{1}/_{8}$" stainless steel 316L tube with the length of 1m coiled around the reactor (see figure 4.25) and the whole structure was then wrapped up with heating tape and insulated. This improvisation then allowed the feed gas and the membrane reactor to be heated up to the same operating temperature by using the same heating jacket and controller, thus saving space and cost.

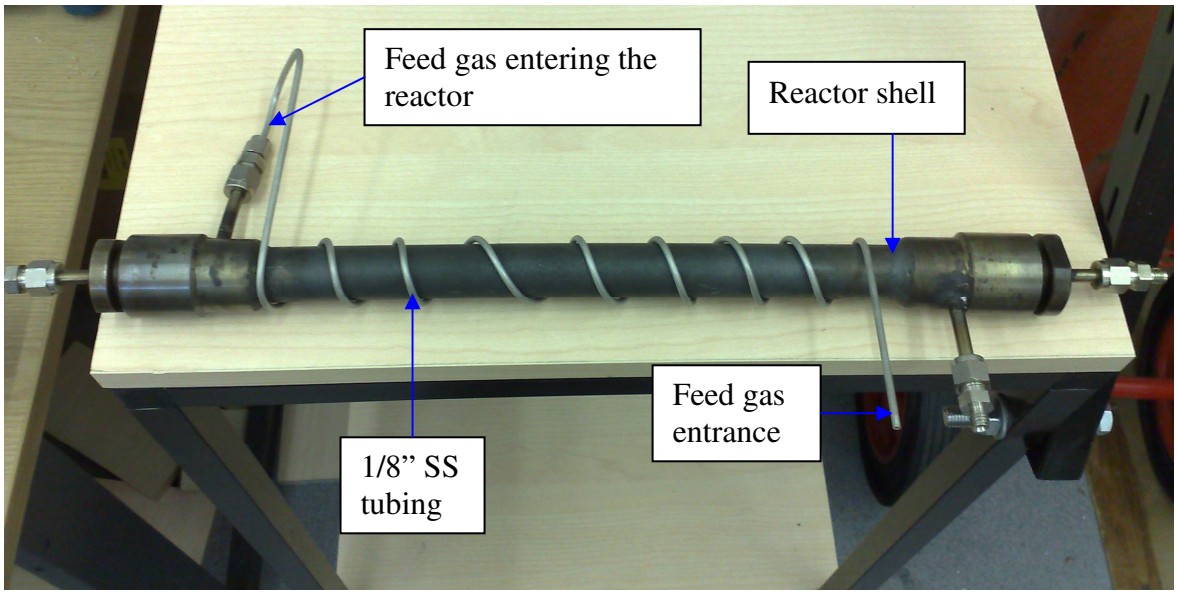

Figure 4.23: Picture showing the new membrane reactor incorporating the pre-heater for the feed gas.

4.4 Final Investigation and Analysis

As the previous membrane produced (membrane C) was damaged by hydrogen embrittlement, a new membrane has to be produced in order to be tested in the new reactor design. Hence, another membrane (membrane 8.0) was produced using the exact same procedure used for membrane C. The estimated membrane thickness obtained this time was about 8.25 microns as compared to 8.67 microns for membrane C. The membrane also exhibits a smooth and silvery surface finish as its predecessor. The ability to produce the membrane with almost the same thickness was encouraging as it shows the reproducibility of the plating method.

As most of the exploratory works has already been conducted, the plan of work this time will concentrate on the effects of:

1. Varying the operating temperature of the membrane reactor.
2. Varying the differential pressure across the membrane.
3. Gas permeation test and GC analysis using:
    a. Nitrogen gas.
    b. Hydrogen gas
    c. H_2 Mixture: *67% hydrogen (H_2), 32% carbon dioxide (CO_2), 0.1% carbon monoxide (CO) and 0.9% of methane (CH_4).*
4. SEM analysis of the Pd membrane layer.

4.4.1 Experimental Plan

Initially, the membrane was subjected to N_2 gas permeation test with the reactor operating at 250 ^{0}C and the pressure slowly increased from 0.1 to 0.8 bar. The experiment was then repeated with the reactor operating at 300 and 400 ^{0}C, and by using pure H_2 and H_2 mixture as feed gas respectively. Figure 4.24 shows the diagram of the experimental work executed. The product was then measured by the flow-meter to obtain the total permeate flow-rate before being analysed by the GC.

However, due to the high concentration of H_2 in the product gas, the GC was not able to provide an accurate reading for H_2 concentration since it was not originally configured for high purity gas analysis. Therefore the percentage of H_2 was obtained by residual gas analysis (i.e. by subtracting the present of other gases instead). Besides that, the GC is more accurate in quantifying smaller concentration of gases.

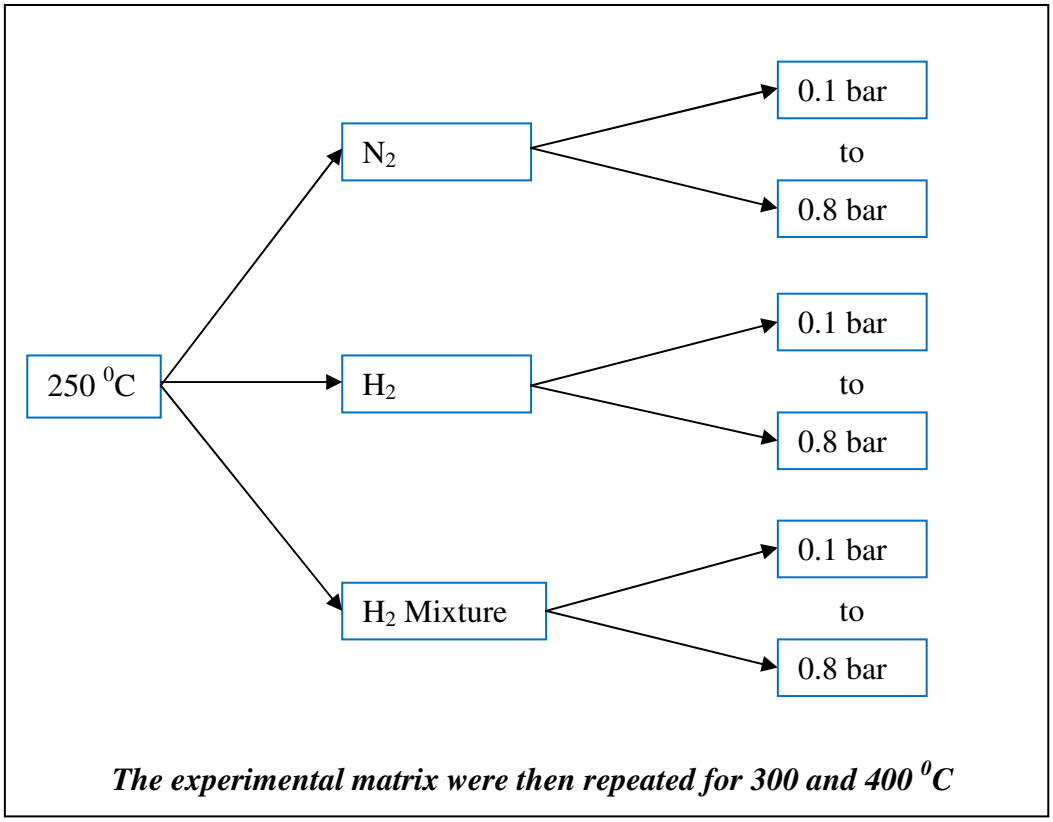

Figure 4.24: Diagram showing the matrix of experimental works planned and conducted.

4.4.2 Gas Permeation with Pure Nitrogen and Hydrogen

In theory, a defect free Pd membrane are impermeable to other gases, so the presence of N_2 flux through the membrane is an indication that the membrane layer might contain pinholes or a possibility of a leak with the membrane sealing. Nonetheless, the average H_2/N_2 selectivity of the membrane is about 140 (at 400 ^{0}C), which is the highest obtained in this study so far. While the estimated thickness calculated from weight gain is ~ 8.23 microns as compared to membrane C at ~ 8.67 microns. The results obtained showed that this is the best membrane produced so far in this work. For the ease of analysis and comparison purpose, the results obtained from experiments are summarises in table 4.8 and the data's were used to plot figure 4.25 to 4.29.

Figure 4.25 shows the pure N_2 and H_2 flux and depict their dependence on differential pressure and temperature for the composite membrane. An increase in the operating temperature and pressure difference will lead to an increase of the H_2 flux. However, the nitrogen flux is also increasing with increasing pressure due to the present of pinholes or leakage within the graphite sealing system (the leak reduces when the reactor seals were tightened harder as the seal will then be further compressed).

Gas Feed	Permeate	Temp °C	Pressure Drop (bar)									
			0.10	**0.15**	**0.20**	**0.25**	**0.30**	**0.40**	**0.50**	**0.60**	**0.70**	**0.80**
Pure H_2	H_2 flux (mol\m^2.s)	400	0.016397	0.030406	0.044609	0.058230	0.073573	0.100966	0.128984	0.153644	0.176885	0.203999
		300	0.014396	0.025500	0.037249	0.046093	0.058553	0.080696	0.105873	0.124594	0.144607	0.167201
		250	0.014009	0.023563	0.029373	0.039057	0.046158	0.064557	0.080696	0.098771	0.118138	0.131050
Pure N_2	N_2 flux (mol\m^2.s)	400	0.000082	0.000113	0.000145	0.000171	0.000210	0.000298	0.000382	0.000472	0.000554	0.00630
		300	0.000115	0.000168	0.000216	0.000281	0.000337	0.000469	0.000588	0.000720	0.000845	0.000980
		250	0.000132	0.000180	0.000252	0.000318	0.000394	0.000521	0.000665	0.000807	0.000980	0.001110
H_2/CO_2 (67/33)	H_2 flux (mol\m^2.s)	400	0.000566	0.000994	0.001749	0.002350	0.003822	0.008328	0.015364	0.023628	0.033892	0.046222
		300	0.000614	0.001143	0.001834	0.002524	0.003802	0.007876	0.013815	0.020271	0.028469	0.036991
		250	0.000598	0.001033	0.001833	0.002526	0.003880	0.006972	0.011233	0.015752	0.020335	0.024854
	H_2 Purity (%)	400	77.813	81.268	84.760	86.681	89.639	93.193	95.447	96.465	97.003	97.306
		300	75.244	78.102	81.414	83.959	87.156	91.742	94.298	95.450	96.103	96.477
		250	73.740	76.123	80.214	83.139	86.351	90.016	92.365	93.484	94.022	94.338

Table 4.8: Gas permeation results obtained with varying temperature and pressure drop for pure N_2, pure H_2 and H_2 mixtures.

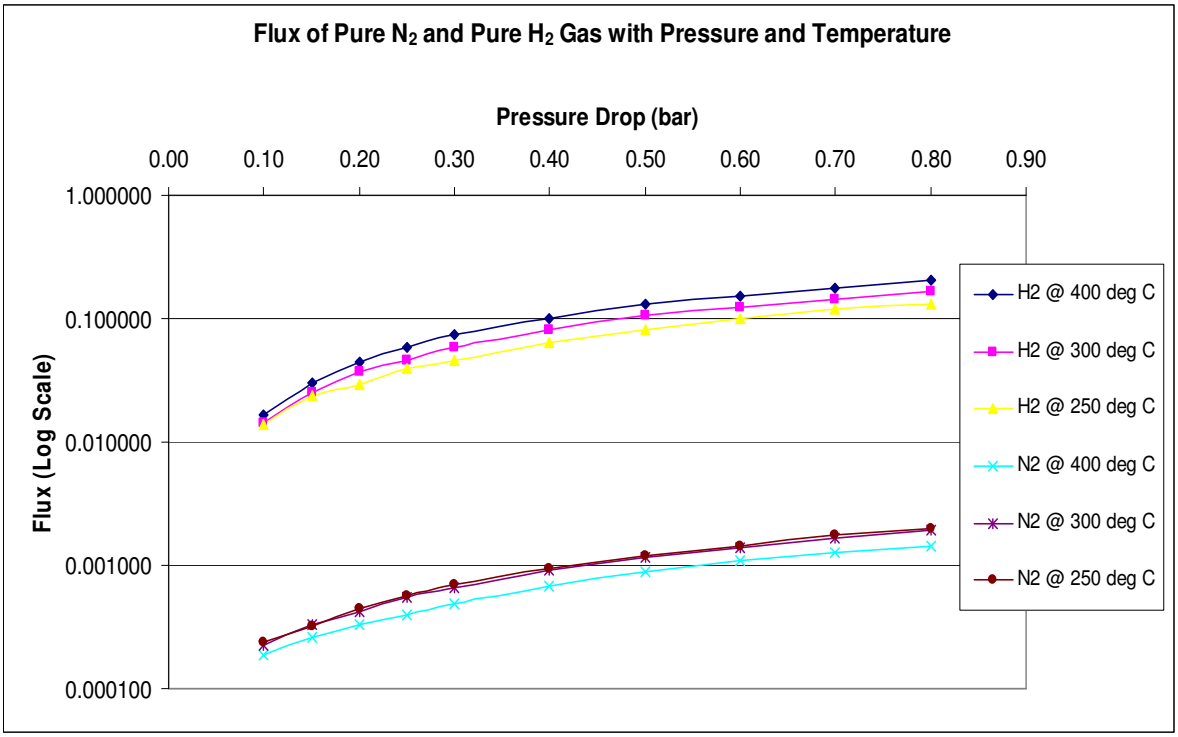

Figure 4.25: Graph showing the fluxes of pure H_2 and N_2 gas in Log scale with temperature and pressure drop.

On the other hand once Pd metal is activated at temperature, in theory only H_2 gas is allowed to pass through it while N_2 gas molecules can only pass through pinholes or leaks from the graphite seal. Thus, the N_2 fluxes will drop with increasing temperature but will increase with increasing pressure. This is due to more molecules of N_2 are forced through the pinholes or leaks by increasing the pressure but not by increasing temperature.

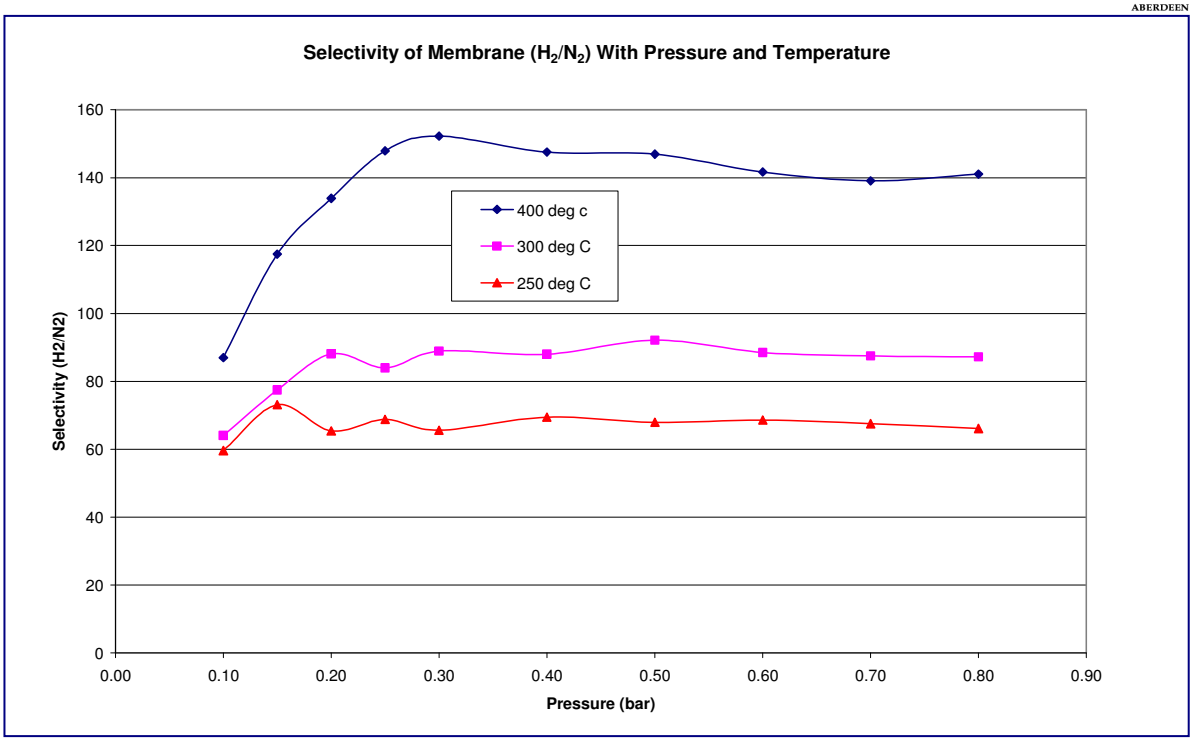

Figure 4.26: Graph showing the selectivity (H_2/N_2) of the membrane with temperature and pressure drop.

Figure 4.26 shows the H_2/N_2 selectivity of the membrane in relation with pressure and temperature. The results show that the selectivity of the membrane increases with increasing temperature but remains almost constant with increasing pressure due to the same reasons mentioned above. In theory, the selectivity of dense Pd membrane to H_2/N_2 is infinity as it only permeable to H_2 gas. However, in practice the Pd film deposited is not perfect and there are always pinholes present and thus there is a finite number for selectivity.

The fluctuation of the selectivity at lower pressures shown in the graph is due to the structural changes induced by the atomic re-odering/re-crystallization between the Pd film and the titania layer when the feed gases are introduced, and will become stable after that a period of time. This trend can be seen in all the graphs plot at lower pressures drop region of 0.1 – 0.5 bar.

4.4.3 Gas Permeation for Using H_2 Mixtures

Similar experiments of varying pressure and temperature were repeated by using mixed gases as feed and the results obtained are then summarized in figure 4.27 to 4.29 and table 4.8 to 4.9.

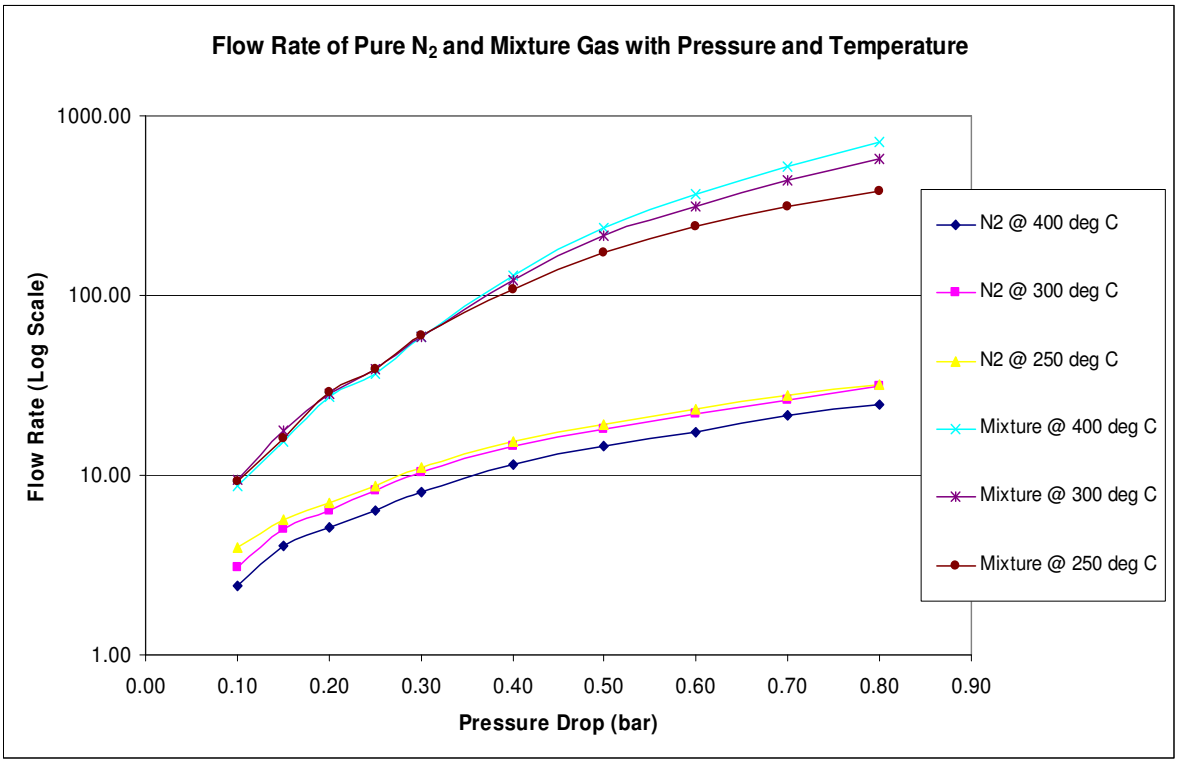

Figure 4.27: Graph showing the flowrate of N_2 and product gases of H_2 mixture in Log scale with temperature and pressure.

It is known that the hydrogen flux/permeation is dependent on the trans-membrane pressure difference, and hydrogen diffusivity through the Pd metal. Therefore, as expected from figure 4.27, the hydrogen flow/permeation data shows a strong dependence on pressure and temperature, as seen from previous results obtained. Figure 4.28 show their comparison with pure H_2 feed gas while figure 4.29 shows the concentration of H_2 gas in the permeate stream.

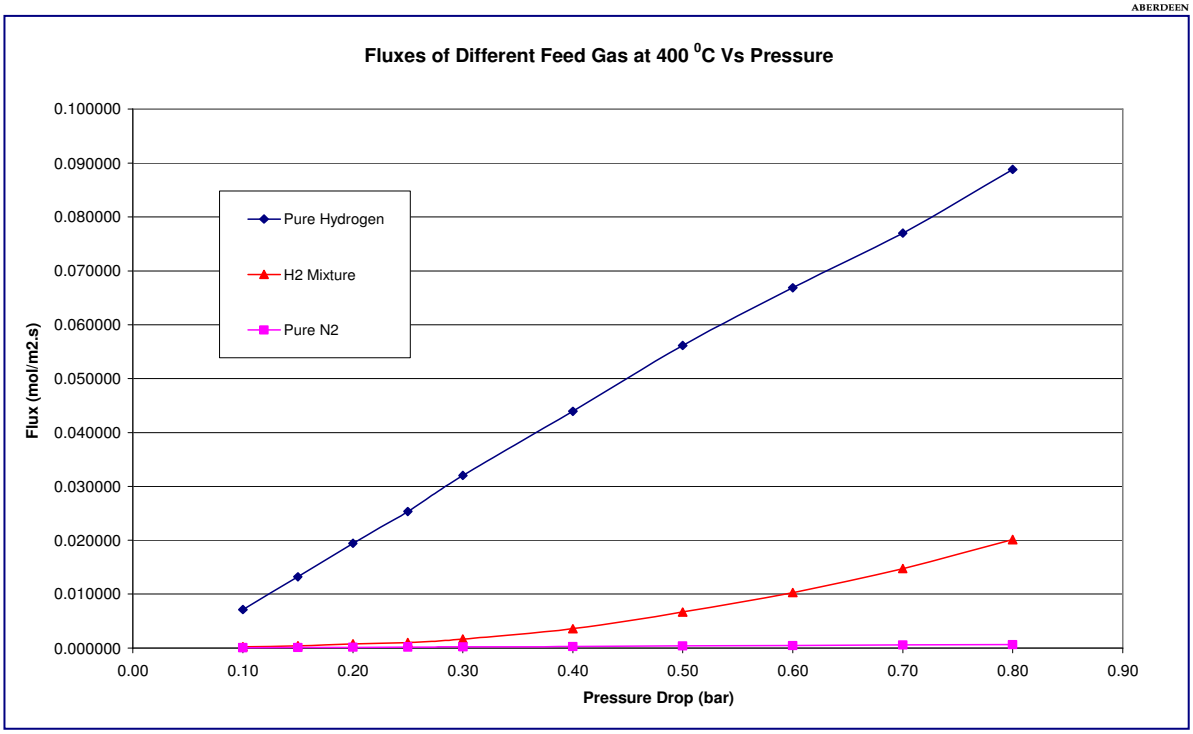

Figure 4.28: Graph showing the comparison of fluxes for pure N_2, pure H_2 and H_2 mixture as feed gases.

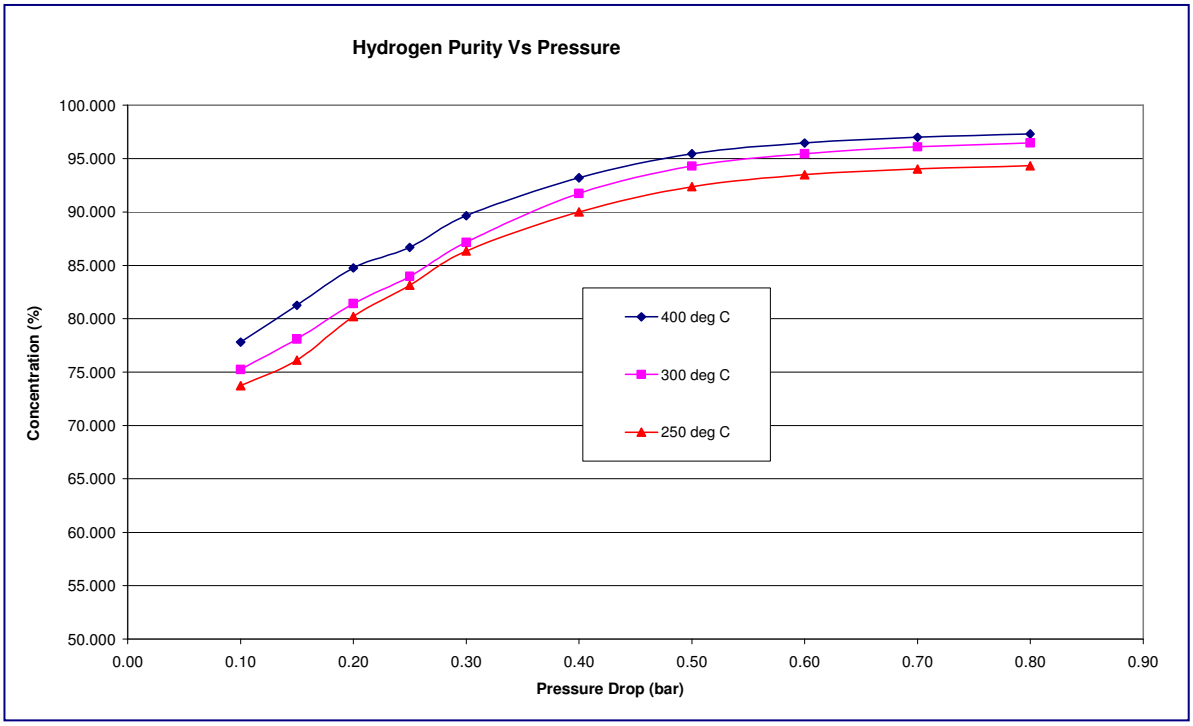

Figure 4.29: Graph showing the purity of H_2 in the product stream using the H_2 mixture as feeds at temperature and pressure.

The non-linearity of H_2 flux shown in figure 4.28 is due to the presence of other gases within the mixture that will certainly obstruct the adsorption of H_2 molecules (boundary layer effect), thus lowering the H_2 flux across the membrane. The results also suggest the existence of a concentration profile across the membrane which leads to a decrease of the hydrogen concentration in the upstream side of the membrane, and thus reduces the actual permeation driving force.

As H_2 gas starts to permeate across the membrane, the concentration of H_2 in the downstream side will also increase. Meanwhile, the concentration of H_2 in the upstream (retentate) side will remain the same as it is constantly being supplied from the cylinder bottle. As a result, the partial pressure of H_2 in the downstream (permeate) side will slowly increase and will eventually reduce the permeation driving force due to equilibrium in mass transfer.

The actual partial pressure of H_2 across the membrane would be low and the operating pressure has to be set higher to compensate for this. An example would be a mixed gas containing 50% H_2 and 50% N_2 and in order to attain a hydrogen partial pressure of 0.8 bar across the membrane, the operating pressure has to be set to 1.6 bar.

The hydrogen purity plot (figure 4.29) also shows the same trend of strong dependence on pressure and temperature but it is apparent from the results obtained that the purity of H_2 increases significantly at the beginning but then the increase eventually levelled off with increasing pressure. This is because the increasing H_2 purity will lead to a reduction of driving force across the membrane as it will increase the partial pressure of H_2 in the downstream side. Hence, in order to obtain a higher purity, the operating pressures have to be set higher.

Unfortunately, the reactor was only pressure tested up to 3 bars at atmospheric temperature. Therefore, for safety reasons the experiments were not conducted higher than 1.6 bar at 400 ^{0}C. However, the purity of the H_2 gas obtained is sufficient to run a fuel cell (see table 4.8 & 4.9).

Partial Pressure of H_2 Upstream (bar)	Purity of H_2 @ 400 ^{0}C (Downstream) (%)	Purity of H_2 @ 300 ^{0}C (Downstream) (%)	Purity of H_2 @ 250 ^{0}C (Downstream) (%)
0.10	77.81	75.24	73.74
0.15	81.27	78.10	76.123
0.20	84.76	81.41	80.21
0.25	86.68	83.96	83.14
0.30	89.64	87.16	86.35
0.40	93.19	91.74	90.01
0.50	95.45	94.30	92.36
0.60	96.465	95.45	93.49
0.70	97.00	96.10	94.02
0.80	97.31	96.48	94.34

Table 4.9: Table showing the purity of H_2 gas in the product stream at different temperature and pressure using H_2 mixture as feed.

4.4.4 SEM Analysis

For SEM analysis, the membrane was broken into small pieces for SEM imaging. Images obtained from the SEM are shown in figure 4.30 to 4.32.

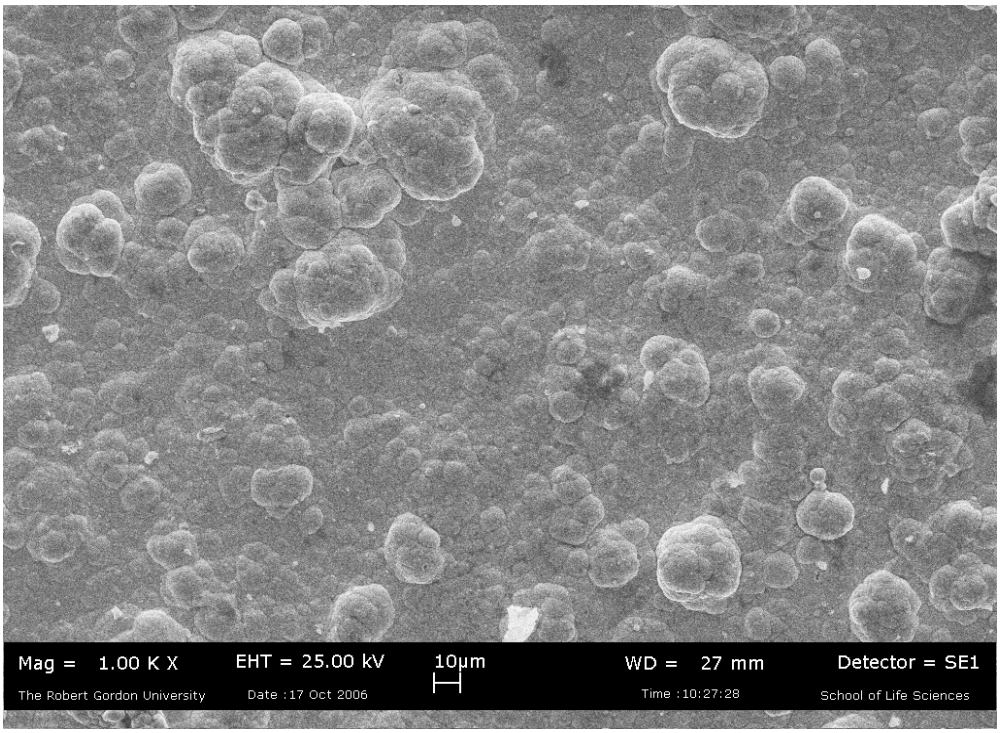

Figure 4.30: SEM image of the Pd membrane surface at 1000X magnification.

SEM micrographs obtained show that the films produced by this modified technique are dense and uniform in cross-section. Figure 4.30 shows the surface of the membrane and it shows a rough texture with many features larger than 10µm in diameter. The high surface roughness might be an advantage as it will help to increase the surface area for which the hydrogen dissociation reaction may take place.

The image in figure 4.32 shows that the thickness of the membrane layer is abut 6 microns (µm), which is slightly lower then the estimated thickness from weight gain of 8.25 µm, calculated by assuming a dense film, and then extrapolating from the weight and area of the sample. The discrepancy in weight is due to the fact the SEM analysis does not take into consideration that some Pd metals would have been deposited into the support pores during plating.

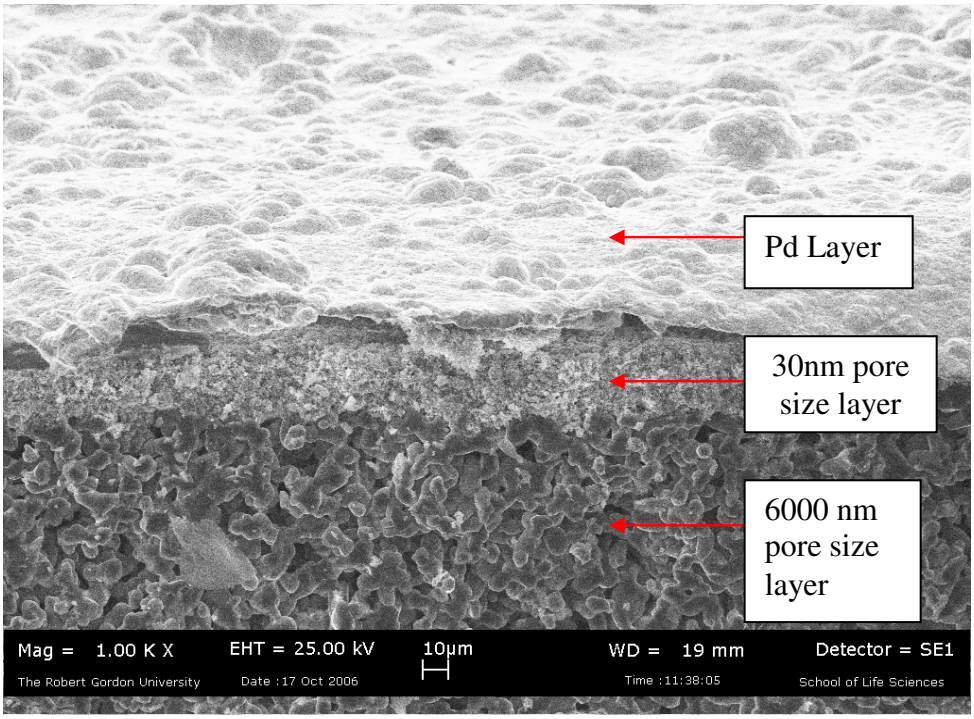

Figure 4.31: SEM cross-section image of the membrane at 1000 X magnification.

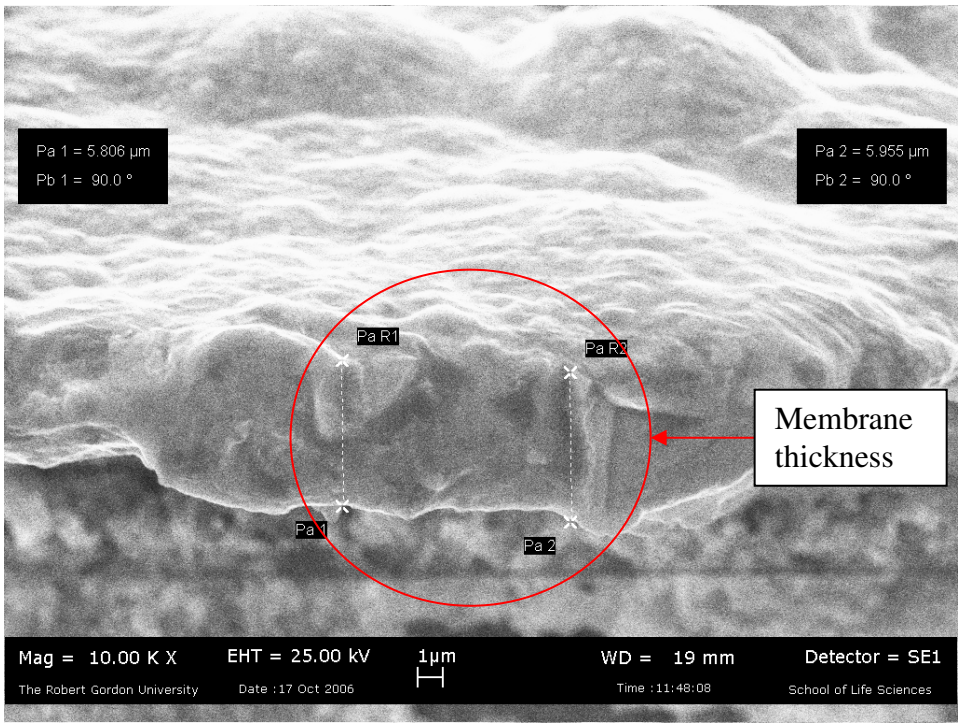

Figure 4.32: SEM image of the membrane layer at 10,000X magnification.

4.5 References

1. JOHN P. COLLINS and J. DOUGLAS WAY, 1993. **Preparation and Characterization of a Composite Palladium-Ceramic Membrane**, *Industrial and Engineering Chemistry Research 32*, pg. 3006-3013.
2. J.N. KEULER, L. LORENZEN, R.D. SANDERSON, V. PROZESKY, W. J. PRZYBYLOWICZ, 1999. **Characterization of Electroless Plated Palladium-Silver Alloy Membranes**, *Thin Solid Films 347*, pg. 91-98.

CHAPTER 5

5.0 Discussions

Electroless plating of Pd membranes have been carried out on the surface and within the pores of a γ-Al_2O_3 layer elaborating a thin film. The thickness of the film was estimated by weight gain. The film growth rate depicts a maximum, a common feature of ELP of Pd and is attributed to a combination of an increasing mass transfer of Pd from the membrane surface to the of bath ingredients.

The initial rate of Pd transfer to the support is determined by the coverage of Pd nuclei. As more nascent crystallites of Pd are deposited an increase in the hydrazine oxidation rate is enhanced, thereby corresponding to an increase in the Pd growth rate. Eventually the entire substrate is completely covered with Pd. The weight Pd loading enables an estimate of the "equivalent Pd membrane thickness''. The permeation measurements for the several membrane types have a linear dependence of the H_2 flow on Δp_{H2}

5.1 Discussions on Fabrication Methods

5.1.1 Discussions for Initial Investigation

At this stage, a number of different experiments have been conducted in order to gain the fundamental knowledge of the ELP process and to better understand the effects of variables such:

1. *Type of Pd precursor used for plating*
2. *Effect of composition of the plating solution*
3. *Effect of the number of plating deposition*
4. *Pore size of the ceramic support used*

These experiments were designed to relate the effect of the ceramic support and plating solution used. Although the membranes produced show a metallic surface finish, they still have a large number of pinholes on them as evidenced by the leak test. Therefore, it was essential to modify the procedure for electroless plating, or the plating process itself. Nonetheless, the knowledge obtained by doing all these experiments is extremely encouraging and constructive. The following conclusions were drawn from conducting these preliminary tests:

a. The chloride precursor is more suitable as it contained higher concentration of Pd metal than nitrate precursor, thus offering more metal for transfer during each plating step. Apart from that, it reduces the amount of plating steps required to produce a thin Pd film. This will then lead to the reduction in time and cost of fabrication.

b. The composition of the plating solution is an important factor in order to provide a stable plating environment for the support. From the tests conducted, it can be observed that plating with an electroless bath with higher Pd composition will definitely increase the thickness of the palladium film. However, it will also affect the film stability, formation of a dense layer and membrane. The deposition rate of the solution is observed to be extremely high, as the solution also started to coat the wall of the glass cylinder vessel used. The test has also indicated that the rate of reaction/plating can be controlled by varying the amount of reducing agent (hydrazine) and the amount of Pd metal added to the solution.

c. The pore size of the ceramic support also plays a crucial role. The lower pore size allows the support to form a dense Pd film at a shorter time and performs better in leak tests than the higher pore size support. The reason is that at higher pore size, the Pd metal will get deposited deeper into the layer of the support to fill up the big pore instead of being deposited on top of each another to form a dense layer. Therefore, higher pore size supports are certainly not suitable for this application. Hence, all the membrane fabrication from this point onward will be coated/plated on 30 nm supports.

d. The Pd film thickness will undoubtedly increase with the number of plating steps. However, it does not necessary follow that a denser layer can be produced as there are other variables, such as the one mentioned above. Beside that, the ELP process has mass transfer limitation too. For example, as the amount of Pd metal deposited on the support approaches the amount of Pd available in the solution, an equilibrium state is attained and the metal transfer will tend to go from the membrane to the solution instead. Therefore, the fundamentals involved in the pinhole reduction are going to be elucidated and more tests carried out in the next set of experiments that are designed to address these issues

5.1.2 Discussions for Pinhole Reduction Methodologies

The following discussions and conclusions are presented for the Pd membranes prepared using different methodologies targeted for pinhole reduction:

a. ELP under Osmosis involved the damage to the Pd film due to the subsequent locking up of salt solution in the micropores which eventually caused interfacial stresses during membrane drying.

b. ELP with water circulation and partial vacuum has not materialised to provide the type of surface finish and results desired.

c. ELP with total suction provided intermediate results with a surface smoothness improvement from the roughness observed with conventional methods. The membrane permeances is still high, which means that the technique still unable to reduce the amount of pinholes.

d. ELP with partial suction was identified as the breakthrough in this work with the desired finish on the membrane surface (which indicates the present of Pd film). However, there is still room for improvement with wide range of flow rate available in peristaltic pump (7 – 700 ml/min) to control the amount of pressure acting on the membrane surface.

e. The developed technique is believed to be suitable and applicable for supports with wide variety of pore size (ranging from 30 nm – 6000 nm pore size) by varying the parameters (varying the pump flow rate) during deposition. In other words, the novelty of the technology is not constrained to the support but to the process itself.

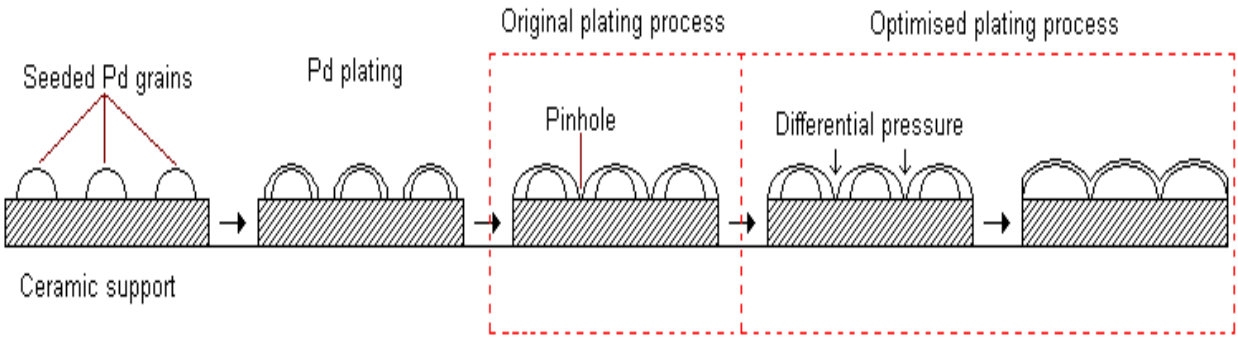

Figure 5.1: Schematic diagram of ELP with partial suction.

f. Figure 5.1 shows the schematic diagram of deposition during ELP with partial suction. The membrane produced also displays a smoother surface finish due to the densification of deposited palladium owing to the pressure applied.

g. ELP with partial suction also allows for a quicker deposition of Pd metal and the silvery surface finish appear much sooner than the conventional method. Figure 5.2 shows the comparison of the membrane surface finish for the conventional and optimised plating process.

h. The future work shall look forward to the development of a longer palladium membrane that can be tested using the stainless steel membrane reactors to obtain the membrane selectivity, stability and performance at higher temperature.

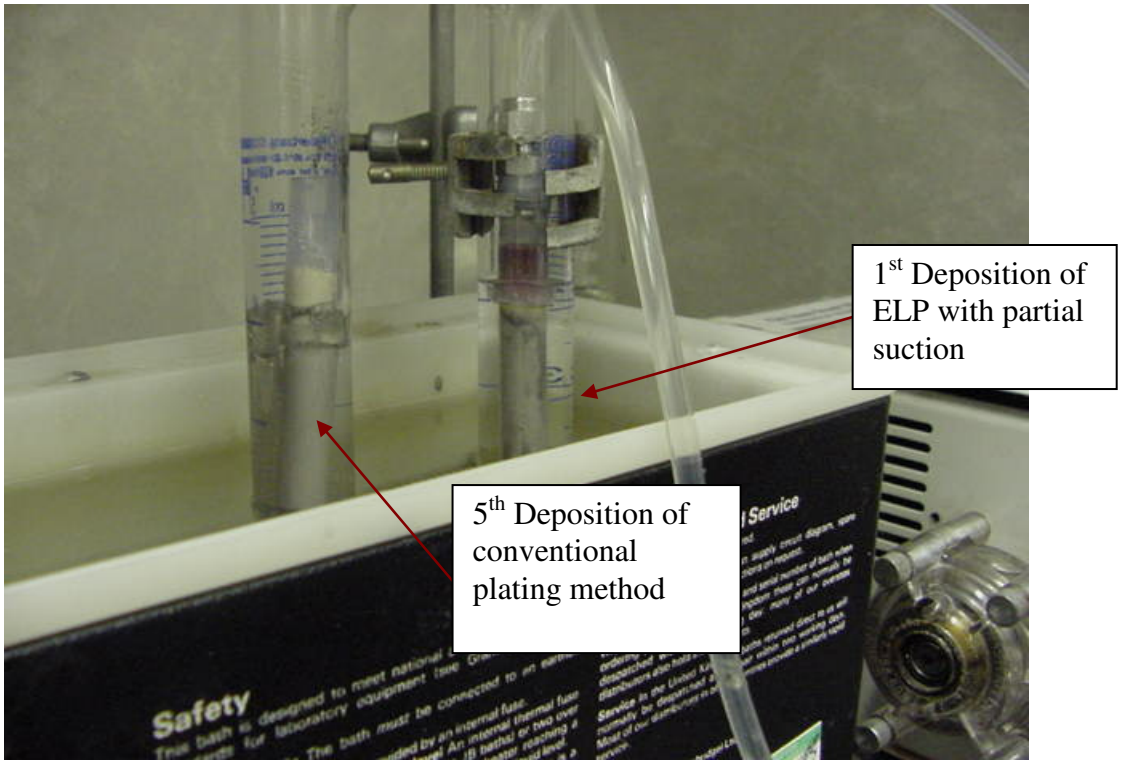

Figure 5.2: Picture showing the evidence of a faster deposition using the optimised method.

5.1.3 Discussion for Further Investigation (*Longer Membrane*)

Findings from the experiments conducted for this subchapter is presented as follows:

i. Fabrication of the 1st longer membrane was successful using the original ELP under partial suction method without any modification for 16 consecutive steps for one hour each (the same parameters used for the shorter membrane produced with EP under partial suction). However, the permeation result obtained for the membrane revealed the present of a significant amount of pinholes.

ii. The procedure for ELP under partial suction method has to be modified in order to reduce the amount of pinholes present and to increase the density of the Pd layer.

iii. The first modification involves the reduction of the number of plating steps. From observation, the ELP under partial suction has a high metal deposition rate, as some peeling effect could be seen at later plating steps during plating. Therefore, it is deemed unnecessary to have the eight conventional ELP plating steps as it is time consuming and the metal deposition rate is slow. Besides that, it is easier to control the rate of metal deposition by adjusting the flow rate on the peristaltic pump.

iv. The thickness of the Pd layer produced this time is thinner and also denser than the 1st membrane. Although, the results obtained are better, it still shows the presence of pinholes. Therefore, better control on how the Pd layer is formed will be crucial.

v. Hence, the next modification involves varying the flow rate of the peristaltic pump for each plating steps in order to have a better control of the deposition rate. The reaction rate was adjusted slower for the initial stages of plating so that the Pd metal can formed slower and have enough time to adhere on to the support surface. Then, increasing the flow rate of the pump for the later stages of plating to provide enough pressure for the Pd metal formed to be compressed on to the already formed layer to give a final dense Pd layer.

vi. The Pd layer produced was much thinner and the N_2 permeance was also lower, which suggested that the hypothesis for the modification has work. Unfortunately, the membrane has undergone H_2 embrittlement before any more meaningful result was extracted from it. Therefore, the reactor has to be modified before anymore test can be conducted.

5.1.4 Discussions for Final Investigation (*Validation for Reproducibility*)

The successful fabrication of an additional long membrane validated the reproducibility of the modified ELP under partial suction method. The membrane produced exhibit the same surface properties as membrane C, which has a smooth and uniform silvery surface finish. However, a higher magnification of the surface (figure 4.30) using SEM analysis showed a rough surface texture with many Pd particles larger than 10µm in diameter.

Nonetheless, it is still too early to judge whether the surface roughness would have any significant influence in its performance as another membrane with a finer Pd particles at the same thickness would have to be produced for comparison. But in order to do so, the EP method would have to be modified again so that the Pd metal contained in the plating solution can dissolve better and thus creating a much finer Pd grain. Consequently, more research work is still required in order to verify this hypothesis.

The membrane produced in this chapter still contains pinholes as indicated by the presence of N_2 gas in the permeate stream. Nonetheless from works done in previous subchapters, it is known that the amount of pinholes can be reduce or eliminate by adjusting the flow rate of the partial suction technique and plating steps required either by slowing or increasing the metal deposition rate and pressure applied.

Results obtained show the hydrogen flux/permeation data have a strong dependence on pressure and temperature. The permeation rate of H_2 increases significantly once the membrane is activated at temperature and the permeation will also increase with increasing pressure, and will display an opposite trend for other gases, as Pd metal is only permeable to H_2.

In an ideal situation, the permeation rate of N_2 should decrease with increasing temperature and pressure. However, it can be clearly seen from the results that the permeation rate of N_2 is increasing with increasing pressure. This is because the increasing differential pressure across the membrane will force the N_2 molecules through the pinholes or leaks with the graphite seal.

Previous experiments conducted have also showed that the fluxes of N_2 gas are significantly reduced by simply replacing the graphite seal. This in turn has showed the possibility of gas leak through the graphite sealing system, therefore the membrane seal has to be improved by either replacing the type of material used or designing a new reactor with a better sealing system. In any case, either option would still require a significant amount of research time and cost.

Despite all these, the performance of the membrane produced this time is by far the best compared to its predecessors. This indicated that all the modifications to the plating technique and reactor design does improve its performance. Embrittlement which occurs at the top part of membrane C (entrance of feed gas) had been eliminated as the feed gas is now preheated to the reactor temperature.

5.1.5 Advanced Electroless Plating

At the Centre for Process Integration & Membrane Technology, I have successfully applied an advanced electroless plating technique to deposit thin Pd films on 30 nm pore ceramic supports. In this patent pending process, a *controlled sustained partial vacuum* process has been developed and applied to assist uniform densification of the palladium film and simultaneously prevent mass transfer from the film back into the solution, which is the major problem with conventional electroless plating techniques.

SEM photographs showing the cross-section of Pd/γ-Al_2O_3 membrane with a 6 micron thick Pd layer membrane obtained by the advanced electroless plating technique are illustrated in figure 5.3. It clearly shows the composite structure with Pd top layer, and base γ-Al_2O_3 support (which is also shown in page 140).

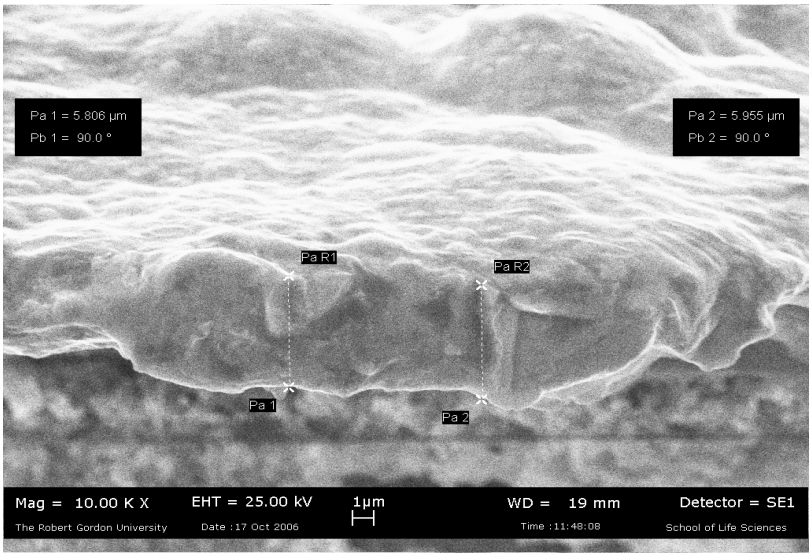

Figure 5.3: Cross-section Scanning Electron Micrograph (SEM) showing the thickness of the Pd film.

Figure 5.4: Photograph of a 365 mm long by 10 mm OD membrane coated with palladium using the advanced electroless plating technique.

5.2 Discussion of The Results Obtained From Gas Permeation Test

5.2.1 The Mechanism of Hydrogen Transport in Palladium Membranes

The mechanism of hydrogen transport (figure 5.5) involves a series of steps which include the mechanism of hydrogen involves a series of steps:

1) adsorption
2) dissociation
3) ionization
4) diffusion
5) re-association
6) desorption

When H_2 molecules contact the Pd metal, adsorption will occur at the metal surface. Within the metal, hydrogen will lose its electron to the palladium structure and diffuses through the membrane as an ion (or proton). At the exit surface the reverse process occurs. Only hydrogen appears to possess the ability to diffuse through palladium or palladium alloys. Assuming no pinholes or micro-cracks, the hydrogen issuing from the low-pressure side of a membrane may be looked upon as a standard of absolute purity. Attempts to detect the presence of impurities show only traces in the parts-per-billion range. These trace impurities, if indeed there are any; probably reflect either mechanical defects or incomplete out-gassing of the walls of the downstream of parts of the system itself.

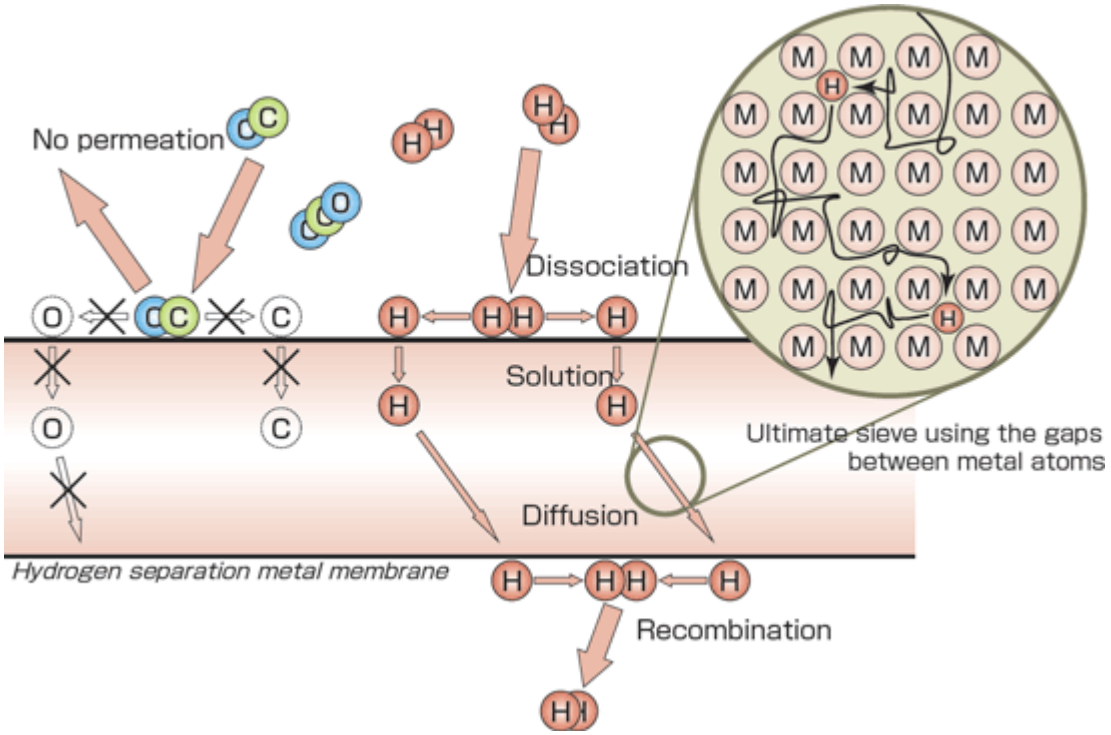

Figure 5.5: Principle of hydrogen separation through metal membrane [21].

5.2.2 Hydrogen Flux

Thin membranes (~2 µm thick) give a moderate flux of the order of ~0.1 mol/m^2s, but at the expense of selectivity towards H_2.and comparatively thick membranes (10-15 µm) gives high selectivity (>1000) but poor H_2 flux of the order of 10^{-2}mol/m^2s [1-17]. The described example, if viewed from the theory of limits, implies that the thinner a membrane can be made; the more cost-effective it will be in terms of performance and materials. While theoretically true, there are limits on the physical material properties for a given set of operational conditions that will define how thin a membrane can be manufactured and still maintain its integrity.

Membrane performance is a function of the quality of the film and, in particular, the presence of defects in the film. As the scientists attempt to produce ultra-thin membranes over larger areas, surface contaminants and particulates, even in the sub-micron range, become problematic. The final thickness of the membrane material incorporated into a design is also influenced by the design and choice of materials for components directly associated with the membrane material.

Uemiya [1] reported that the thickness of palladium layer strongly depended on the supports quality, such as narrow pore size distribution and the amount of defects on the surface. The suggested relations between the thickness of Pd layer and pore size were 13µm in thickness versus 0.3µm in pore size, 4.5µm versus 0.2µm, 2.2µm versus 0.1µm and 0.8µm versus 5nm. Mardilovich et al. [2 & 3] showed that the minimum thickness of palladium required to achieve a dense layer by electroless plating was approximately three times the diameter of the largest pores in the support.

5.2.3 Hydrogen Permeation

The hydrogen permeation through palladium-based membranes is described by Equation (1), [4] & [5]:

$$J = Q_H (P_{high}^{\ n} - P_{low}^{\ n}) \quad \text{..... (Eq 1)}$$

Where J is the gas flux, Q_H is temperature dependent constant, n is a constant power of the pressure, P_{high} and P_{low} are respectively the hydrogen partial pressure on feed and permeate sides. The value of n indicates the rate-limiting step of H_2 permeation through Pd membranes. If the bulk diffusion of atomic hydrogen is the rate-determining step, n equals to 0.5. When surface process involving the H_2 dissociative adsorption on Pd membrane and/or atomic H recombination and desorption at the permeate side controls the H2 permeation, n is 1. When both the surface process and bulk diffusion are responsible for determining H_2 permeation rate, n will vary between 0.5 and 1.

Our observed value of 1.0 for n (figure 5.6) implies that surface process involving the H_2 dissociative adsorption on Pd membrane and/or atomic H recombination and desorption at the permeate side controls the H_2 permeation.

The measured hydrogen fluxes through palladium-based membranes at different temperatures enabled an estimate of the activation energy as described by an Arrhenius law as follows:

$$Q_H = Q_o \exp(-E_A/RT) \quad \text{..... (Eq 2)}$$

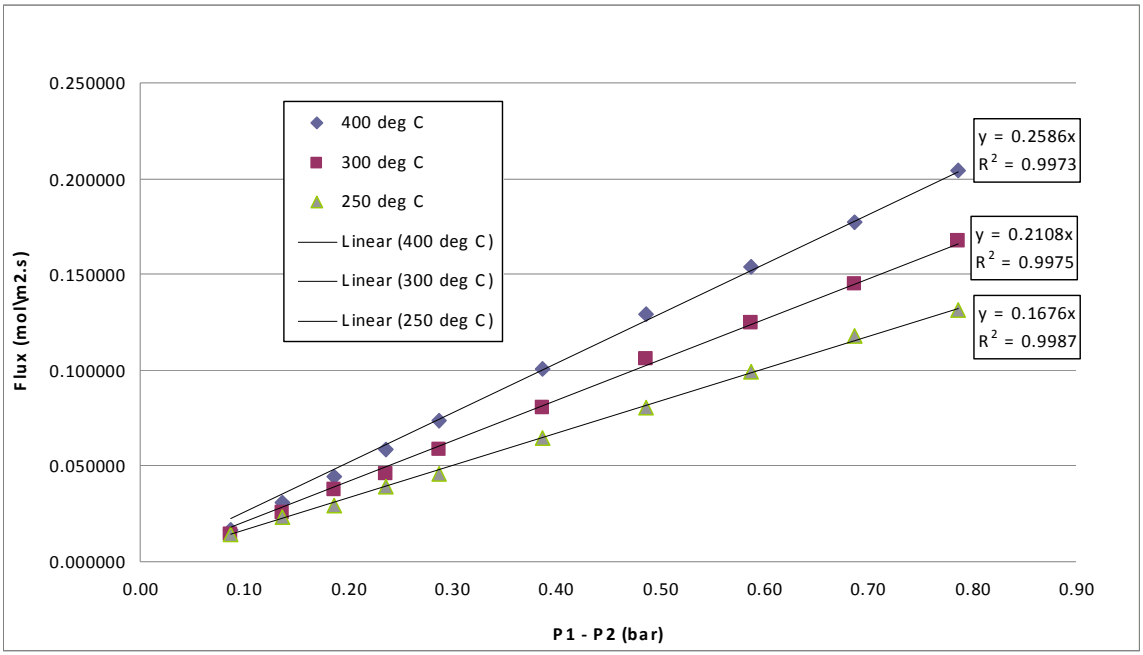

Figure 5.6: Hydrogen flux versus partial pressure difference for pure hydrogen feed (lines: predictions, points: measurements).

Where Q_o is the pre-exponential factor, E_A is the activation energy, T the permeation temperature and R the ideal gas constant (8.3144 $JK^{-1}mol^{-1}$ in SI units). Figure 5.7 shows the plot of Ln (Q_H) against 1/T and the regression of the hydrogen permeance at different reciprocal temperatures with the Arrhenius equation. From the slope it was possible to calculate that the activation energy is 8.43 KJ/mol. This value is in good agreement with literature data for different Pd-based membranes as shown in Table 5.1.

For electroless plated Pd membranes or cold rolling Pd disks, the activation energy lies between 8–15 kJ/mol if bulk diffusion is a rate-limiting step, or both bulk diffusion and surface process are responsible for determining the whole permeation process [6,7–9].

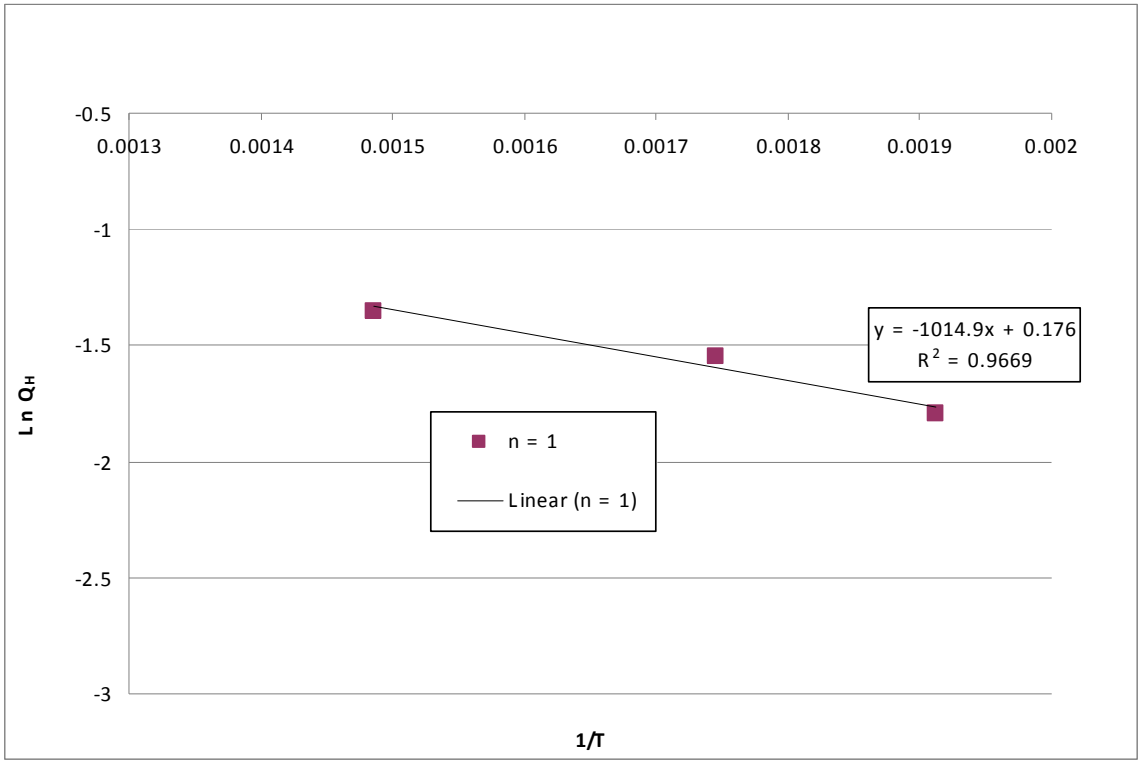

Figure 5.7: Arrhenius plot of pure hydrogen permeation (lines: predictions, points: measurements).

Membrane	Preparation Method	Pore Size of The Support	Pd Thickness (μm)	Activation Energy (kJ/mol)	n-value	Ref.
Self Supporting						
Pd Disk	Cold rolling	Not applicable	27-154	11.9	0.68	7
Pd Disc	Cold rolling	Not applicable	50	11.4	n/a	8
$P_{75}Ag_{25}$ Disc	*	Not applicable	198	6.2	0.5	13
$P_{75}Ag_{25}$ Tube	**	Not applicable	124	6.6	0.5	14
Composite						
$P_{77}Ag_{23}/Al_2O_3$	ELP	150 nm	8.6	8.22	0.5	9
Pd/Al_2O_3	ELP	10-200 nm	11.4	8.88	0.58	6
$P_{77}Ag_{23}$ $/\gamma\text{-}Al_2O_3$	Sputtering	3-6 nm	0.35	23.0	n/a	12
$P_{75}Ag_{25}$ $/\gamma\text{-}Al_2O_3$	Sputtering	3-6 nm	0.1 – 1.5	27.9 – 32.0	n/a	15
Pd/316L stainless steel	ELP	200 nm	0.3 – 0.4	n/a	n/a	16
Pd/porous silver	ELP	200 nm	5	6.6	0.5	5
$P_{75}Ag_{25}$/ porous stainless steel	ELP	500 nm	24	9	0.5	18
This Work	**Advanced ELP**	**30 nm**	**6**	**8.43**	**1.0**	

Table 5.1: Comparison of activation energy for hydrogen transport through Pd-based membranes based on available literatures (Disc supplied by KfK Karlsruhe; **The tube was supplied by Engelhard Industries)*

5.2.4 Hydrogen Flux and Purity (Permeate)

In order to better understand the nature of the perm-selectivity losses in the Pd-composite membranes, experiments were carried out to quantify single gas H_2 and N_2 (both 99.999%) permeation tests and the WGS-shifted dry reformate mixture (ca.67% H_2, 32% CO_2, 0.1% CO, and 0.9% CH_4) were undertaken for comparison at 250^{O}C, 300^{O}C, and 400^{O}C respectively. Permeation through the palladium membrane with a reformate (H_2+Y) having a hydrogen concentration at 67% hydrogen shows that above a partial pressure drop of 0.3 bar hydrogen, there was substantial deviation from linearity indicating distortion due to component Y.

With a molecular type impurity diffusing through the lattice structure, the normal atomic type hydrogen permeation is expected to be disturbed from the normal mode of transportation. Such perturbation is expected to become more severe as the concentration of the second gas increases. The linear coordination between hydrogen flux and pressure would then deviate further from a linear coordination as the concentration of Y gas increase. This was indeed observed when the concentration of carbon dioxide in hydrogen mixture increased as shown in Fig 5.8 and Fig 5.9. When hydrogen and carbon dioxide was only 25%, the hydrogen permeate was almost negligible unless the upstream pressure increased to a high value.

Based on theory of palladium relaxation, Lewis and Schirber and Morosin calculated the atomic distance between Pd atoms increase from 3.890Å to 4.025Å when chemisorbed. H/Pd ratio increases from 0.06 to 0.6, following a relationship of $\Delta v = 2.9$ Å^3 and $\Delta L/L = 0.198$ for each additional chemisorption of hydrogen atom to the lattice [18, 19]. Since the kinetic diameter of N_2, CO, CO_2, H_2 and CH_4 [20] is 3.64, 3.69, 3.30, 2.89 and 3.80 Å respectively are slightly smaller than the lattice opening, these gas molecules can conceivably penetrate through the expanded cubic structure if the membrane is getting thinner. Without hydrogen chemisorption on the palladium, the lattice structure is tighter and thus seals better for these gases molecule to penetrate through and show a satisfactory leak proof when the test was conducted with a single gas.

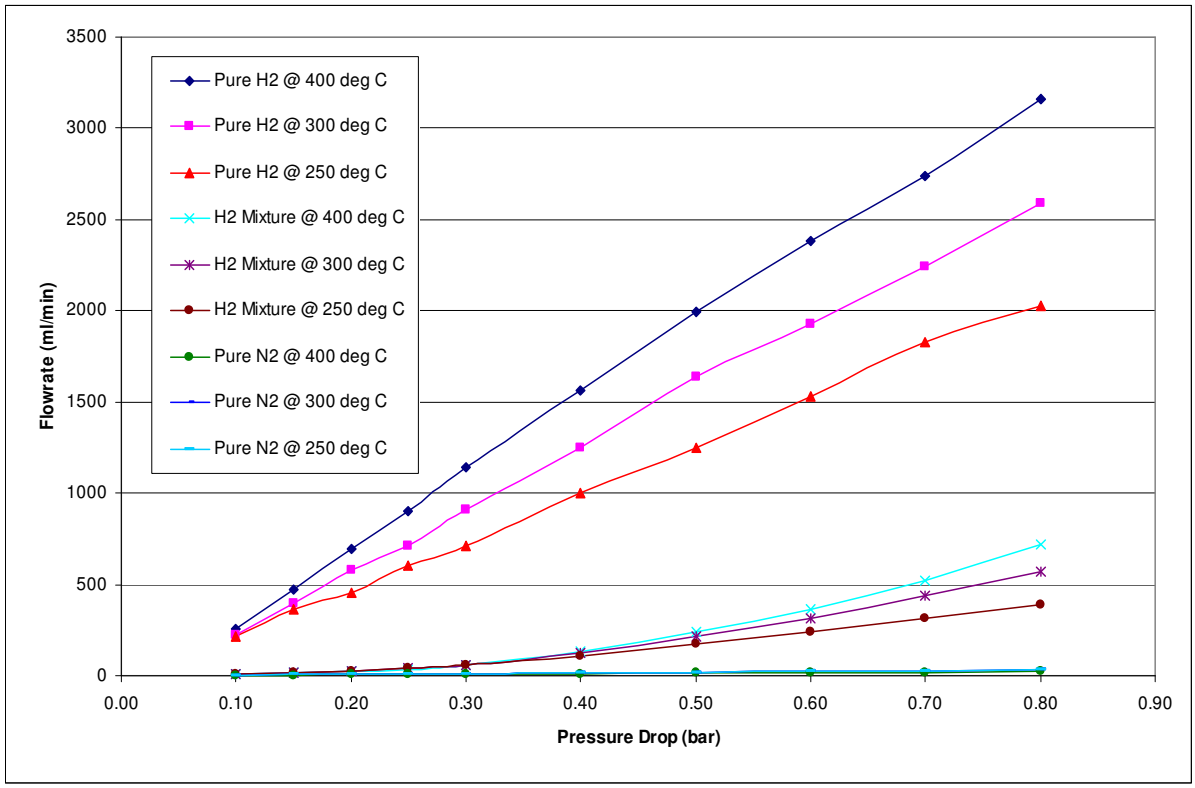

Figure 5.8: Flowrate of pure H_2 and pure N_2 in comparison to that of the WGS-shifted dry reformate (ca 67% H_2, 32% CO_2, 0.1% CO, and 0.9% CH_4) versus partial pressure drop at 250^{O}C, 300^{O}C, and 400^{O}C respectively.

Very minor N_2 permeation could be detected at temperatures of 250^{O}C, 300^{O}C, and 400^{O}C. The N_2 flux was found to be almost constant at 2 x 10 $^{-8}$ mol/m2-s-Pa. The magnitude of the N_2 leak was comparable to those reported by Ma et al. (2005). Moreover, the N_2 permeance is nearly independent of the pressure. The results, however, does not support N_2 diffusing interstitially just like H_2 through Pd. When the permeation source gas was a 100% H_2, the hydrogen flux is generally linear and shows marked temperature dependence. Of the reduction, carbon dioxide is thought to cause the most severe reduction than others in the WGS dry reformate mixture; this was attributed to the poisoning effect of carbon monoxide brought about by the reduction of carbon dioxide. Such a plot provides some information about the nature of the non-selective transport through membrane defects.

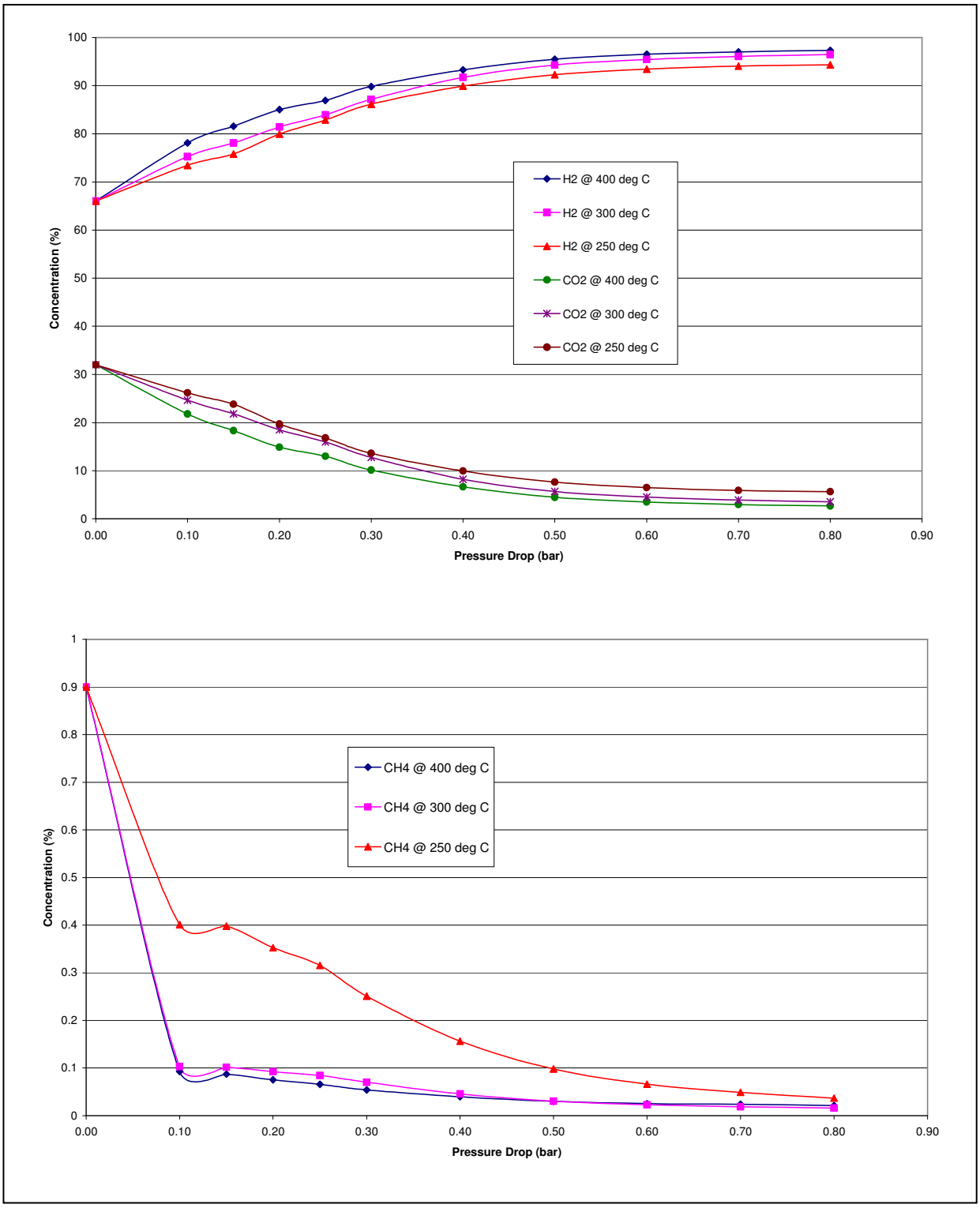

Figure 5.9: Graph showing the permeate component obtained by the membrane, simulating concentration from a feed-stream consisting of WGS dry reformate mixture (ca.67% H_2, 32% CO_2, 0.1% CO, 0.9% CH_4) at 250^{O}C, 300^{O}C, and 400^{O}C respectively.

5.3 References

1. S. UEMIYA, 1999. **State of the Art of Supported Metal Membrane for Gas Separation**, *Separation and Purifications Review 28*, pg. 51-85.
2. MARDILOVICH I.P., SHE Y., MA Y.H., 1998. **Defect Free Palladium Membranes on Porous Stainless Steel Support**, *AIChE Journal 44 (2)*, pg. 310 – 322.
3. MARDILOVICH I.P., SHE Y., MA Y.H., 2002. **Dependence of Hydrogen Flux on the Pore size and Plating Surface Topology of Asymmetric Pd-porous Stainless Steel Membranes,** *Desalination 144 (1-3)*, pg. 85 – 89.
4. GOBINA, E., HUGHES, R., MONAGHAN, D. and ARNELL, D. 1994. **High-Temperature Selective Membranes for Hydrogen Separation**. *Dev. Chem. Eng. Min. Proc*., *2*, pg. 105-114.
5. GOVIND, R. and ATNOOR, D., 1991. **Development of a Composite Palladium Membrane for Selective Hydrogen Separation at High Temperature**, *Ind. Eng. Chem. Res. 30*, pg. 591-594
6. COLLINS JP, WAY JD., 1993. **Preparation and Characterization of a Composite Palladium-Ceramic Membrane**. *Ind Eng Chem Res. 32*, pg. 3006–3013.
7. HURLBERT RC, KONECNY JO, 1961. **Diffusion of hydrogen through Palladium**. *J Chem Phys. 34*, pg. 655–658.
8. JUNG SH, KUSAKABE K, MOROOKA S, KIM SD., 2000. **Effects of Co-existing Hydrocarbons on Hydrogen Permeation Through a Palladium Membrane**. *J Membr Sci. 170*, pg. 53–60.
9. GUO Y, LU G, WANG Y, WANG R., 2003. **Preparation and Characterization of Pd-Ag/ceramic Composite Membrane and Application to Enhancement of Catalytic Dehydrogenation of Isobutane**. *Sep Purif Technol. 32*, pg. 271–279.
10. MCCOOL BA, LIN YS., 2001. **Nanostructured Thin Palladium-Silver Membranes: Effects of Grain Size on Gas Permeation Properties**. *J Mater Sci. 36*, pg. 3221–3227.
11. YEUNG KL, CHRISTIANSEN SC, VARMA A., 1999. **Palladium Composite Membranes by Electroless Plating Technique: Relationships between Plating**

Kinetics, Film Microstructure and Membrane Performance. *J Membr Sci. 159*, pg. 107–122.

12. JAYAMARAN V, LIN YS, PAKALA M, LIN RY., 1995. **Fabrication of Ultrathin Metallic Membranes on Ceramic Supports by Sputter Deposition**., *J Membr Sci. 99*, pg. 89–100.
13. E. SERRA, M. KEMALI, A. PERUJO, D.K. ROSS., 1998. **Hydrogen and Deuterium in Pd-25 Pct Ag Alloy: Permeation, Diffusion, Solubilization, and Surface Reaction**, *Metallurgical And Materials Transactions, Vol. 29A*, pg. 1023-1028.
14. FRANK J. ACKERMAN, GEORGE J. KOSKINAS, 1972. **Permeation of Hydrogen and Deuterium Through Palladium-Silver Alloys**, *Journal of Chemical and Engineering Data, Vol. 17, No. 1*, pg. 51-55.
15. XOMERITAKIS G, LIN YS., 1997. **Fabrication of Thin Metallic Membranes by MOCVD and Sputtering**. *J Membr Sci.* 133, pg. 217–230.
16. ZHONGLIAN SHI and JERZY A. SZPUNAR, 2007. **Synthesis of an Ultra-Thin Palladium Membrane for Hydrogen Extraction**, *Rev.Adv.Mater.15*, pg. 1-9.
17. JAMES R. BRENNER, GAURAV BHAGAT and PAREEN VASA, 2008. **Hydrogen purification with palladium and palladium alloys on porous stainless steel membranes,** *Int. J. Oil, Gas and Coal Technology, Vol. 1, Nos. 1/2, pg.109-124.*
18. M. KRUKOWSKI and B. BARANOWSKI, 1976. *J. Less-common Metals 49*, pg. 385.
19. Y. DE RIBAUPIERRE and F.D. MAMCHESTER, 1974. *K. Phys. C: Solid State Phys. 7*, pg. 2126.
20. S. SIRCAR and A. L. MYERS, 2003. "**Gas Separation by Zeolite**" in *Handbook of Zeolite Science and Technology*, Ed by S.M. AUERBACH, K. A. CARRADO and P.K. DUTTA, *Marcel Dekker Inc. New York, 2003, Chapter 22.*

CHAPTER 6

6.0 Conclusions and Recommendations for Future Work

The future of Palladium membranes to a large extent will depend on its ability to become widely recognised as a suitable alternative to other conventional hydrogen separation technologies. In order to be economically feasible to compete with other separation technologies, the cost of membrane fabrication and amount of Pd metal used is extremely crucial. Its success will depend on the formation of thin and dense layer of Pd metal.

6.1 Conclusions

The research work conducted here has yielded some very interesting and new results. Most importantly, all the objectives initially set out have been achieved. With the results and information obtained from this work, it can be concluded that

1. Although the most cost effective way of producing a composite Palladium membrane would be the electroless plating technique, the partial vacuum has enhanced the method compared to other available techniques due to it's relatively ease of fabrication setup, and most importantly the degree of freedom provided for future modification and coupling with other techniques.

2. The investigated technique is applicable for supports with wide variety of pore sizes ranging from 30 nm – 6000 nm pore size and can handle longer supports. In other words, the novelty of the technology is not constrained to the support but to the optimisation process itself.

3. The investigation has revealed that the ELP under partial suction is the best way forward for membrane fabrication. This modified method is extremely versatile for variation and process optimisation studies. It can easily be adjusted to control the metal deposition rate, which will eventually determine the thickness and density of the Pd membrane layer.

4. The improved method has also resulted in the reduction of the amount of time and material required, thus significantly reducing the cost of membrane fabrication.

5. This work also showed the ability of the method in scaling up the membrane process/size as different lengths of Pd membrane varying from 6 – 32cm have been successfully produced

6. The final membrane produced has also proved its capability in purifying H_2 gas using a reformate gas mixtures containing 67% of H_2, up to the value of 97.3% pure H_2 in a single stage pass at 400 ^{0}C at low pressure differentials.

7. It should be noted that the membrane is capable of purifying H_2 gas to a higher value than the one obtained if it is operated at a higher operating pressure and temperature. This is because the membrane performance shows a strong dependence on pressure and temperature from the results obtained. Unfortunately, there was no suitable equipment available at the time to do the test at higher pressure and temperature safely

6.2 Recommendations for Future Work

Although a great deal of experimental work has been conducted for this project, the author feels that there is still room for further improvement. The main focus of the future work should look toward:

- The use of an even larger and longer ceramic support in order to validate whether the new ELP method is capable of coating supports with a wide range of sizes.

- To design a new reactor that is capable of operating at a much higher pressure and temperature of about 5 bars at 400 ^{0}C (pressure tested and certified). This is crucial for generating more results at high operating pressure and temperature.

- To investigate the stability of the Pd membrane layer or possible deactivation of the membrane by performing long term stability test for a period of up to 1 or 3 months. This will certainly require the development of a fully automated experimental rig where real time on-line measurement/analysis of the permeate gas are achieved via computer controls of temperature, mass flow-meter, digital pressure gauges, control valves, pressure relief valves, automated shutdown and alarm systems. This facility would then allow the test to be conducted safely and will eventually free-up the researcher to perform other experiments or investigation.

- An investigation into the overall mass transfer resistance (boundary layer effect) of the membrane through a systematic evaluation of the porous support, permeation rate, thickness of membrane, alloying with other metals, pressure and temperature. Information obtained can then be used to develop a model to predict the performance of membrane and minimising resistance to H_2 transport.

- Studying the dependence on the pressure applied by the different flow rate used to create the partial suction in order to gain more understanding on the deposition reaction during plating and how it can actually affect the metal deposition.

- Finally, the continuing development and advancing of the ELP under partial suction method by exploring the use of alloying Pd with other metals to produce a multi-metallic/Pd-alloy membrane. The benefit of these types of membrane is to reduce the amount of Pd needed without compromising its performance and thus reducing the cost of membrane production. Besides that, Pd-alloy membranes are capable of operating at a lower temperature therefore reducing the chances of hydrogen embrittlement occurring and membrane poisoning caused by impurities with the feed gas.

The list of recommendations provided here is drawn up to evaluate and facilitate the suitability of the ELP process for scale-ups and the stability of Pd membranes in long-term operations. Besides that, the proposed development of a model can then be used to predict the performance, understanding and improving the overall membrane process. Knowledge gained here will eventually provide essential information required for future commercialization purposes.

APPENDICES

Appendix A: Sample of GC Chromatogram and Result

As mentioned earlier, the original GC used (CP-3800) was not configured to measure high purity H_2 gas. Hence, it was instead used to measure the presence of N_2 gas and subtracting it to give the H_2 value. The result obtained was then verified by the use of 2nd GC (Micro-GC). Figure A1 show the value obtained from using CP-3800 and figure A2 shows the value obtained from Micro-GC. The value for N_2 obtained using Micro-GC is slightly higher but the total percentage is more than 100%. Therefore after normalizing, the actual value for N_2 is only 17.1428 %, which close to the value of 17.2644% obtained from CP-3800

Print Date: Tue Oct 02 12:52:37 2007 Page 1 of 1

Title :
Run File : C:\Star\data\CHEN\2007-10-02\2007-10-02-1.0.run
Method File : e:\star\gc2\gc2-h2n2-ret.mth
Sample ID : 2007-10-02-1.0

Injection Date: 10/2/2007 12:14 PM Calculation Date: 10/2/2007 12:52 PM

Operator : Ali Detector Type: 3800 (10 Volts)
Workstation: Bus Address : 45
Instrument : Varians GC 2 Sample Rate : 10.00 Hz
Channel : Front = TCD Run Time : 2.000 min

** Star Chromatography Workstation Version 5.31 ** 00756-2460-4c1-0094 **

Run Mode : Analysis
Peak Measurement: Peak Area
Calculation Type: External Standard

Peak No.	Peak Name	Ret. Time Result ()	Time (min)	Offset (min)	Width Area (counts)	Sep. Code	1/2 (sec)	Status Codes
1	N2	17.264458	1.461	0.021	125135	BB	4.0	
Totals:		17.264458		0.021	125135			

Total Unidentified Counts : 0 counts

Detected Peaks: 2 Rejected Peaks: 1 Identified Peaks: 1

Multiplier: 1 Divisor: 1 Unidentified Peak Factor: 0

Baseline Offset: 3 microVolts

Noise (used): 3 microVolts - monitored before this run

Manual injection

****

Figure A1: A scan copy showing the result obtained from Varian GC model CP-3800 (using mixture of H_2/N_2 gas as feed at 400 ^{0}C and 1.0 bar pressure differential)

```
Print Date: Wed Aug 19 10:22:09 2009                    Page 1 of 1

Title        :
Run File     : C:\star\data\Pd\4900.44168.run
Method File  : 4900.44168-b.mth
Sample ID    : Manual Sample

Injection Date: 5/12/2009 1:25 PM     Calculation Date: 5/12/2009 1:28 PM

Operator    : ccc                     Detector Type: 4900 (21 Volts)
Workstation:                          Bus Address  : 44
Instrument : varian 1                 Sample Rate  : 100.00 Hz
Channel     : B = MS 5A               Run Time     : 2.500 min

** GC Workstation Version 6.41 ** 04981-27c0-826-1335 **

Run Mode         : Analysis
Peak Measurement: Peak Area
Calculation Type: External Standard

                                  Ret.     Time                          Width
 Peak      Peak        Result     Time    Offset       Area     Sep.     1/2    Status
  No.      Name          ()       (min)    (min)     (counts)  Code    (sec)   Codes
 ---- ------------ ----------  -------- -------- ----------  ----  -----  ------
    1 H2              87.3123     0.636    0.021 1237784832    BB     3.3  C
    2                  0.0000     0.646    0.000      10087    BV     0.1
    3                  0.0000     0.937    0.000    3761203    VV     0.0
    4                  0.0000     1.276    0.000    4213744    VV     0.0
    5                  0.0000     1.489    0.000     387384    VB     0.0
    6 N2              18.6118     1.613    0.033   25687342    BB     2.7
 ---- ------------ ==========  -------- ======= ==========  ----  -----  ------
      Totals:        105.9241              0.054 1271844592

Status Codes:
C - Out of calibration range

Total Unidentified Counts :     8372419 counts

Detected Peaks: 6            Rejected Peaks: 0       Identified Peaks: 2

Multiplier: 1          Divisor: 1           Unidentified Peak Factor: 0

Baseline Offset: 0 microVolts           LSB:  0.01 microVolts

Noise (used): 8 microVolts - monitored before this run

Manual injection

Calib. out of range; No Recovery Action Specified

********************************************************************************
```

Figure A2: A scan copy showing the result obtained from Varian Micro-GC (using mixture of H_2/N_2 gas as feed at 400 ^{0}C and 1.0 bar pressure differential)

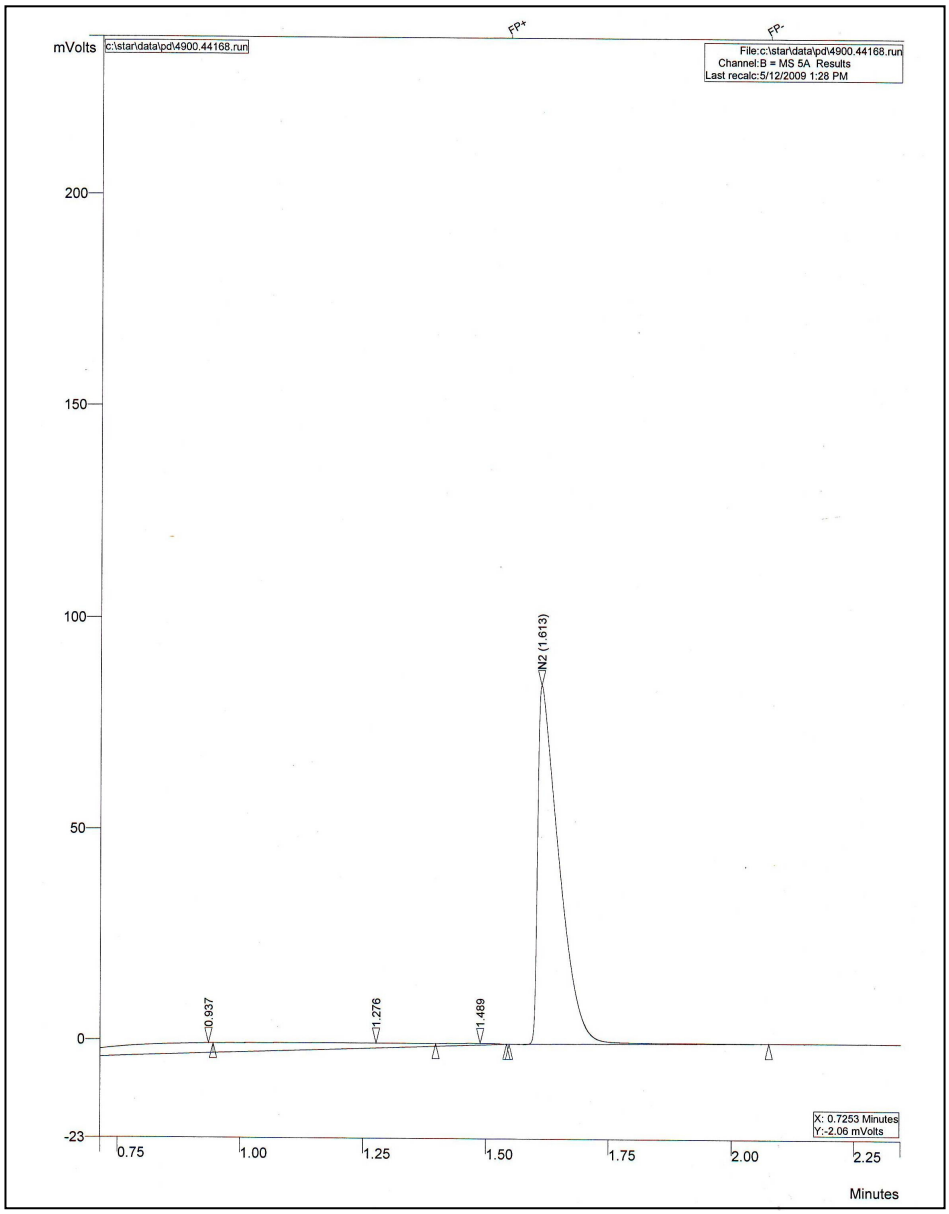

Figure A3: A scan copy of the gas chromatogram (Micro-GC) showing the presence of N2 gas peak.

Appendix B: A Sample of EDXA Graph and Result

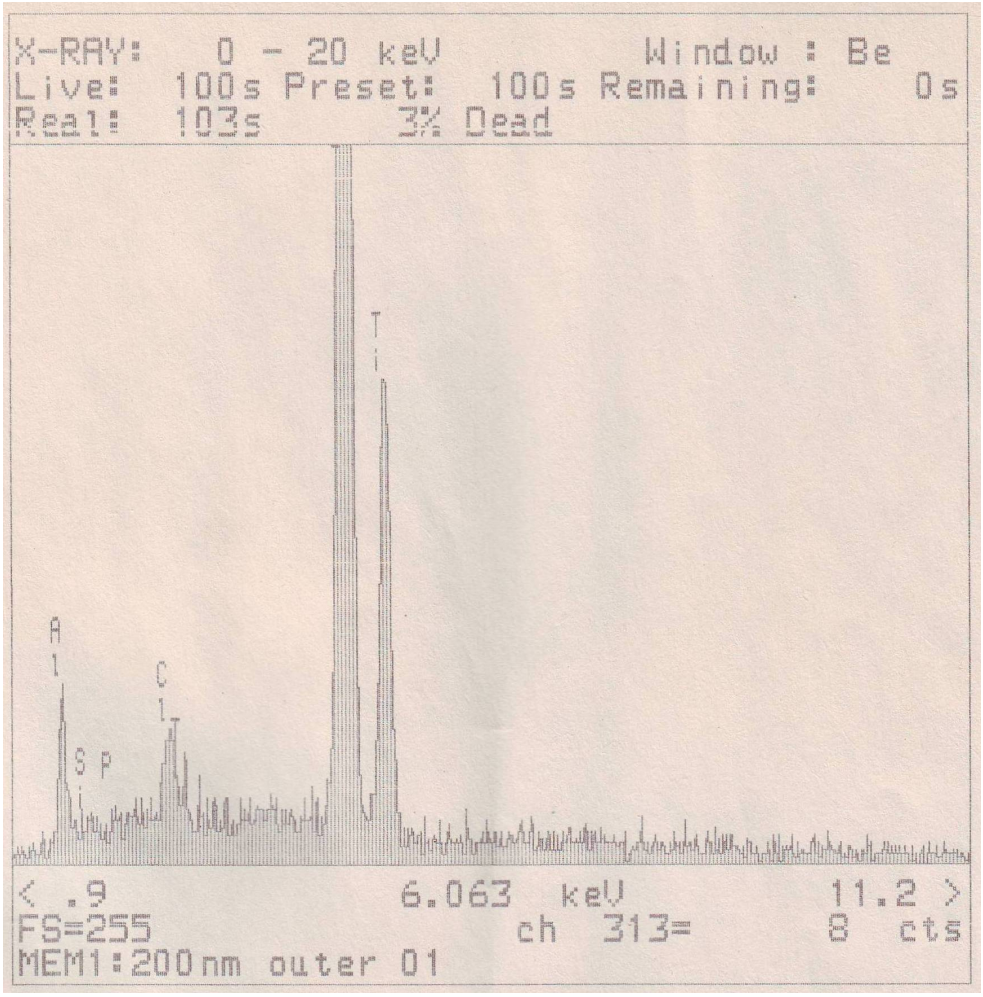

Figure B1: A scan copy of the EDXA graph obtained for a 200 nm ceramic support (outer layer)

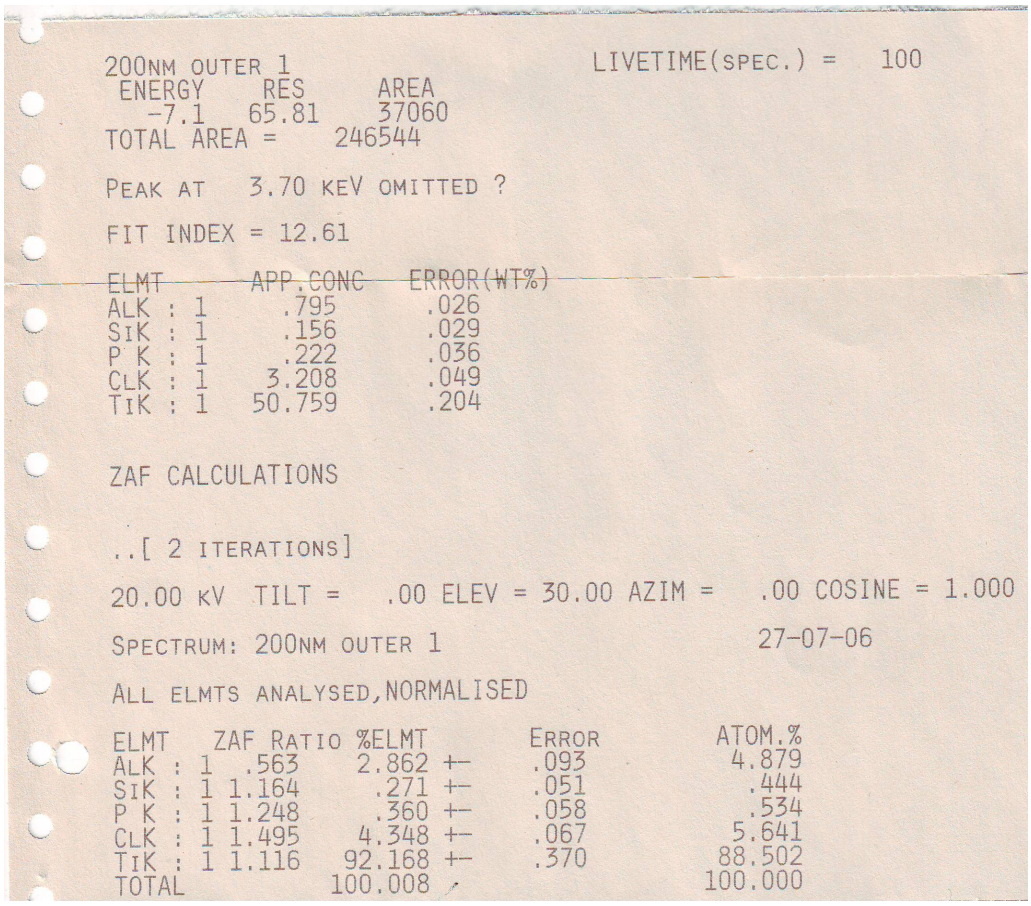

200NM OUTER 1 LIVETIME(SPEC.) = 100

ENERGY	RES	AREA
-7.1	65.81	37060

TOTAL AREA = 246544

PEAK AT 3.70 KEV OMITTED ?

FIT INDEX = 12.61

ELMT	APP.CONC	ERROR(WT%)
ALK : 1	.795	.026
SIK : 1	.156	.029
P K : 1	.222	.036
CLK : 1	3.208	.049
TIK : 1	50.759	.204

ZAF CALCULATIONS

..[2 ITERATIONS]

20.00 KV TILT = .00 ELEV = 30.00 AZIM = .00 COSINE = 1.000

SPECTRUM: 200NM OUTER 1 27-07-06

ALL ELMTS ANALYSED,NORMALISED

ELMT	ZAF RATIO	%ELMT	ERROR	ATOM.%
ALK : 1	.563	2.862 +-	.093	4.879
SIK : 1	1.164	.271 +-	.051	.444
P K : 1	1.248	.360 +-	.058	.534
CLK : 1	1.495	4.348 +-	.067	5.641
TIK : 1	1.116	92.168 +-	.370	88.502
TOTAL		100.008		100.000

Figure B2: A scan copy showing the composition (88% titania) of the outer layer of the 200 nm ceramic support.

Appendix C: Sample Calculation of Membrane Permeances

Permeation experiment refers to the measurement of permeation flow rates at different trans-membrane pressure differentials. Usually, the permeate stream (outlet from membrane tube) is left open to atmosphere and hence, zero gauge pressure. The gas stream that enters the permeation cell shell offers a pressure higher than atmosphere pressure and has values above 0.0 gauge pressure. The permeation experiments are then conducted at specified gauge pressure.

The following presents a sample calculation of how the measured values from using Helium gas as feed are transformed to membrane permeances:

Measured Values:

Pressure Differential set:	= 0.08bar	= 8000 pa
Temperature:	= 23 ^{0}C	= 296 K
Membrane Length:	= 5.9 cm	
Membrane Diameter:	= 1.0 cm	
Helium flow rate:	= 20.4 ml\min	= 20.4 x 10^{-3} L\min

Calculations:

Flux = Gas Flow (mol\s) / Area (m^2)

$$Gas\ Flow = \frac{20.4\times10^{-3}}{60}(L \setminus s) = 0.00034(L \setminus s)$$

$$= \frac{0.00034(L \setminus s)}{22.4(\frac{296}{273})(L \setminus mol)} = 0.00001399(mol \setminus s)$$

$$Area = \pi \times d \times l = 3.142 \times 1 \times 5.9(cm^2) = 18.538(cm^2) = 0.001853(m^2)$$

$$Therefore,\ flux = \frac{0.00001399(mol \setminus s)}{0.001853(m^2)} = 0.007556(mol \setminus m^2.s)$$

Permeances = Flux (mol\m^2.s)/ Pressure Differential (Pa)

$$= \frac{0.007556(mol \setminus m^2.s)}{8000(Pa)}$$

$$= 9.4456 \times 10^{-7}(mol \setminus m^2.s.Pa)$$

Appendix D: Sample Calculation of Membrane Thickness from Weight Gain Measurement

The following present the steps involved for a sample calculation of an *estimated* palladium film thickness based on weight gain. In order for the equation to be valid, the coating is assumed to be distributed uniformly on the membrane surface.

Weight of the support before deposition	= 13.08 g
Weight of the support after deposition (membrane) (after cleaning and drying)	= 13.54 g
Weight gained	= 13.54 – 13.08 = 0.46 g
Support length for deposition	= 6.1 cm
Diameter of the support	= 1.05 cm
Support surface area	= 3.142 x 1.05 x 6.1 = 20.1117 cm^2
Palladium metal density	= 12 g/cm^3
Palladium film volume (weight/density)	= 0.46/12 = 0.03833 cm^3
Palladium film thickness (Pd film volume/surface area)	= 0.03833/20.1117 = 0.001906 cm = 19.06 µm